Published for SISSA by Springer

Received: November 4, 2025
Accepted: May 13, 2026
Published: July 2, 2026

Differential cross-section measurements of coherent production of singly and doubly resonant top-quark in $WWbb$ events with one lepton at $\sqrt{s} = 13$ TeV with the ATLAS detector

The ATLAS collaboration

Full author list at the end of the paper

E-mail: atlas.publications@cern.ch

Abstract: This paper presents differential cross-section measurements of events containing a charged lepton, missing transverse momentum, two b-jets, and two light jets, consistent with the $W^+W^-b\bar{b}$ final state. The analysis is based on 140 fb^{-1} of proton-proton collision data at $\sqrt{s} = 13$ TeV recorded with the ATLAS detector during Run 2 of the Large Hadron Collider (2015–2018). Differential cross-sections are unfolded at particle level for a range of kinematic observables and in three kinematic regions. Both regions and observables are optimised for sensitivity to the interference between $W^+W^-b\bar{b}$ produced with singly and doubly resonant top quarks. Results are compared with various theoretical predictions and deviations are observed in regions sensitive to the interference between singly and doubly resonant top-quark production. The unfolded results provide new information about the modelling of interference and off-shell effects of the $W^+W^-b\bar{b}$ final state, improving the understanding of top-quark production mechanisms and providing new inputs for future Monte Carlo generator development.

Keywords: Hadron-Hadron Scattering

ArXiv ePrint: 2510.26476

Open Access, Copyright CERN,
for the benefit of the ATLAS Collaboration.
Article funded by SCOAP^3.

https://doi.org/10.1007/JHEP07(2026)028

JHEP07(2026)028

Contents

1 Introduction **1**

2 Experimental and simulation setups **3**
- 2.1 The ATLAS experiment 3
- 2.2 Object reconstruction 4
- 2.3 Modelling and simulation of Standard Model processes 5

3 Event selection **8**

4 Unfolding procedure **12**

5 Systematic uncertainties **13**

6 Differential cross-section results **19**

7 Conclusions **28**

The ATLAS collaboration **39**

1 Introduction

The study of the top quark is a cornerstone of the Large Hadron Collider (LHC) [1] physics programme. At the LHC, top quarks are predominantly produced in top-antitop-quark pairs. This process is referred to as doubly resonant top-quark production, or $t\bar{t}$, in the following. Additionally, top quarks can be produced individually via singly resonant top-quark production, which occurs through three main channels: the t-, s-, and tW-channels. The t-channel involves the exchange of a virtual W boson and is characterised by the scattering of a light quark, making it the most abundant single-top production mode. The s-channel proceeds through the production of a virtual W boson that yields a top-quark and a bottom quark. Lastly, the tW-channel involves the production of a single top quark in association with a W boson. The top quark decays into a W boson and a bottom quark (b) with a branching fraction of approximately 100%. When considering all processes at next-to-leading (NLO) accuracy in quantum chromodynamics (QCD), the associated production of a single resonant top-quark and a W boson, or tWb, has the same final state as doubly resonant top-quark production. Traditionally these processes have been treated separately in theory calculations and experimental measurements, due to their large cross-section differences and the non-trivial interplay between leading order (LO) and NLO between the two processes.[1]

Differential cross-sections for $t\bar{t}$ production have been measured by the ATLAS [2–6] and CMS [7–10] collaborations and accurate theory calculations have been performed [11–13].

[1] At NLO, the $gb \to WWb$ process receives radiative corrections that include contributions overlapping with the LO $gg \to W^+W^-b\bar{b}$ process ($t\bar{t}$). The contribution of the latter, being $t\bar{t}$ mediated, is much larger than the former.

JHEP07(2026)028

Differential cross-sections for tW production have also been measured by the two LHC experiments [14–20]. A dedicated procedure [21–25] is used to define single-top-quark cross-sections and Monte Carlo predictions not including the doubly resonant top-quark production. The separation of single and double top-quark production is subject to a certain degree of arbitrariness, related to the treatment of interferences and off-shell top-quark (finite-width) effects. This theory approximation provides a significant source of uncertainty for many measurements [3, 26–28] and searches for physics beyond the Standard Model (BSM) [29–39]. For this reason, a coherent treatment of singly and doubly top resonant production is desirable. This can be achieved considering the complete process $pp \to W^+W^-b\bar{b}$. The $W^+W^-b\bar{b}$ topology can arise from doubly resonant top-quark processes (figure 1(a)), singly resonant top-quark processes (figure 1(b)), non-resonant diagrams without intermediate top quarks (figure 1(c)) and their interference. The consistent calculation of the $W^+W^-b\bar{b}$ process was performed up to NLO order in QCD [40] and supplemented with parton showers [41, 42]. Calculations of the process $pp \to \ell\nu bbjj$ were performed up to NLO QCD [43] and NLO QCD including NLO electroweak corrections in ref. [44]. The only existing measurements to assess these predictions in a region sensitive to the interplay between singly and doubly resonant top-quark processes have been performed in final states with two light charged leptons [6, 45, 46].

This paper considers events with at least one leptonically decaying W boson. The final state is characterised by a light charged lepton (e or μ), missing transverse momentum, and three or four jets, of which two identified as originating from b-quarks (b-jets). The focus of this measurement is singly and doubly resonant top quark production: $t\bar{t}$ and tWb. Differential cross-sections on key top-quark physics observables are extracted using an unfolding procedure at particle level. The analysis selections, fiducial volumes and observables are optimised to probe a kinematic phase space where the interplay (and interference) between the two processes is enhanced, using dedicated requirements to actively suppress the pure doubly resonant top-quark production. The non-resonant $W^+W^-b\bar{b}$ production is not explicitly enhanced in these selections and has therefore a negligible contribution to the analysis selections. In comparison with measurements requiring two light charged leptons in the final state, the single-lepton channel provides the opportunity to measure the W boson kinematic properties directly, since the hadronically decaying W boson can be fully reconstructed. In addition, the larger branching ratio gives access to kinematic regions of the phase space characterised by more extreme momenta. The analysis therefore focusses on three kinematic regions. The inclusive region (IR), designed to study both single and double top-quark processes and their interference in the broadest possible phase space; the W-hadronic region (WR), which directly probes the $W^+W^-b\bar{b}$ process by studying the kinematic properties of the W boson and b-jet kinematic observables and thus provides constraints on higher-order corrections or the modelling of real emissions; and the search-like region (SLR), which takes inspiration from a number of BSM searches [29–32, 47, 48] that probe less inclusive corners of the phase space where the interference effects between $t\bar{t}$ and tWb processes are found to be enhanced.

The results of this paper are compared with various state-of-the-art simulations and can be used in the development of new predictions. The full data sample collected with

JHEP07(2026)028

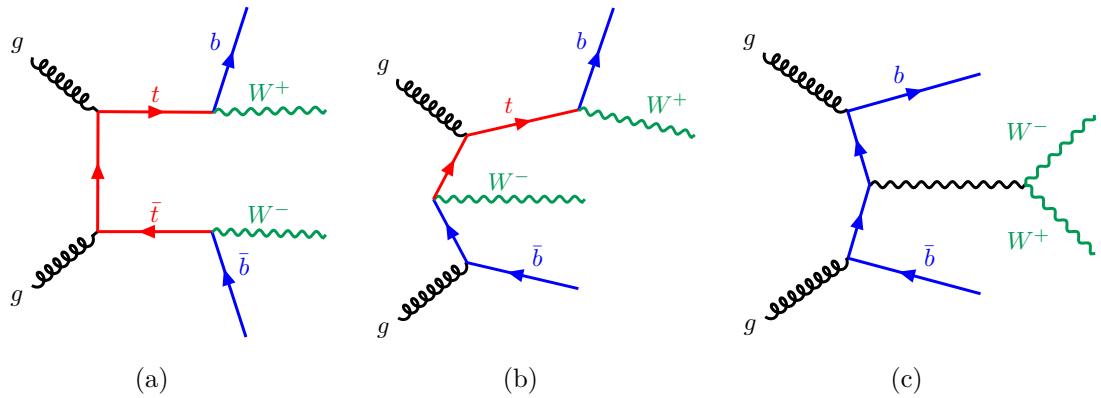

Figure 1. Feynman diagram of the $W^+W^-b\bar{b}$ production. The $W^+W^-b\bar{b}$ topology can arise from 1(a) doubly resonant top-quark processes, 1(b) singly resonant top-quark processes, 1(c) diagrams without intermediate top-quarks, and their interference.

the ATLAS detector between 2015 and 2018 at centre-of-mass energy $\sqrt{s} = 13\,\text{TeV}$ with an integrated luminosity of $\mathcal{L} = 140\,\text{fb}^{-1}$ is used for the measurement.

2 Experimental and simulation setups

2.1 The ATLAS experiment

The ATLAS experiment [49] at the LHC is a multi-purpose particle detector with a forward-backward symmetric cylindrical geometry and a near 4π coverage in solid angle.[2] It consists of an inner tracking detector surrounded by a thin superconducting solenoid providing a 2 T axial magnetic field, electromagnetic and hadronic calorimeters, and a muon spectrometer. The inner tracking detector (ID) covers the pseudorapidity range $|\eta| < 2.5$. It consists of silicon pixel, silicon microstrip, and transition radiation tracking detectors. Lead/liquid-argon (LAr) sampling calorimeters provide electromagnetic (EM) energy measurements with high granularity within the region $|\eta| < 3.2$. A steel/scintillator-tile hadronic calorimeter covers the central pseudorapidity range ($|\eta| < 1.7$). The endcap and forward regions are instrumented with LAr calorimeters for EM and hadronic energy measurements up to $|\eta| = 4.9$. The muon spectrometer surrounds the calorimeters and is based on three large superconducting air-core toroidal magnets with eight coils each. The field integral of the toroids ranges between 2.0 and 6.0 T m across most of the detector. The muon spectrometer includes a system of precision tracking chambers up to $|\eta| = 2.7$ and fast detectors for triggering up to $|\eta| = 2.4$. The luminosity is measured mainly by the LUCID-2 [50] detector which is located close to the beampipe. A two-level trigger system is used to select events [51]. The first-level trigger is implemented in hardware and uses a subset of the detector information to accept events at a rate close to 100 kHz. This is followed by a software-based trigger

[2] ATLAS uses a right-handed coordinate system with its origin at the nominal interaction point (IP) in the centre of the detector and the z-axis along the beam pipe. The x-axis points from the IP to the centre of the LHC ring, and the y-axis points upwards. Polar coordinates (r, ϕ) are used in the transverse plane, ϕ being the azimuthal angle around the z-axis. The pseudorapidity is defined in terms of the polar angle θ as $\eta = -\ln\tan(\theta/2)$. Angular distance is measured in units of $\Delta R \equiv \sqrt{(\Delta\eta)^2 + (\Delta\phi)^2}$.

JHEP07(2026)028

that reduces the accepted rate of complete events to 1.25 kHz on average depending on the data-taking conditions. A software suite [52] is used in data simulation, in the reconstruction and analysis of real and simulated data, in detector operations, and in the trigger and data acquisition systems of the experiment.

2.2 Object reconstruction

Each physics object included in the event selection is defined by a collection of detector information and is reconstructed using dedicated algorithms. These reconstructed particles are referred to as detector-level objects in the following text.

Electron candidates are reconstructed from energy deposits (clusters) in the electromagnetic calorimeter associated with reconstructed tracks in the inner detector [53]. Candidates that have a transverse momentum $p_{\mathrm{T}} > 10\,\mathrm{GeV}$ and $|\eta| < 2.47$ are selected, excluding the calorimeter transition region $1.37 < |\eta| < 1.52$. Electrons in this measurement must satisfy the *Tight* likelihood-based identification criterion [53]. Muon candidates are reconstructed from track segments in the various layers of the muon spectrometer, and matched with tracks from the inner detector [54]. The final muon candidates are refitted using the complete track information from both detector systems, and required to satisfy $p_{\mathrm{T}} > 10\,\mathrm{GeV}$ and $|\eta| < 2.5$. Muons are required to satisfy the *Medium* identification requirements. Both electrons and muons are required to meet the tight working point of the prompt-lepton isolation discriminant [55], trained to separate prompt and non-prompt leptons. Electrons (muons) are further required to have $|z_0 \sin(\theta)| < 0.5\,\mathrm{mm}$ and $|d_0/\sigma(d_0)| < 5$ (3), where the longitudinal and transverse impact parameters d_0 and z_0 are computed relative to the primary vertex, and $\sigma(d_0)$ is the resolution of the track transverse impact parameter d_0 [56]. Calibrations of the electron and muon energy scale and resolution, as well as corrections to the reconstruction, identification and isolation efficiencies are applied following refs. [53, 54, 57, 58]. A secondary set of (fake) electrons and muons candidates is used in the estimate of background arising from misidentified and non-prompt lepton sources. Electron candidates in the fakes category are required to fulfil all kinematic requirements of standard electrons. They are additionally required to satisfy the *Loose* likelihood-based identification criterion but fail to meet either the tight identification requirement or the isolation requirements. Muon candidates in the fakes category are required to fulfil all kinematic and identification requirements of standard muons, but fail to satisfy the isolation requirements.

Jets are reconstructed using the anti-k_t algorithm [59] as implemented in FastJet [60] with a jet radius parameter $R = 0.4$. The inputs to this algorithm are particle flow (PFlow) objects [61], which combine measurements from the ATLAS inner detector and calorimeters [62] to improve the jet energy resolution and increase the jet reconstruction efficiency, especially at low jet p_{T}. Jets are required to have $p_{\mathrm{T}} > 25\,\mathrm{GeV}$ and $|\eta| < 2.5$. Jets originating from pile-up interactions are rejected using the *jet vertex tagger* (JVT) tool [63], which uses a combination of track-based variables providing discrimination against pile-up jets. The `Tight` working point is used for jets in the momentum range $20 < p_{\mathrm{T}} < 60\,\mathrm{GeV}$ and $|\eta| < 2.4$. Calibrations (and their associated uncertainties) are applied in the measurement to the jet energy scale (JES) and resolution (JER) [64], which include components derived both from simulation and in situ measurements. The identification of b-jets is made using the `DL1r`

JHEP07(2026)028

b-tagging algorithm [65], a high-level tagger based on a deep neural network and it is applied to jets satisfying the selections stated above. In this measurement, a working point with a b-tagging efficiency of 77% is used, as evaluated in simulated $t\bar{t}$ events. The corresponding rejection factors are 6 for charm-jets and 134 for light-jets, respectively. Correction factors are applied to the simulated event samples to compensate for differences between data and simulation in the b-tagging efficiency for $b-$, $c-$ and light-jets.

The missing transverse momentum, with magnitude $E_{\mathrm{T}}^{\mathrm{miss}}$, is defined as the negative vector sum of the transverse momenta of all selected and calibrated electrons, muons and jets in the event, with an extra track-based term added to account for energy in the event that is not associated with any of these objects [66].

To avoid double-counting in the analysis due to reconstruction ambiguities, objects are removed based on the distance $\Delta R_y = \sqrt{(\Delta y)^2 + (\Delta\phi)^2}$, where y is rapidity. If an electron and a muon overlap within $\Delta R_y = 0.1$, the muon is removed if it is reconstructed only from an ID track and calorimeter energy deposits consistent with a minimum-ionising particle, otherwise the electron is removed. Then, jets within $\Delta R_y = 0.2$ of an electron are removed. If a jet within $\Delta R_y = 0.4$ survives, the electron is discarded. Muons are removed if $\Delta R_y < 0.4$ from a jet, but if the jet has fewer than three tracks, the jet is removed instead, ensuring efficient selection of high-energy muons affected by calorimeter energy loss.

2.3 Modelling and simulation of Standard Model processes

Monte Carlo (MC) simulated event samples of all major Standard Model (SM) processes are used to aid in the estimation of the differential cross-sections and the unfolding procedure. They are additionally used to estimate systematic uncertainties arising from the theory modelling of such processes. The ATLAS detector response is simulated using a detailed description of the detector geometry and response [67] based on `Geant4` [68] or through a fast simulation using a parameterisation of the calorimeter response and `Geant4` for the other parts of the detector. Detector-level objects are reconstructed in simulated events using the same algorithms used to process the data, with appropriate performance corrections and calibrations applied. The matrix element (ME) generator, parton shower (PS), cross-section accuracy (CS) and specific tools used for their calculation, parton distribution function (PDF) set and the set of tuned parameters (tune) for these samples are given in table 1, and more details of the generator configurations can be found in refs. [25, 69–71] and are briefly summarised in the following text. All simulation samples, except for Sherpa, use EvtGen [72] to model the decays of bottom and charm hadrons. The effect of multiple interactions in the same and neighbouring bunch crossings (pile-up) is modelled by overlaying the simulated hard-scattering event with inelastic proton-proton (pp) events generated with Pythia 8.186 [73] using the NNPDF2.3lo set of PDFs [74] and the A3 set of tuned parameters [75]. Events are weighted to reproduce the distribution of the average number of interactions per bunch crossing ($\langle\mu\rangle$) observed in the data. The $\langle\mu\rangle$ value in data is rescaled by a factor of 1.03 ± 0.04 to improve agreement between data and simulation in the visible inelastic pp cross-section [76].

Modelling of the signal processes. This measurement targets singly and doubly resonant top quark production: $tW(b)$ and $t\bar{t}$. Simulation samples of these processes are used to

JHEP07(2026)028

estimate the unfolding parameters needed to extract fiducial differential cross-sections at particle-level and to estimate the systematic uncertainties associated with the modelling of these processes. These simulation samples are also used to construct the pseudo-data sample used to estimate the closure and robustness of the unfolding procedure.

The production of both final states is modelled using the Powheg Box v2 [77–80] generator, which provides MEs at NLO in the strong coupling constant α_s, and is interfaced with Pythia 8.2 [81] for the parton shower and hadronisation according to the settings described in table 1. The generation of both processes uses the five-flavour scheme. The top quark mass, m_{top}, is set to 172.5 GeV. The h_{damp} parameter, which controls the matching in Powheg and effectively regulates the high-p_{T} radiation against which the $t\bar{t}$ or tW system recoils, is set to $1.5\,m_{\text{top}}$ [25]. The functional form of the renormalisation and factorisation scales is set to the default dynamic scale $\sqrt{m_{\text{top}}^2 + p_{\text{T}}^2}$. The definition of the tW sample is chosen to enable combination with the corresponding $t\bar{t}$ calculation. This is non-trivial at NLO, where care must be taken to avoid double-counting tWb events with $m_{bW} \sim m_{\text{top}}$. Interference effects between the tW and $t\bar{t}$ processes are included in the predictions. The default scheme for combining the $t\bar{t}$ and tW processes at NLO adopted here is diagram removal (DR) [22]. Other choices exist (see ref. [24] for a review), for example the case where doubly resonant contributions are canceled out by gauge-invariant subtraction terms (diagram subtraction, DS) [22, 25]. The $t\bar{t}$ sample is normalised to a cross-section of $831.8^{+29.3}_{-36.5}$ pb. The cross-section prediction is calculated at next-to-next-to-leading-order (NNLO) in QCD including the resummation of next-to-next-to-leading logarithmic (NNLL) soft-gluon terms calculated using Top++ 2.0 [11, 82–87]. The tW sample is normalised to a cross-section of $79.3^{+2.9}_{-2.8}$ pb. This cross-section prediction is calculated at NLO in QCD with NNLL soft-gluon corrections [88–90].

Additional uncertainties associated with the modelling of $t\bar{t}$ and $tW(b)$ processes have been considered using alternative simulation samples.

The impact of using a different parton shower and hadronisation model is evaluated with a simulation sample produced with an alternative shower generator (Herwig [91–94]), see table 1. Furthermore, effects associated with the parameters that regulate the matching between ME and PS generators are estimated by varying the $p_{\text{T,hard}}$ parameter according to the studies in ref. [95]. The top-quark recoil model is also varied in such a way that the parton shower of the nominal $t\bar{t}$ sample employs the recoiling against the top-quark instead of b-quarks. Uncertainties from missing higher orders are evaluated [96] using two-point variations of the QCD factorisation and renormalisation scales in the matrix elements by factors of 0.5 and 2.

To assess the uncertainties related to the modelling of the initial-state radiation (ISR), the sample is reweighted using the Var3c up variation from the A14 tune, which changes the scales in the ISR shower in Pythia. The impact of final-state radiation (FSR) is evaluated by varying the renormalisation scale for emissions from the parton shower up and down by a factor of two. The uncertainties in the cross-section due to the PDF and α_s are calculated using the PDF4LHC15 prescription [97] and are added in quadrature to the effect of the scale uncertainty. Alternative simulation samples with varied h_{damp} parameter ($3\,m_{\text{top}}$) value and varied top-quark mass values (equivalent to a variation of $\pm 0.5 m_{\text{top}}$) were also

JHEP07(2026)028

used to estimate the impact of these parameters on the modelling of the $t\bar{t}$ and tW processes. An alternative tW sample generated with the DS scheme is used to estimate the impact of the double-counting removal procedure used to generate $tW(b)$ events. It is also used as an alternative prediction when comparing to the final result.

Finally, a sample aims to model $t\bar{t}$ processes at NNLO QCD and incorporates all-order radiative corrections through parton-shower simulations as detailed in ref. [98]. This sample is generated using a procedure that consists of three steps. In the first step $t\bar{t}$ pairs plus one light parton are generated using the Powheg Box v2 program, which performs an NLO calculation and includes a second light parton. The second step involves computing the limit in which the emitted light partons become collinear with the $t\bar{t}$ system. This step incorporates Sudakov form factors and relevant higher-order corrections to ensure the result remains well-behaved and accurate at NNLO for inclusive $t\bar{t}$ production. The third step explicitly generates the kinematic properties of the second radiated parton using Powheg Box v2, since this was only treated inclusively in the initial stage. This ensures that the NLO accuracy of the $t\bar{t}$ +jet cross-section is maintained. Following this step, additional radiation is simulated using the PS method of Pythia. This sample is referred to as the "MiNNLOPS" sample in the paper and is used only in the final comparison with the unfolded results. The sample is normalised to the same cross-section at NNLO+NNLL in pQCD calculated with the Top++ 2.0 program, as previously mentioned.

Modelling of the background processes. All relevant SM background processes, with the exception of the QCD multi-jet background, are estimated with the aid of MC simulation samples. The most important processes are the production of vector bosons in association with jets ($V+$jets), diboson production (VV), $t\bar{t}H$, $t\bar{t}V$ and single top (s- and t-channel) production. The production of single-boson and diboson processes is simulated using the Sherpa 2.2.1 [99]. The $V+$jets (VV) processes are simulated at NLO MEs for up to two (one) partons, and LO matrix elements for up to five (three) partons calculated with the Comix [100] and OpenLoops [101–103] libraries.The matrix element calculations are matched and merged with the Sherpa parton shower based on Catani-Seymour dipole factorisation [100, 104] using the MEPS@NLO prescription [105–108]. The diboson simulation samples include off-shell effects and Higgs boson contributions, where appropriate. The $V+$jets simulation samples include electroweak virtual corrections [109, 110]. An additional data-driven normalisation correction is applied to the $W+$jets processes as described in section 4. Single-top-quark (s- and t-channel) processes are simulated using the Powheg Box v2 generator interfaced with Pythia. The $t\bar{t}H$ and $t\bar{t}V$ processes are simulated using the Powheg Box v2 and MadGraph5_aMC@NLO [111] generators, respectively.

The background arising from QCD multi-jets events containing misidentified or non-prompt leptons is estimated using a data-driven *fake-factor* method as described in section 4. Simulation samples as described in this section are used to subtract the prompt-lepton contamination of the non-prompt estimation region and to estimate the systematic uncertainties, including the ones associated with the extrapolation to the phase space of this measurement.

JHEP07(2026)028

Process	ME	PS	CS	PDF	Tune	b/c decays
$t\bar{t}$	Powheg Box v2	Pythia 8.230	NNLO+NNLL (Top++2.0)	NNPDF3.0nlo	A14 tune + NNPDF2.3lo	EvtGen 1.6.0
tW	Powheg Box v2	Pythia 8.230	NLO+NNLL	NNPDF3.0nlo	A14 tune + NNPDF2.3lo	EvtGen 1.6.0
$t\bar{t}$ (alt.)	Powheg Box v2	Herwig 7.1.3	NNLO+NNLL	NNPDF3.0nlo	H7 def. + MMHT2014lo	EvtGen 1.6.0
tW (alt.)	Powheg Box v2	Herwig 7.2.3	NLO+NNLL	NNPDF3.0nlo	H7 def. + MMHT2014lo	EvtGen 1.6.0
$t\bar{t}$ MiNNLOPS	MiNNLOPS + Powheg Box v2	Pythia 8.230	NNLO+NNLL	NNPDF3.0nlo	A14 tune + NNPDF2.3lo	EvtGen 1.6.0
V+jets	Sherpa 2.2.11	Sherpa	NLO	NNPDF3.0nnlo	Sherpa tune	
VV	Sherpa 2.2.11	Sherpa	NLO	NNPDF3.0nnlo	Sherpa tune	
s and t- channel single-t	Powheg Box v2	Pythia 8.230	NLO (Hathor 2.1 [112, 113])	NNPDF3.0nlo	A14 tune + NNPDF2.3lo	EvtGen 1.6.0
$t\bar{t}H$	Powheg Box v2	Pythia 8.230	NLO QCD & EW [114]	NNPDF3.0nlo	A14 tune + NNPDF2.3lo	EvtGen 1.6.0
$t\bar{t}V$	MG 2.3.3	Pythia 8.210	NLO QCD & EW	NNPDF3.0nlo	A14 tune + NNPDF2.3lo	EvtGen 1.2.0

Table 1. Summary of the generator settings used for the Monte Carlo simulation samples. The columns indicate the physics process, the matrix element (ME) generator, the parton shower (PS) generator, the cross-section accuracy (CS), the parton distribution function (PDF) set, the tune used for the underlying event, and the program used for the b/c hadron decays. MadGraph5_aMC@NLO is here referred to as MG. See text for further details.

3 Event selection

The results presented in this paper are based on data collected with the ATLAS experiment between 2015 and 2018 during Run 2 of the LHC. The data sample corresponds to an integrated luminosity of 140 fb^{-1} [50, 115] of pp collisions at a center-of-mass energy of 13 TeV. The measurement of the integrated luminosity is obtained using the LUCID-2 detector for the primary measurement and complemented by measurements in the inner detector and calorimeters. Every detector subsystem must have been in operation during data collection. Moreover, stringent data quality criteria are applied to ensure the reliability of the data [116]. Events are required to be triggered by a collection of single-electron or single-muon triggers [51, 117, 118] operating at different thresholds of transverse momentum and identification criteria through the data-taking periods. Events are required to contain at least one collision vertex with two or more associated tracks with $p_{\mathrm{T}} > 500$ MeV, and the vertex with the highest p_{T}^2 sum of the associated tracks is taken as the primary vertex (PV) [119] of the event.

The target topology of this measurement are events containing two W bosons, one decaying leptonically and one hadronically, and two b-jets, arising from $t\bar{t}$ or tWb production. To select this topology, the events are required to contain exactly one light charged lepton (ℓ, either an electron or a muon) with $p_{\mathrm{T}} > 30$ GeV, which ensures the full efficiency of the triggers. Any event containing an additional lepton with $p_{\mathrm{T}} > 10$ GeV is rejected. Events are also required to have at least four jets, of which at least two are b-jets. An additional requirement on the sum of the $E_{\mathrm{T}}^{\mathrm{miss}}$ and the m_{T}^{ℓ}, the transverse mass between the $E_{\mathrm{T}}^{\mathrm{miss}}$ and the lepton,[3] of greater than 60 GeV is applied to suppress contaminations from the misidentified and non-prompt lepton background.

As introduced before, three kinematic regions are used in this measurement: the inclusive region IR, the W-hadronic region WR and the search-like region SLR. The selection criteria described so far define the IR.

[3]This transverse mass is defined as $m_{\mathrm{T}}^{\ell} = \sqrt{(E_{\mathrm{T}}^{\mathrm{miss}} + E_{\mathrm{T},\ell})^2 - (\vec{p}_{\mathrm{T}}^{\mathrm{miss}} + \vec{p}_{\mathrm{T},\ell})^2}$.

JHEP07(2026)028

	Requirements	
preselection	$N_{b\text{-jets}}$	≥ 2
	$N_\ell(p_\mathrm{T} > 10\,\mathrm{GeV})$	$= 1$
	$E_\mathrm{T}^\mathrm{miss} + m_\mathrm{T}^\ell$	$\geq 60\,\mathrm{GeV}$
	$p_\mathrm{T}(\ell)$	$\geq 30\,\mathrm{GeV}$
IR	N_jets	≥ 4
WR	N_jets	≥ 3
	$p_\mathrm{T}(W_\mathrm{had.})$	$\geq 80\,\mathrm{GeV}$
	$60 < m(W_\mathrm{had.}) < 100\,\mathrm{GeV}$	
SLR	N_jets	≥ 4
	$m_{b\ell}^\mathrm{min}$	$\geq 150\,\mathrm{GeV}$
	$p_\mathrm{T}(j_1), p_\mathrm{T}(j_2)$	$\geq 50\,\mathrm{GeV}$
	$p_\mathrm{T}(b_1), p_\mathrm{T}(b_2)$	$\geq 160, 50\,\mathrm{GeV}$
	$1.4 < \Delta R(b_1, b_2)$	
	$E_\mathrm{T}^\mathrm{miss} \geq -0.625 p_\mathrm{T}(\ell) + 270\,\mathrm{GeV}$	

Table 2. Summary of the selections used in the three measurement regions: inclusive region (IR), W-hadronic region (WR) and search-like region (SLR). Details on the definition of the hadronic W candidate, $W_\mathrm{had.}$, and the invariant mass quantities m_T^ℓ and $m_{b\ell}^\mathrm{min}$ are given in the text.

The WR is defined by explicitly requiring a hadronically decaying W boson in the final state. A W boson reconstruction algorithm is optimised to maximize the overall W identification purity with a procedure that is equally easy to apply on detector-level objects and particle-level objects. This procedure identifies the W candidate as either the leading jet, the subleading jet, or their vectorial sum, with b-jets excluded from this procedure. This approach aims to increase the purity of W identification in the high-p_T region, where the boosted W boson decay products are collimated and the W boson is reconstructed as a single jet. The candidate with a mass closest to the W mass is selected. The mass of the candidate is required to be between $60 < m_W < 100\,\mathrm{GeV}$ and its p_T is required to be at least $80\,\mathrm{GeV}$. These requirements ensure a signal purity of at least 75%, which becomes larger than 90% for events with a W boson transverse momentum larger than $180\,\mathrm{GeV}$.

The SLR is optimised for an extreme phase space and it takes inspiration from BSM physics searches that probed phase spaces where the interference modelling between $t\bar{t}$ and tWb processes resulted in large systematic uncertainties. The unfolded results in this peculiar phase space are very sensitive to the modelling of interference effects. To optimise the selection, the tWb purity and the yield difference between the tW DR and DS simulation samples are used as key metrics. The optimisation aims to minimise this yield difference while maintaining high tWb purity. The minimum invariant mass obtained by pairing the lepton with each

JHEP07(2026)028

of the b-jets in the event, $m_{b\ell}^{\min}$, is an important observable to enhance topologies where at least one top quark is produced off-shell, where interference effects between $t\bar{t}$ and tWb can be probed best. A requirement of $m_{b\ell}^{\min} \geq 150\,\text{GeV}$ exploits the characteristic kinematic endpoint of $t\bar{t}$ events and suppresses events with an on-shell semileptonically decaying top quark. Further requirements are embedded into the selection to suppress on-shell $t\bar{t}$ events: the transverse momentum of the leading (subleading) b-jet is required to be greater than 160 (50) GeV. The leading and subleading b-jets are required to have a relatively large spatial separation ($\Delta R(b_1, b_2) > 1.4$). Finally, $E_{\text{T}}^{\text{miss}}$ and $p_{\text{T}}(\ell)$ are required to satisfy the following condition in the SLR:

$$E_{\text{T}}^{\text{miss}} \geq -0.625 p_{\text{T}}(\ell) + 270\,\text{GeV}.$$

This requirement is chosen to maximise the overall $t\bar{t} + tWb$ acceptance, while enhancing the interference effects in this phase space using easily-interpretable observables. The selection criteria for the three measurement regions are summarised in table 2.

In the WR selection, observables are chosen study the kinematic properties of the hadronically decaying W boson. These are:

- $p_{\text{T}}(W_{\text{had.}})$: the transverse momentum of the hadronically decaying W boson candidate.
- $y(W_{\text{had.}})$: the rapidity of the hadronically decaying W boson candidate.
- $m(W_{\text{had.}}bb\ell)$: the invariant mass of the $Wbb\ell$ system.
- m_{bW}^{minimax}: variation of the min-max variable from ref. [45], which takes into account the different final state considered in this paper. The variable is defined using the hadronic W candidate ($W_{\text{had.}}$) and the two leading b-jets as:

  $$m_{bW}^{\text{minimax}} = \min\left(\max(m_{W_{\text{had.}}b_1}, m_{\ell b_2}), \max(m_{\ell b_1}, m_{W_{\text{had.}}b_2})\right).$$

  This observable considers all possible pairings of the two b-jets with either $W_{\text{had.}}$ or the lepton. It exhibits a kinematic endpoint at

  $$m_{bW}^{\text{minimax}} < \sqrt{m_{\text{top}}^2 - m_W^2}$$

  for doubly resonant top-quark topologies, where m_{top} and m_W denote the top-quark and W masses, respectively. This makes it sensitive to regions of phase space enriched in singly resonant processes, where this endpoint is exceeded.
- $m_{b\ell}^{\text{selected}}$: a variation of the $m_{b\ell}^{\min}$ observable which uses the b-jets assignment from the m_{bW}^{minimax} observable to calculate the invariant mass between the lepton and the selected b-jet.

A variation of the $m_{b\ell}^{\min}$ observable, $m_{\text{T}}^{\min}(b\ell)$, is studied in the IR and SLR selections. It considers also the $E_{\text{T}}^{\text{miss}}$ information to constrain the mass of the leptonically decaying top. This is defined as the minimum transverse invariant mass between the $E_{\text{T}}^{\text{miss}}$, the lepton and the b-jet.

JHEP07(2026)028

Physics process	IR		WR		SLR	
tW DR	139 000	$^{+8000}_{-8000}$	34 000	$^{+1900}_{-1900}$	1680	$^{+100}_{-80}$
tW DS (alt.)	120 000	$^{+8000}_{-8000}$	28 400	$^{+1900}_{-1900}$	234	$^{+15}_{-15}$
$t\bar{t}$	4 000 000	$^{+200\,000}_{-200\,000}$	850 000	$^{+40\,000}_{-40\,000}$	1170	$^{+80}_{-80}$
W + jets	120 000	$^{+22\,000}_{-18\,000}$	10 300	$^{+2000}_{-1600}$	344	$^{+90}_{-56}$
Other t	91 000	$^{+24\,000}_{-24\,000}$	9300	$^{+2400}_{-2400}$	104	$^{+27}_{-27}$
Other V	25 000	$^{+4000}_{-16\,000}$	2210	$^{+230}_{-1600}$	61	$^{+4}_{-61}$
Mis-ID lep.	20 000	$^{+8000}_{-14\,000}$	1900	$^{+1300}_{-700}$	45	$^{+33}_{-34}$
Total MC w/ DR	4 400 000	$^{+230\,000}_{-220\,000}$	910 000	$^{+50\,000}_{-50\,000}$	3400	$^{+210}_{-190}$
Data	4 303 650		849 115		2403	

Table 3. Summary of the contributions of all SM processes and observed data in the three measurement regions. All statistical and systematic uncertainties are included, with the exception of the signal modelling, in the total uncertainty in the yields and are summed in quadrature. Both diagram removal (DR) and diagram subtraction (DS) yields are shown for the tW process for comparison.

The total yields observed in data and predicted from the simulation in each region are shown in table 3. The breakdown by SM process is also shown.

In addition to the detector-level objects, corresponding particle-level objects are defined using generator-level information from stable particles, identified as those with a proper lifetime $c\tau > 10$ nm. These objects are identified without simulating their interactions with the detector and are used to define the fiducial phase-space regions and observables of interest in the measurement.

Particle-level electrons and muons are required not to originate from hadrons, either directly or through intermediate τ-lepton decays. A lepton is retained if it arises from a τ-lepton that itself originates directly from a W boson. The lepton four-momenta are corrected for final-state radiation from photons not originating from hadron decays and located within $\Delta R = 0.1$ of the lepton direction. The same transverse momentum and pseudorapidity requirements as for detector-level leptons are applied.

Particle-level jets are reconstructed by clustering all stable particles, excluding those identified as leptons or as neutrinos from electroweak boson decays, using the anti-k_t algorithm with a radius parameter of $R = 0.4$. The identification of b-jets is performed via the ghost-association technique: all b-hadrons are included in the jet clustering with their momentum set to a negligible value, and jets containing a b-hadron with $p_{\mathrm{T}} > 5$ GeV are classified as b-tagged.

The particle-level missing transverse momentum is computed as the negative vector sum of the transverse momenta of all neutrinos, excluding those originating from hadron decays, either directly or via τ-leptons.

An overlap removal is applied among particle-level objects where electrons and muons located within $\Delta R = 0.4$ of any jet are removed.

JHEP07(2026)028

The particle-level selections for the three measurement regions used for the differential measurements are constructed to match the detector-level regions by applying the same selection criteria.

4 Unfolding procedure

The differential cross-section measurement is performed in each of the three measurement regions (IR, WR and SLR), using the fiducial volumes definitions described in the previous section. An unfolding procedure is applied to extract the results at particle-level, following the methodology outlined in refs. [120, 121]. The unfolding is performed using the `TUnfold` package [122].

The differential cross-section for a variable X at particle-level is defined as follows:

$$\frac{d\sigma_{\text{fid}}}{dX_i} = \frac{1}{\mathcal{L}_{\text{int}} \cdot \Delta X_i} \cdot \frac{1}{\epsilon_i} \cdot \sum_j M^{-1}_{i,j} f^j_{\text{acc}} (N_{d,j} - N_{b,j}).$$

The index i runs over all the bins of the particle-level definition of the variable X while the index j runs over all the bins of the reconstructed-level definition of the variable X. $\mathcal{L}_{\text{int}}$ is the integrated luminosity. The differential cross-section is obtained from the data distribution $N_{d,j}$ after subtracting the background contribution $N_{b,j}$. The unfolding efficiency ϵ_i and the unfolding acceptance f^j_{acc} are obtained from the simulation of the target processes of the analysis ($t\bar{t} + tWb$). The efficiency is defined as the fraction of particle-level events that satisfy the detector-level selections and corrects for detector inefficiencies in the fiducial phase space. The acceptance is defined as the fraction of detector-level signal simulated events that satisfy the particle-level selection in each bin and corrects for events that are generated outside the fiducial phase-space but satisfy the detector-level selection. The migration matrix $M_{i,j}$, or normalised response matrix, is derived from the simulation and it describes the fraction of events that migrate from particle-level bin i to reconstructed bin j. The bin width is indicated by ΔX_i. The bin boundaries are chosen such that, in most cases, the diagonal of the migration matrix contains at least 60% of particle-level events of a row. The number of reconstructed distribution bins is chosen to be twice the number of particle-level bins, according to the `TUnfold` default configuration [122]. The migration matrix inversion, M^{-1}, is estimated using a Tikhonov-Phillips regularisation scheme [123, 124], which reduces the statistical uncertainty associated with the inversion at the price of a possible deviation from the true value (bias). The bias is quantified with a closure test and found to be negligible.

Typical efficiency values across the three measurement regions range between 20 and 30% for most of the phase space and observables considered in the unfolding results. The acceptance values exhibit stronger variability across regions and phase space. In the IR and WR selections, typical acceptance values range between 60 and 80%, while in the SLR selections, the acceptance values are lower, with typical values around 40%. The migration matrix is almost diagonal for observables with small reconstruction uncertainties, such as the lepton p_{T}, while it is more off-diagonal for observables with larger reconstruction uncertainties, such as the (b)-jet momenta or the $m^{\text{min}}_{b\ell}$ observable.

The unfolding is performed in each of the three measurement regions and the results are compared with the predictions of the simulation on key observables that allow for a

JHEP07(2026)028

thorough assessment of the data and its comparison with the MC models across all relevant kinematic phase space.

All SM processes other than $t\bar{t}$ and tWb are subtracted from data as the first step of the unfolding procedure. The dominant processes are $W+$jets, $Z+$jets and diboson (referred to as "Other V"), $t\bar{t}V$, $t\bar{t}H$ and sub-dominant single-top channels (referred to as "Other t") and QCD multi-jets processes with fake and non-prompt leptons (referred to as "Mis ID. lep."). $W+$jets is an important background for the IR and SLR selections. Its normalisation is constrained in a dedicated control region, WCR, enriched in this process with the purpose of better controlling the impact of systematic uncertainties related to this background. Events in the WCR are required to fulfil all requirements of the IR selection, except for the jet multiplicity requirement that is reduced to exactly three jets to ensure orthogonality. The overlap with the WR is removed by vetoing events that fulfil the WR selection, which is a small fraction of the total events in WCR. The $W+$jets contribution is further enhanced by requiring 40 GeV $< m_{\mathrm{T}}^{\ell} <$ 100 GeV and $m_{b\ell}^{\mathrm{min}} > 180$ GeV. A purity of 50% is achieved, with a contamination of 39% from $t\bar{t}+tWb$ events. The normalisation of the $W+$jets background is estimated by means of a likelihood fit in the WCR, where detector and modelling uncertainties of all processes are treated as nuisance parameters in the fit. The resulting normalisation factor is 1.10 ± 0.10. The data is within the uncertainty in the expected yields after the fit. The normalisation factor is used to correct the $W+$jets process in all measurement regions (and is applied also in table 3).

Misidentified and non-prompt leptons are estimated by using a data-driven method called *fake-factor method* that estimates the non-prompt contamination from a control region rich in this background and with high statistical power as described in detail in ref. [125]. This process is found to be the smallest source of background in every region of the analysis. The electron and muon requirements used to select this fakes control region are described in section 2.2. The prediction is validated in a dedicated and statistically independent validation region selecting events failing the requirement on $E_{\mathrm{T}}^{\mathrm{miss}}+m_{\mathrm{T}}^{\ell}$ and applying looser requirements on the jet multiplicity. All other backgrounds are estimated from simulation.

The unfolding procedure is tested using pseudo-experiments and the self-consistency of the procedure (closure) is quantified. The unfolding is found to be stable and the bias is found to be negligible. In addition, stress tests are performed to verify that the unfolding is able to recover an alternative truth-level distribution. The stress tests include the reweighing of the unfolding observable with a linear function, the reweighting of the unfolding observable to match the data distribution, and the reweighing of the unfolding observable with a histogram of the ratio of observed-to-expected signal in the unfolded variable at detector level. The unfolding is able to recover an alternative distribution in all cases, with discrepancies always consistent with the statistical precision of the test.

5 Systematic uncertainties

The sources of systematic uncertainties that affect the measurements of the differential cross-sections include the detector-related uncertainties that affect the calibration and the reconstruction efficiency of detector-level particles, the background and signal modelling, and the size of the data and MC samples. All systematic uncertainties related to the detector

JHEP07(2026)028

performance and calibration and the modelling of the SM processes (as described in section 2) are propagated through the unfolding procedure.

The integrated luminosity has an uncertainty of 0.83% [115], which is propagated as a systematic uncertainty in the measurement to all physics processes other than the QCD multi-jet background. The pile-up uncertainty is assessed through the uncertainty on the factor used for the μ reweighting.

Charged leptons have uncertainties in the efficiency of the reconstruction, identification, isolation requirements, and trigger, which are derived from studies using $Z \to ee$ and $Z \to \mu\mu$ events [53, 54, 117, 118]. The impact of the lepton energy scale and resolution uncertainty is evaluated using resonance decays [57, 58]. The JER and JES uncertainties are derived using a combination of data and MC samples, using measurements of (for example) the jet p_{T} balance in dijet, Z+jet and γ+jet events [64]. Further jet-related uncertainties originate from efficiency corrections for tagging pile-up jets [63] and the identification of b-jets [126–128]. Uncertainties in the $E_{\mathrm{T}}^{\mathrm{miss}}$ are estimated by propagating the uncertainties in the energy and momentum scale of each of the objects entering the calculation of $E_{\mathrm{T}}^{\mathrm{miss}}$, with additional terms taking into account the uncertainty in the resolution and scale of the soft term [66].

Modelling uncertainties are considered for both signal and background processes. Uncertainties associated with the modelling of $t\bar{t}$ and $tW(b)$ processes have been considered using alternative simulation samples as described in section 2.3. The most important uncertainty is found to be the one related to different schemes used as double-counting removal procedure in the generation of $tW(b)$ events (DS versus DR removal schemes), followed by those related to the use of a different parton shower and hadronisation model and to variations of ISR and FSR. Additional uncertainties include factorisation and renormalisation scale variations, effects associated with the parameters that regulate the matching between ME and PS generators ($p_{\mathrm{T,hard}}$ parameter), top-quark recoil model, and PDF choice. Since the $t\bar{t}$ and $tW(b)$ cross-sections are known at different perturbative orders in QCD and the two processes are treated here coherently, the modelling uncertainties in the two processes are treated consistently at NLO in QCD. The impact of the assumed value of the top quark mass on the results is evaluated using additional simulation samples with varied top-quark mass values of 172 GeV and 173 GeV. The resulting uncertainty is usually found to be negligible, but can grow up to 5% in the most extreme regions of phase space. Furthermore, uncertainties related to the flavour composition of extra jets radiated in association with top pairs are estimated and found to be negligible.

All signal modelling uncertainties are treated as correlated between the two processes. A dedicated uncertainty is included to account for the approximations used to model the shape of the top-quark mass with a proper width and high off-shell behaviours. This uncertainty is estimated by comparing two existing implementations from Powheg and MadGraph5_aMC@NLO [129]. Uncertainties related to the modelling of additional $b\bar{b}$ or $c\bar{c}$ pairs in the parton shower are estimated by varying their respective contributions in the nominal $t\bar{t}$ sample and found to be negligible. The cross-section uncertainties are treated as anti-correlated for the $t\bar{t}$ and tW samples, which is the most conservative approach for a result that is sensitive to the relative normalisation of the two processes. The results are

JHEP07(2026)028

also found to be insensitive to whether the $t\bar{t}$ samples are normalised using NLO+NNLL or NNLO+NNLL cross-sections.

The full uncertainty in the $W+$jets normalisation, as obtained from the profile likelihood fit, is propagated to the unfolding. In addition, the shape component of all systematic uncertainties associated with the $W+$jets background are propagated individually to the unfolding using the corresponding variations.

For all background samples, cross-section uncertainties are estimated by taking into account scales and PDF variations. The uncertainties due to missing higher-order corrections are evaluated by varying the renormalisation and factorisation scales by factors of 2.0 and 0.5. These uncertainties are estimated by keeping one scale at its central value while the other is varied up and down, and vice versa. The PDF uncertainties are estimated by using the PDF4LHC15 prescription. Electroweak correction uncertainties are estimated for single and multi boson processes [109, 110].

The uncertainties related to the modelling of the QCD multi-jet background are estimated by varying the control region selection criteria used in the fake-factor method and by varying the Monte Carlo predictions by 10% around their nominal values. These procedures result in a conservative uncertainty of 50% to 70% in the total yield of this background, which does not affect the final results because of the small contribution of this background in all regions.

Detector and modelling uncertainties in backgrounds are propagated from detector to particle level by calculating varied unfolding corrections ($M_{i,j}$, ϵ_i and f^j_{acc}). The data is then unfolded with these varied corrections and the difference to the nominal unfolded data defines the uncertainty. Modelling uncertainties in signal are treated differently. Pseudo-data built using alternative predictions are unfolded using the nominal setup. These results are compared with the alternative simulation sample at particle-level and the difference defines the uncertainty.

Overall, small uncertainties are observed for the variables that are reconstructed only from leptons or dominated by $t\bar{t}$ only, thanks to the large number of data events and small migrations between the bins. The more statistically limited SLR results in unfolded observables with relatively large statistical uncertainties.

One of the dominant uncertainties is the uncertainty in the modelling of the interference between $t\bar{t}$ and tWb arising from using the alternative tWb DS MC sample in the unfolding procedure. This comparison estimates whether the unfolding is able to recover an alternative truth-level distribution and it is particularly important when no simulation is available that models the data well, as in this case. This uncertainty particularly strongly affects the SLR selection, where the large difference both in acceptance and normalisation of the two simulation approaches changes the relative fractions of $t\bar{t}$ and tWb processes in the unfolding and affects the unfolded result in a significant way. This uncertainty is presented separately in all unfolded cross-sections in section 6 as it is the one with the largest potential for reduction in the future.

The uncertainties of the unfolded distributions range approximately from 5% to 20% in the higher statistics regions and from 20% to 80% in extreme phase spaces. The more extreme phase spaces, especially in the SLR selection, are strongly affected by the DR-DS

JHEP07(2026)028

uncertainty. The results for these selections achieve a precision at the level of 20% or better overall when the DS-DR uncertainty is not taken into account.

A detailed breakdown of systematic uncertainties is presented in figures 2 to 4 for all observables discussed in this paper. Depending on the region and observable the dominant systematic uncertainties are found to be detector systematic uncertainties related to jet tagging and calibration, and modelling of the signal processes. Observables that exhibit end-points, e.g. $m_{b\ell}^{\mathrm{min}}$, $m_{\mathrm{T}}^{\mathrm{min}}(b\ell)$, $m_{b\ell}^{\mathrm{selected}}$ and m_{T}^{ℓ}, are particularly sensitive to variations of the jet energy scale and resolution, which create sharp increases in the uncertainties around the top-quark mass in figures 2(a), 2(c), 3(a) and 3(b). Uncertainties related to the modelling of the $t\bar{t}$ signal processes are also significant around those end-points, where different modelling of the parton shower or the initial and final state radiation can lead to different shaping of the distributions.

JHEP07(2026)028

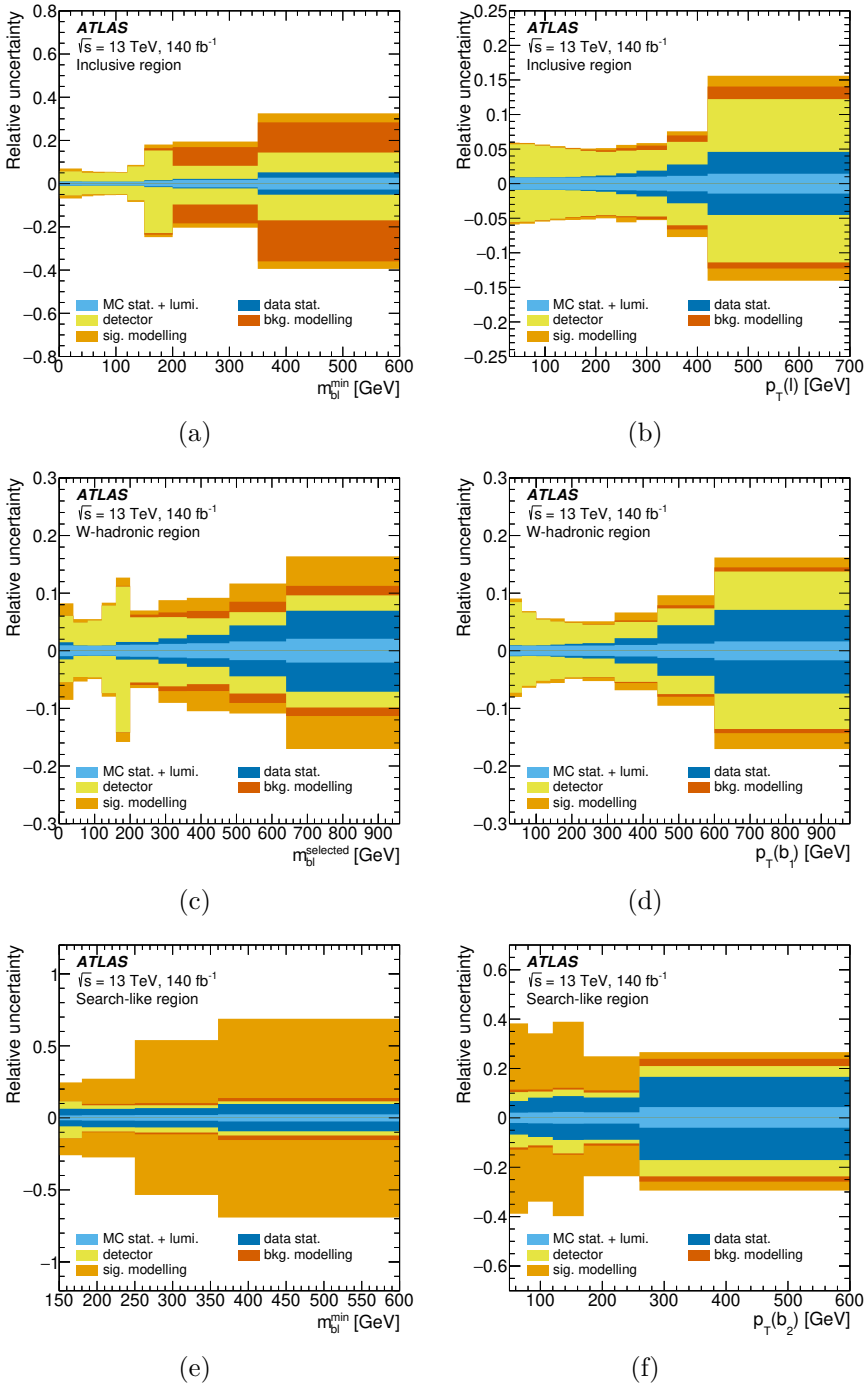

Figure 2. Breakdown of the systematic uncertainties in the unfolded differential cross-section measurement for 2(a) $m_{b\ell}^{\min}$ for the inclusive region, 2(b) the lepton p_{T} for the inclusive region, 2(c) $m_{b\ell}^{\mathrm{selected}}$ for the W-hadronic region, 2(d) leading b-jet p_{T} for the W-hadronic region, 2(e) $m_{b\ell}^{\min}$ for the search-like region, and 2(f) the subleading b-jet p_{T} for the search-like region. The coloured bands represent each individual source of systematic uncertainty. The envelope of the coloured band represents the total systematic uncertainty, where each component is added in quadrature.

JHEP07(2026)028

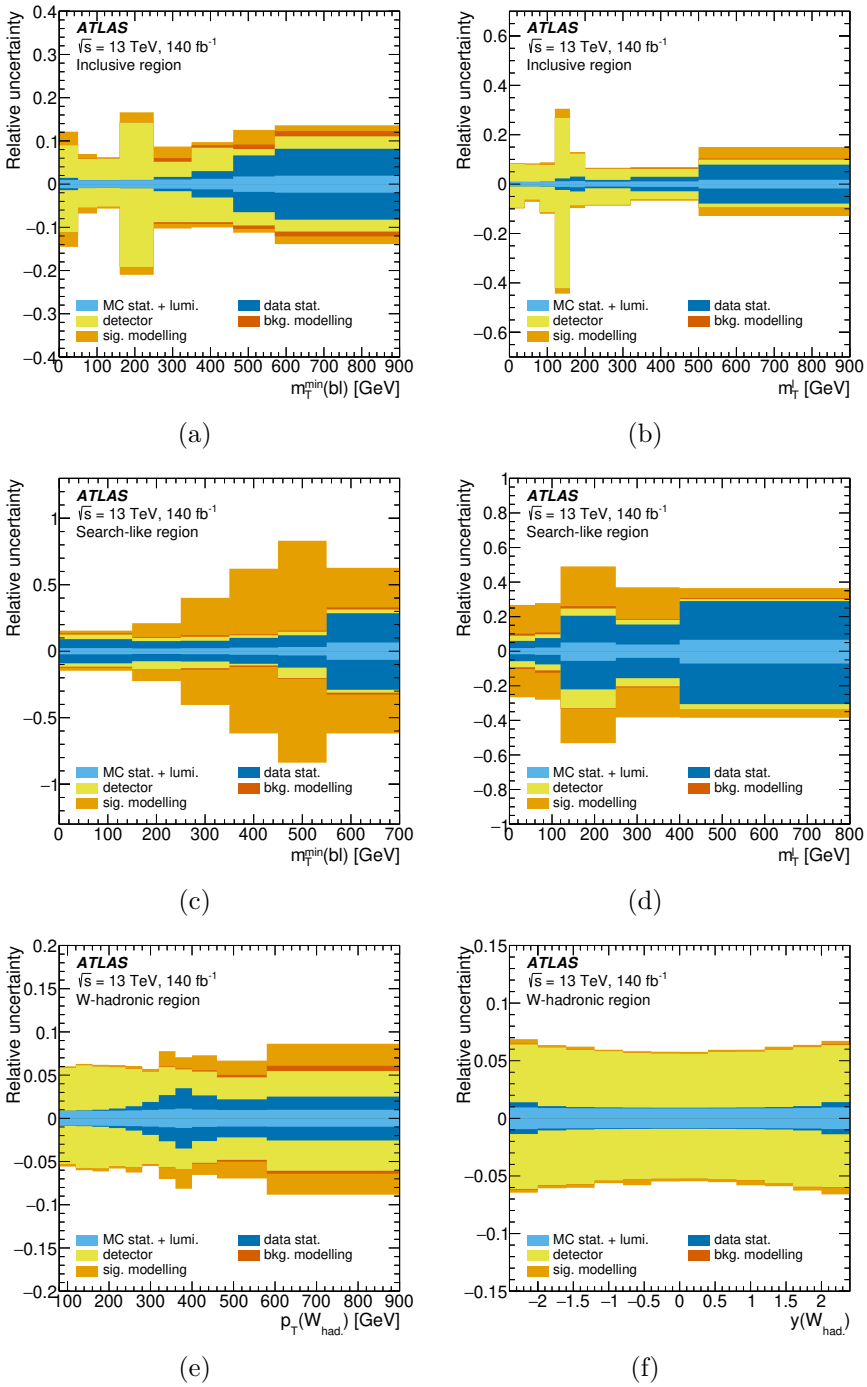

Figure 3. Breakdown of the systematic uncertainties in the unfolded differential cross-section measurement for 3(a) $m_{\mathrm{T}}^{\mathrm{min}}(b\ell)$ for the inclusive region, 3(b) the transverse mass of the lepton, m_{T}^{ℓ}, for the inclusive region, 3(c) $m_{\mathrm{T}}^{\mathrm{min}}(b\ell)$ for the search-like region, 3(d) the transverse mass of the lepton, m_{T}^{ℓ}, for the search-like region. 3(e) the hadronic W candidate transverse momentum for the W-hadronic region, and 3(f) the rapidity $y(W_{\mathrm{had.}})$ for the W-hadronic region. The coloured bands represent each individual source of systematic uncertainty. The envelope of the coloured band represents the total systematic uncertainty, where each component is added in quadrature.

JHEP07(2026)028

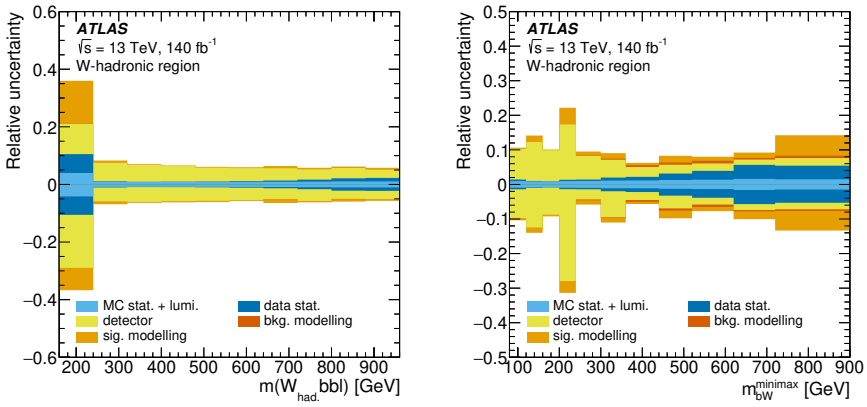

(a) (b)

Figure 4. Breakdown of the systematic uncertainties in the unfolded differential cross-section measurement for 4(a) the invariant mass of the $Wbb\ell$ system and 4(b) m_{bW}^{minimax} for the W-hadronic region. The coloured bands represent each individual source of systematic uncertainty. The envelope of the coloured band represents the total systematic uncertainty, where each component is added in quadrature.

6 Differential cross-section results

The differential cross-sections are measured in the three measurement regions (IR, WR and SLR) for a set of kinematic variables. The variables are chosen to probe the phase space where the interference effects between $t\bar{t}$ and tWb processes are most prominent. In the WR region, the observables are chosen to represent all relevant kinematic quantities of the $W^+W^-b\bar{b}$ process. The variables are defined at particle level and are unfolded from the detector level using the procedure described in the previous sections. Selected unfolded differential cross-section results as a function of $m_{b\ell}^{\text{min}}$ and characteristic kinematic observables for the three measurement regions are presented in figures 5 and 6, together with their detector-level distributions. Cross-sections in the IR and SLR as a function of the minimum transverse invariant mass between the $E_{\text{T}}^{\text{miss}}$, the lepton and the b-jets, $m_{\text{T}}^{\text{min}}(b\ell)$, and as a function of the transverse mass between the lepton and the $E_{\text{T}}^{\text{miss}}$, m_{T}^{ℓ}, are presented in figures 7 and 8.

The observable presenting the largest overall disagreement between the unfolded data and the simulation is $m_{b\ell}^{\text{min}}$. This observable is a proxy for the invariant mass of the leptonically decaying top quark and is particularly sensitive to effects related to processes with virtual top contributions in the $t\bar{t} + tWb$ production. Detector-level and particle-level distributions are presented in figure 5 for IR, WR and SLR selections. The ratio panel of each figure compares the reconstructed or unfolded data with the prediction from simulation. The full set of systematic uncertainties affecting the unfolded data, arising from detector and modelling sources, is presented as a shaded band. In the detector-level results, only the nominal simulation prediction is shown, which includes tWb processes simulated with the DR approach. Various unfolded $t\bar{t} + tW$ differential cross-section predictions are shown in the figures. The details of each prediction are given in section 2.3. They are: PH+PY8 DR (nominal prediction which includes the tWb process with DR treatment), PH+PY8 DS

JHEP07(2026)028

(prediction with the tWb process simulated with DS treatment), MiNNLOPS (using NNLO QCD description for the $t\bar{t}$ process), and PH+H7 DR (using Herwig as shower model).

The unfolded results in figure 5 show that none of the available predictions are well suited to simultaneously describe all the kinematic properties of the phase space under investigation. The various predictions exhibit a varying level of agreement in different observables and regions of the phase space. The disagreement is particularly enhanced in those parts of the kinematic phase space that are not dominated exclusively by doubly resonant top production, such as the tails of the $m_{b\ell}^{\min}$ observable for the IR and WR selection. Additionally, a discrepancy is observed across the entire phase space and with a more pronounced deviation in the SLR selection, because of the interference-dominated phase space selected by this region. This discrepancy is about one standard deviation if all systematic uncertainties are considered. The uncertainties in these selections are dominated by the modelling of the singly resonant top quark production (DS/DR uncertainty). Recent progress in event generators [42] could not yet be included in this work but will contribute to future studies of the modelling in this region. The PH+PY8 DR and PH+PY8 DS predictions enclose the unfolded data distributions, with discrepancies at the level of approximately one standard deviation. The unfolded results were found not to depend strongly on the choice of the nominal MC for unfolding. The largest impact of this choice is on the magnitude of the out-of-acceptance corrections used in the unfolding, affecting the absolute cross-section. As a result, when using the PH+PY8 DS predictions as the nominal MC for unfolding, the unfolded data moves away from the PH+PY8 DS prediction and closer to the PH+PY8 DR prediction.

The modelling of the lepton and the b-jets' momenta in the event crucially characterises the phase space kinematic properties, as they are directly linked to the modelling of the boost of the tWb or $t\bar{t}$ systems. In the three representative distributions shown for the three measurement regions in figure 6 it can be observed that no prediction is within one sigma of the unfolded data in the p_{T} spectrum of the lepton and the b-jets for highly energetic objects ($p_{\mathrm{T}} \gtrsim 200\,\mathrm{GeV}$). In the IR the discrepancy can be mitigated by $t\bar{t}$ higher order corrections (MiNNLOPS prediction) when doubly resonant top-quark production dominates in the phase space. This is however not true everywhere, as for example the MiNNLOPS prediction exhibits slightly worse modelling of the data than the nominal prediction for events with leading b-jet momenta $< 200\,\mathrm{GeV}$ in the WR selection (figure 6(d)) and the MiNNLOPS prediction is very similar to the nominal PH+PY8 DR prediction in the SLR selection (figure 6(f)). Observables related to the invariant mass of the leptonic W, like m_{T}^{ℓ}, which are instead independent of the boost of the tWb or $t\bar{t}$ system, are well modelled in the inclusive (IR) phase space (see figure 7). The $m_{\mathrm{T}}^{\min}(b\ell)$ observable is presented in figure 8 for IR and SLR selections, as a proxy for the transverse component of the invariant mass of the leptonically decaying top quark. Such an observable exploits the $E_{\mathrm{T}}^{\mathrm{miss}}$ information from the neutrino and is less sensitive to contaminations from the $W+$jets background in the interference-enhanced phase space of the regions and therefore overall affected by smaller systematic uncertainties. Despite the overlap between events in the tail of the $m_{b\ell}^{\min}$ and $m_{\mathrm{T}}^{\min}(b\ell)$ distributions in the inclusive region (figure 5(b) and figure 8(b)), the two distributions exhibit opposite trends in terms of agreement between unfolded data and predictions. The nominal PH+PY8 DR prediction models best the unfolded data for the $m_{b\ell}^{\min}$ observable. By contrast, the unfolded

JHEP07(2026)028

Inclusive region	PH+PY8 DR		PH+PY8 DS		PH+H7 DR		PH+PY8 DR (MiNNLOPS)	
Observable	χ^2 / NDF	p-value	χ^2 / NDF	p-value	χ^2 / NDF	p-value	χ^2 / NDF	p-value
$m_{b\ell}^{\min}$	7.27 / 9	0.61	10.15 / 9	0.34	6.00 / 9	0.74	23.72 / 9	<001
$p_{\mathrm{T}}(\ell)$	31.67 / 11	<001	19.70 / 11	0.05	13.11 / 11	0.29	7.54 / 11	0.75
m_{T}^{ℓ}	11.20 / 8	0.19	7.91 / 8	0.44	12.13 / 8	0.15	3.68 / 8	0.88
$m_{\mathrm{T}}^{\min}(b\ell)$	21.17 / 8	0.01	7.49 / 8	0.48	16.54 / 8	0.04	17.34 / 8	0.03

Table 4. χ^2 and p-values for each variable (rows) for each prediction (columns) for the absolute differential cross-section in the IR. All systematic uncertainties described in section 5 are included, with no additional uncertainties included on the predictions under test.

data for the $m_{\mathrm{T}}^{\min}(b\ell)$ observable is best described by the PH+PY8 DS prediction. In the SLR instead, the PH+PY8 DR and PH+PY8 DS predictions enclose the unfolded data distributions in similar ways across the $m_{b\ell}^{\min}$ and $m_{\mathrm{T}}^{\min}(b\ell)$ observables, with differences of about one standard deviation.

figure 9 presents the transverse momentum and rapidity of the hadronic W candidate in the WR selection. None of the prediction shows a good modelling of all the unfolded data, with the exception of the alternative PH+H7 DR model. The discrepancy between the predictions and the unfolded data is particularly enhanced for large W boson transverse momenta and central rapidity. The MiNNLOPS prediction exhibits particularly large disagreements, especially in the overall normalisation in this selection. The $m_{bW}^{\mathrm{minimax}}$ and $m(W_{\mathrm{had.}}bb\ell)$ observables are presented in figure 10. The former allows to probe the transition region of the relative abundance of singly versus doubly resonant top-quark processes (at the kinematic endpoint $m_{bW}^{\mathrm{minimax}} < \sqrt{m_t^2 - m_W^2}$). The latter allows to study the modelling of the entire $W^+W^-b\bar{b}$ system. Also in this case, the alternative PH+H7 DR model seems to provide the best description of the unfolded data, while PH+PY8 DS exhibits a worse modelling, especially in the region that is most sensitive to the interference effects between $t\bar{t}$ and tWb processes.

The compatibility of the unfolded distributions and the predictions is quantitatively assessed by calculating χ^2 values, as presented in tables 4 to 6. All uncertainties (statistical and systematic, both symmetrised) associated with the unfolded distributions, described in section 5 are included, taking into account their correlations, with no additional uncertainties included on the predictions under test.

The corresponding p-values are calculated inclusively for each distribution and reflect the various level of disagreement observed between the unfolded data and the simulation in the various observables and regions studied in this paper.

JHEP07(2026)028

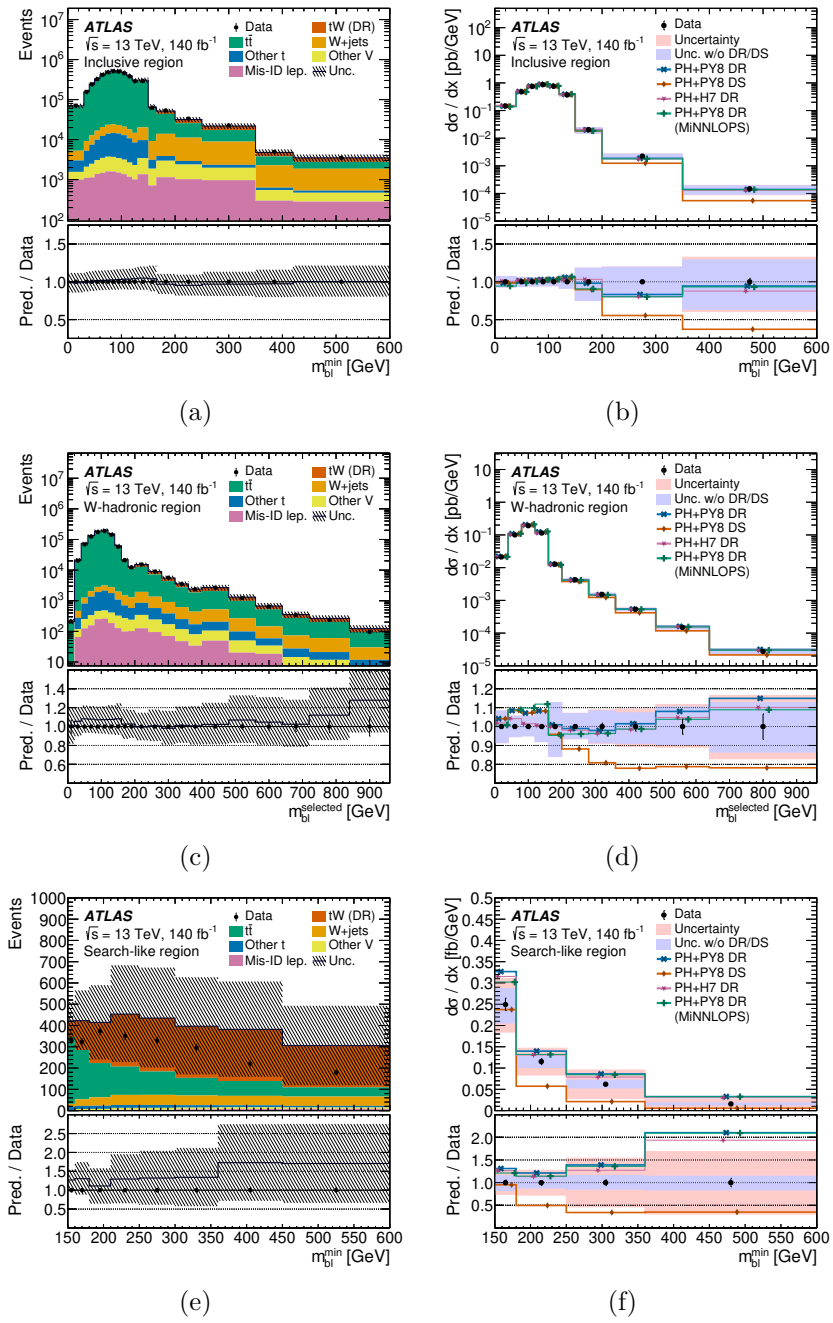

Figure 5. The (5(a), 5(c), 5(e)) detector-level distributions and (5(b), 5(d), 5(f)) unfolded differential cross-sections of the invariant mass between the lepton and the b-jets. The distributions are shown (5(a) and 5(b)) in the inclusive region, (5(c) and 5(d)) in the W-hadronic and (5(e) and 5(f)) in the search-like region. In the bottom panel, the reconstructed or unfolded data are compared with the predictions. The markers representing the different predictions are shifted from the bin centre to improve readability. The data statistical uncertainty is shown as error bars. The total systematic uncertainty is shown as a shaded band. An additional band including all uncertainties except the DS/DR interference modelling is shown for the unfolded results. The unfolded $t\bar{t} + tW$ predictions are shown: PH+PY8 DR (nominal using DR tW), PH+PY8 DS (using DS tW), MiNNLOPS (using NNLO QCD $t\bar{t}$), and PH+H7 DR (using Herwig shower model).

JHEP07(2026)028

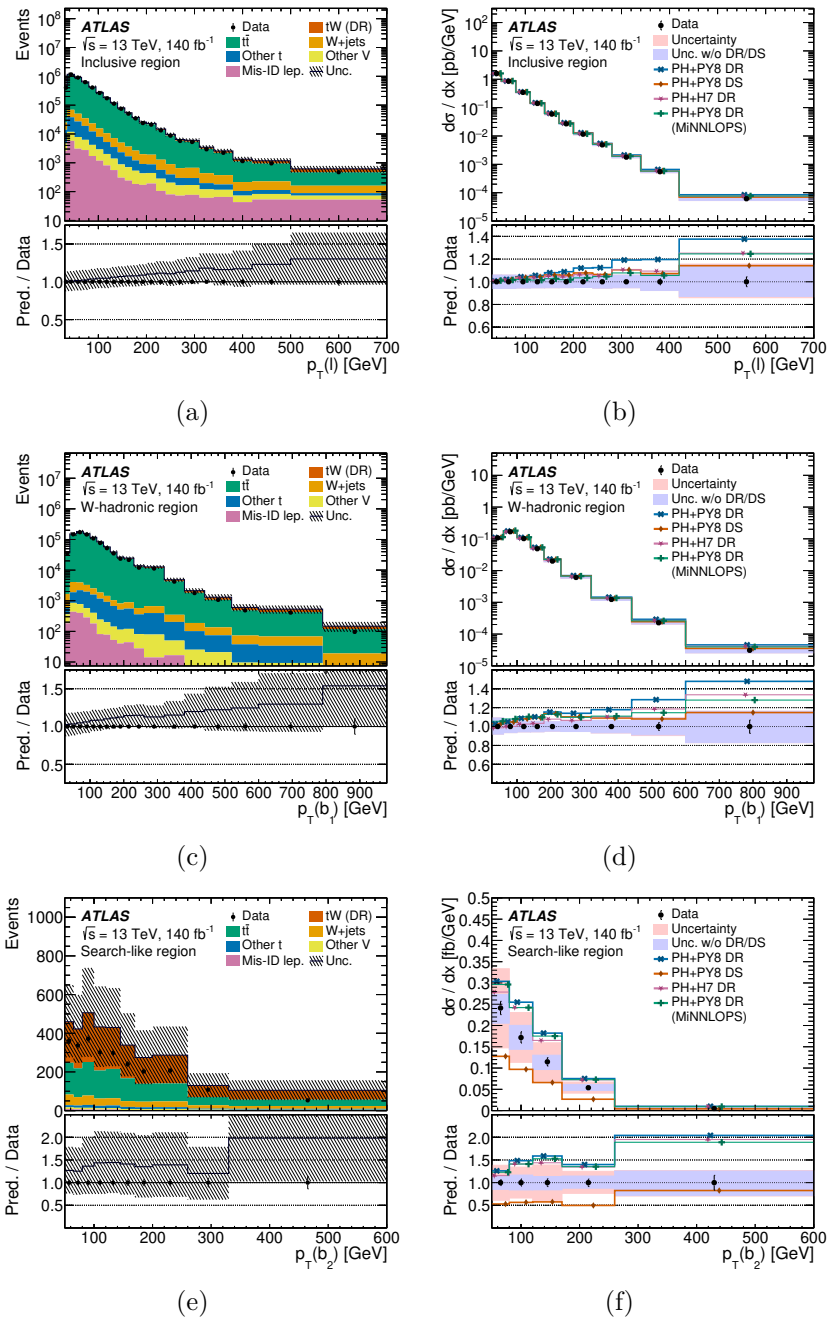

Figure 6. The (6(a), 6(c), 6(e)) detector-level distributions and (6(b), 6(d), 6(f)) unfolded differential cross-sections of (6(a) and 6(b)) the lepton p_{T} for the inclusive region, (6(c) and 6(d)) the leading b-jet p_{T} for the W-hadronic region and (6(e) and 6(f)) the subleading b-jet p_{T} for the search-like region. In the bottom panel, the reconstructed or unfolded data are compared with the predictions. The markers representing the different predictions are shifted from the bin centre to improve readability. The data statistical uncertainty is shown as error bars. The total systematic uncertainty is shown as a shaded band. An additional band including all uncertainties except the DS/DR interference modelling is shown for the unfolded results. The unfolded $t\bar{t} + tW$ predictions are shown: PH+PY8 DR (nominal using DR tW), PH+PY8 DS (using DS tW), MiNNLOPS (using NNLO QCD $t\bar{t}$), and PH+H7 DR (using Herwig shower model).

JHEP07(2026)028

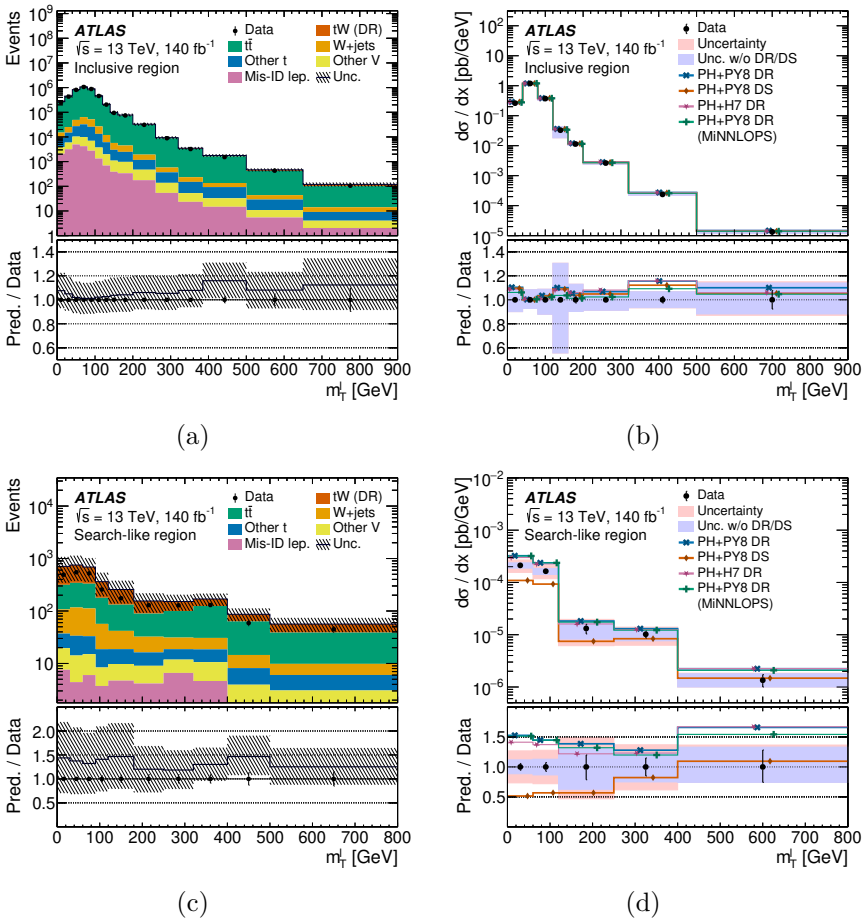

Figure 7. The (7(a), 7(c)) detector-level distributions and (7(b), 7(d)) unfolded differential cross-sections of the lepton transverse mass, m_{T}^{ℓ}. The distributions are shown (7(a) and 7(b)) in the inclusive region and (7(c) and 7(d)) in the search-like region. In the bottom panel, the reconstructed or unfolded data are compared with the predictions. The markers representing the different predictions are shifted from the bin centre to improve readability. The data statistical uncertainty is shown as error bars. The total systematic uncertainty is shown as a shaded band. An additional band including all uncertainties except the DS/DR interference modelling is shown for the unfolded results. The unfolded $t\bar{t} + tW$ predictions are shown: PH+PY8 DR (nominal using DR tW), PH+PY8 DS (using DS tW), MiNNLOPS (using NNLO QCD $t\bar{t}$), and PH+H7 DR (using Herwig shower model).

W-hadronic region	PH+PY8 DR		PH+PY8 DS		PH+H7 DR		PH+PY8 DR (MiNNLOPS)	
Observable	χ^2 / NDF	p-value	χ^2 / NDF	p-value	χ^2 / NDF	p-value	χ^2 / NDF	p-value
$m_{b\ell}^{\text{selected}}$	15.65 / 10	0.11	26.84 / 10	<001	6.95 / 10	0.73	30.53 / 10	<001
$p_{\mathrm{T}}(b_1)$	25.50 / 9	<001	20.56 / 9	0.01	10.19 / 9	0.34	13.62 / 9	0.14
$p_{\mathrm{T}}(W_{\text{had.}})$	20.79 / 11	0.04	14.32 / 11	0.22	10.99 / 11	0.44	7.28 / 11	0.78
$y(W_{\text{had.}})$	14.81 / 12	0.25	14.13 / 12	0.29	7.96 / 12	0.79	11.99 / 12	0.45
m_{bW}^{minimax}	22.37 / 11	0.02	44.24 / 11	<001	12.72 / 11	0.31	34.33 / 11	<001
$m(W_{\text{had.}}bb\ell)$	5.37 / 10	0.87	7.83 / 10	0.65	2.08 / 10	1.00	4.54 / 10	0.92

Table 5. χ^2 and p-values for each variable (rows) for each prediction (columns) for the absolute differential cross-section in the WR. All systematic uncertainties described in section 5 are included, with no additional uncertainties included on the predictions under test.

JHEP07(2026)028

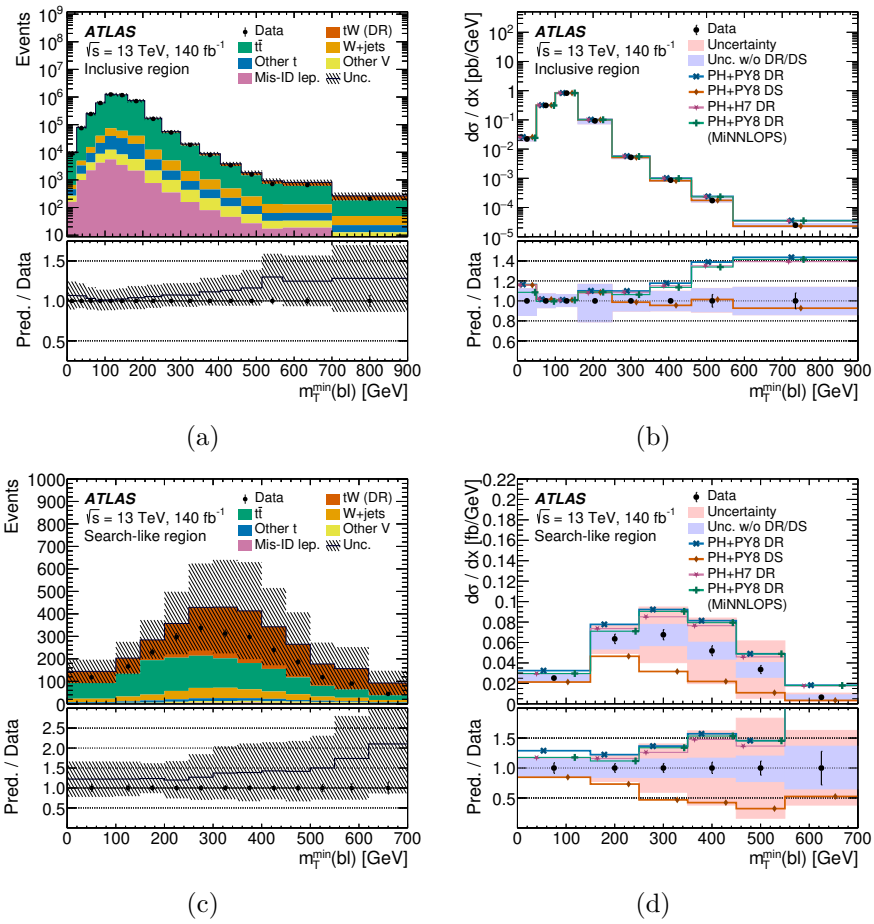

Figure 8. The (8(a), 8(c)) detector-level distributions and (8(b), 8(d)) unfolded differential cross-sections of the transverse component of the minimal transverse mass between the $E_{\mathrm{T}}^{\mathrm{miss}}$, the lepton and the b-jets in the event, $m_{\mathrm{T}}^{\mathrm{min}}(b\ell)$. The distributions are shown (8(a) and 8(b)) in the inclusive region and (8(c) and 8(d)) in the search-like region. In the bottom panel, the reconstructed or unfolded data are compared with the predictions. The markers representing the different predictions are shifted from the bin centre to improve readability. The data statistical uncertainty is shown as error bars. The total systematic uncertainty is shown as a shaded band. An additional band including all uncertainties except the DS/DR interference modelling is shown for the unfolded results. The unfolded $t\bar{t}+tW$ predictions are shown: PH+PY8 DR (nominal using DR tW), PH+PY8 DS (using DS tW), MiNNLOPS (using NNLO QCD $t\bar{t}$), and PH+H7 DR (using Herwig shower model).

Search-like region	PH+PY8 DR		PH+PY8 DS		PH+H7 DR		PH+PY8 DR (MiNNLOPS)	
Observable	χ^2 / NDF	p-value	χ^2 / NDF	p-value	χ^2 / NDF	p-value	χ^2 / NDF	p-value
$m_{b\ell}^{\mathrm{min}}$	9.57 / 4	0.05	7.57 / 4	0.11	9.21 / 4	0.06	10.73 / 4	0.03
$p_{\mathrm{T}}(b_2)$	17.11 / 5	<001	4.12 / 5	0.53	14.72 / 5	0.01	13.00 / 5	0.02
m_{T}^{ℓ}	0.41 / 4	0.98	4.24 / 4	0.38	0.30 / 4	0.99	0.58 / 4	0.96
$m_{\mathrm{T}}^{\mathrm{min}}(b\ell)$	11.54 / 6	0.07	2.76 / 6	0.84	10.01 / 6	0.12	10.45 / 6	0.11

Table 6. χ^2 and p-values for each variable (rows) for each prediction (columns) for the absolute differential cross-section in the SLR. All systematic uncertainties described in section 5 are included, with no additional uncertainties included on the predictions under test.

JHEP07(2026)028

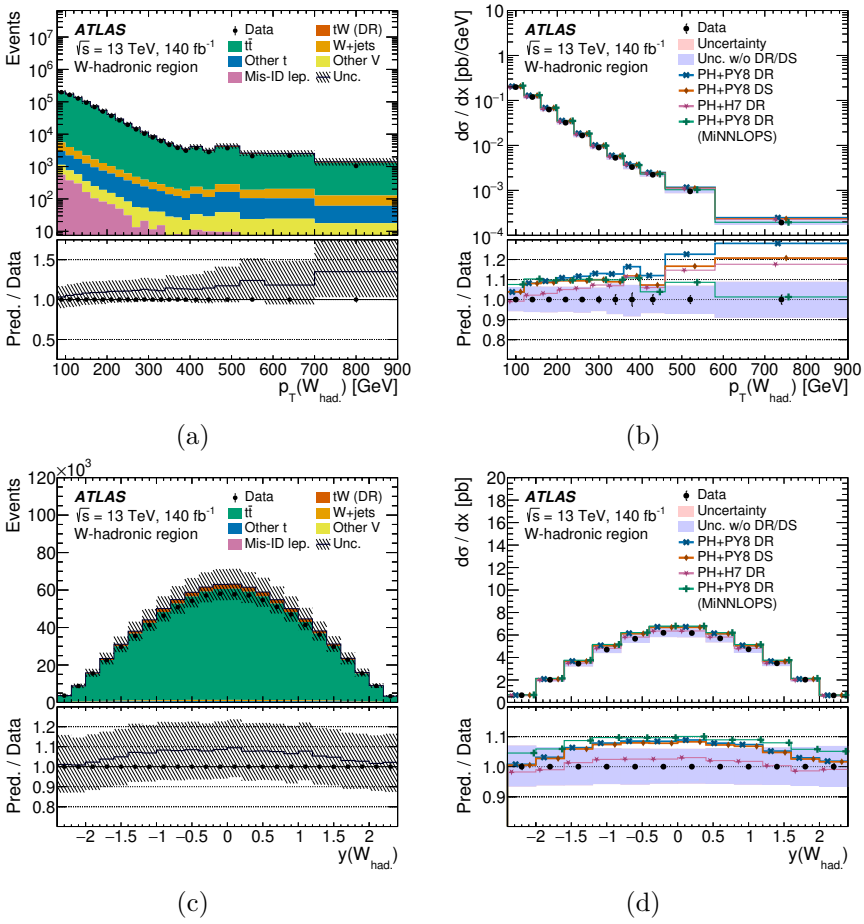

Figure 9. The (9(a), 9(c)) detector-level distributions and (9(b), 9(d)) unfolded differential cross-sections in the W-hadronic region. The distributions are shown for (9(a) and 9(b)) the hadronic W candidate momentum $p_{\mathrm{T}}(W_{\mathrm{had.}})$ and (9(c) and 9(d)) rapidity $y(W_{\mathrm{had.}})$. In the bottom panel, the reconstructed or unfolded data are compared with the predictions. The markers representing the different predictions are shifted from the bin centre to improve readability. The data statistical uncertainty is shown as error bars. The total systematic uncertainty is shown as a shaded band. An additional band including all uncertainties except the DS/DR interference modelling is shown for the unfolded results. The unfolded $t\bar{t} + tW$ predictions are shown: PH+PY8 DR (nominal using DR tW), PH+PY8 DS (using DS tW), MiNNLOPS (using NNLO QCD $t\bar{t}$), and PH+H7 DR (using Herwig shower model).

JHEP07(2026)028

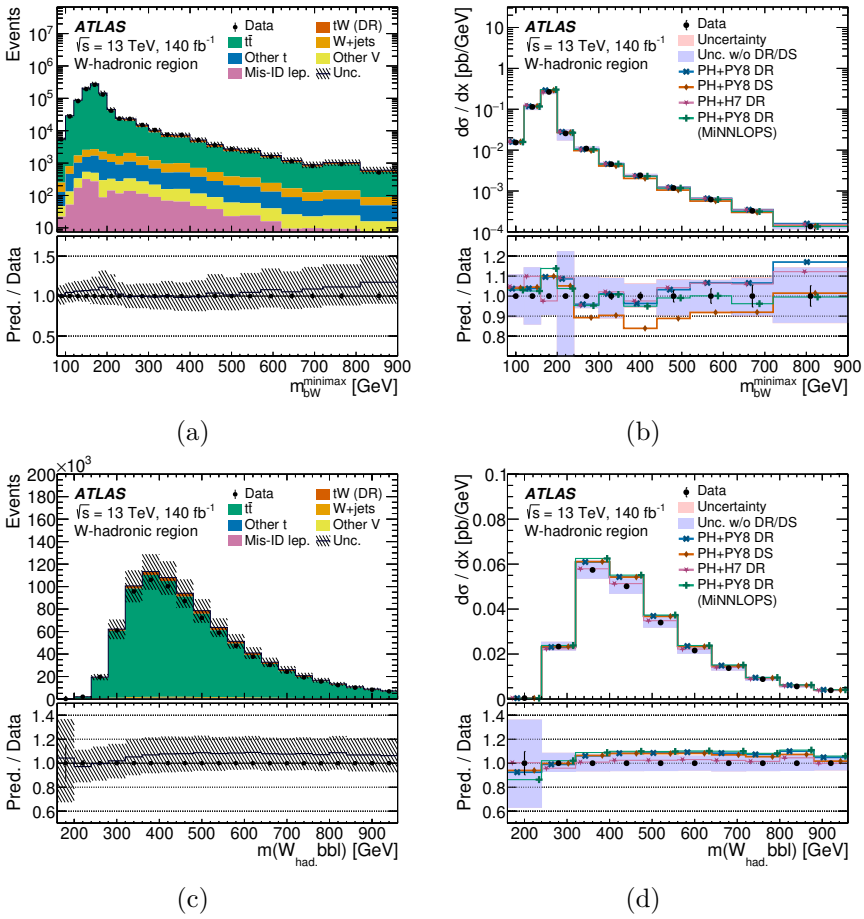

Figure 10. The (10(a), 10(c)) detector-level distributions and (10(b), 10(d)) unfolded differential cross-sections in the W-hadronic region. The distributions are shown for (10(a) and 10(b)) m_{bW}^{minimax} and (10(c) and 10(d)) the invariant mass of the $Wbb\ell$ system. In the bottom panel, the reconstructed or unfolded data are compared with the predictions. The markers representing the different predictions are shifted from the bin centre to improve readability. The data statistical uncertainty is shown as error bars. The total systematic uncertainty is shown as a shaded band. An additional band including all uncertainties except the DS/DR interference modelling is shown for the unfolded results. The unfolded $t\bar{t} + tW$ predictions are shown: PH+PY8 DR (nominal using DR tW), PH+PY8 DS (using DS tW), MiNNLOPS (using NNLO QCD $t\bar{t}$), and PH+H7 DR (using Herwig shower model).

JHEP07(2026)028

7 Conclusions

This paper presented a differential cross-section measurement of the coherent production of singly and doubly resonant top quarks in $W^+W^-b\bar{b}$ events using 140 fb^{-1} of pp collisions at a center-of-mass energy of 13 TeV, collected with the ATLAS experiment in the years from 2015 to 2018 during Run 2 of the LHC. Events requiring one lepton, three or four jets, of which at least two b-jets, were considered. Three measurement regions were defined: the inclusive region, the W-hadronic region, and the search-like region. The analysis selections, fiducial volumes and observables were optimised to isolate a phase space that probes the kinematic properties of the $t\bar{t} + tWb$ processes and their interference, actively suppressing the pure doubly resonant top-quark production.

Differential cross-sections obtained at particle-level from unfolded data are derived for various observables. The results are compared with predictions from several simulations, including the full set of uncertainties affecting the unfolded data and no additional systematic uncertainties in the predictions. The results indicate that none of the considered predictions can simultaneously accurately describe all observables in the fiducial phase-space. For most of the phase space, observables connected to the transverse momentum of the $tW/t\bar{t}$ system are described better by the MiNNLOPS prediction, which describes $t\bar{t}$ processes at NNLO QCD accuracy. These observations are compatible with the findings of other recent analyses targeting dileptonic final states [6, 46].

The measurement is limited by the uncertainties in the signal modelling, in particular those related to the treatment of the $t\bar{t} + tWb$ interference, uncertainties related to the calibration of jets and b-jets. When comparing with the measurement performed in the dilepton channel [46], a larger number of observables sensitive to interference effects has been studied. The overall findings are consistent, with discrepancies between data and predictions at the level of one standard deviation when the comparison between the DS and DR removal schemes is included as modelling uncertainty, increasing to two to three standard deviations when excluding it. Furthermore, statistical uncertainties in the single-lepton measurement are significant only in the tails of the distributions. This measurement represents the first differential cross-section measurement of the coherent production of singly and doubly resonant top-quarks in final states with exactly one lepton. The results of this study provide valuable insights into the modelling of the $W^+W^-b\bar{b}$ process in the fiducial phase-space and can be used to assess the modelling accuracy of future Monte Carlo simulation developments.

Acknowledgments

We thank CERN for the very successful operation of the LHC and its injectors, as well as the support staff at CERN and at our institutions worldwide without whom ATLAS could not be operated efficiently.

The crucial computing support from all WLCG partners is acknowledged gratefully, in particular from CERN, the ATLAS Tier-1 facilities at TRIUMF/SFU (Canada), NDGF (Denmark, Norway, Sweden), CC-IN2P3 (France), KIT/GridKA (Germany), INFN-CNAF (Italy), NL-T1 (Netherlands), PIC (Spain), RAL (U.K.) and BNL (U.S.A.), the Tier-2 facilities

JHEP07(2026)028

worldwide and large non-WLCG resource providers. Major contributors of computing resources are listed in ref. [130].

We gratefully acknowledge the support of ANPCyT, Argentina; YerPhI, Armenia; ARC, Australia; BMWFW and FWF, Austria; ANAS, Azerbaijan; CNPq and FAPESP, Brazil; NSERC, NRC and CFI, Canada; CERN; ANID, Chile; CAS, MOST and NSFC, China; Minciencias, Colombia; MEYS CR, Czech Republic; DNRF and DNSRC, Denmark; IN2P3-CNRS and CEA-DRF/IRFU, France; SRNSFG, Georgia; BMFTR, HGF and MPG, Germany; GSRI, Greece; RGC and Hong Kong SAR, China; ICHEP and Academy of Sciences and Humanities, Israel; INFN, Italy; MEXT and JSPS, Japan; CNRST, Morocco; NWO, Netherlands; RCN, Norway; MNiSW, Poland; FCT, Portugal; MNE/IFA, Romania; MSTDI, Serbia; MSSR, Slovakia; ARIS and MVZI, Slovenia; DSI/NRF, South Africa; MICIU/AEI, Spain; SRC and Wallenberg Foundation, Sweden; SERI, SNSF and Cantons of Bern and Geneva, Switzerland; NSTC, Taipei; TENMAK, Türkiye; STFC/UKRI, United Kingdom; DOE and NSF, United States of America.

Individual groups and members have received support from BCKDF, CANARIE, CRC and DRAC, Canada; CERN-CZ, FORTE and PRIMUS, Czech Republic; COST, ERC, ERDF, Horizon 2020, ICSC-NextGenerationEU and Marie Skłodowska-Curie Actions, European Union; Investissements d'Avenir Labex, Investissements d'Avenir Idex and ANR, France; DFG and AvH Foundation, Germany; Herakleitos, Thales and Aristeia programmes co-financed by EU-ESF and the Greek NSRF, Greece; BSF-NSF and MINERVA, Israel; NCN and NAWA, Poland; La Caixa Banking Foundation, CERCA and AGAUR programs from Generalitat de Catalunya and PROMETEO and GenT Programmes Generalitat Valenciana, Spain; Göran Gustafssons Stiftelse, Sweden; The Royal Society and Leverhulme Trust, United Kingdom; Eric and Wendy Schmidt Fund for Strategic Innovation, United States of America.

In addition, individual members wish to acknowledge support from CERN: European Organization for Nuclear Research (CERN DOCT); Chile: Agencia Nacional de Investigación y Desarrollo (ANID FONDECYT reg. 1230987, FONDECYT 1230812, FONDECYT 1240864, Fondecyt 3240661, Fondecyt Regular 1240721); China: Chinese Ministry of Science and Technology (MOST-2023YFA1605700, MOST-2023YFA1609300), National Natural Science Foundation of China (NSFC — 12175119, NSFC 12275265); Czech Republic: Czech Science Foundation (GACR — 24-11373S), Ministry of Education Youth and Sports (ERC-CZ-LL2327, FORTE CZ.02.01.01/00/22_008/0004632), PRIMUS Research Programme (PRIMUS/21/SCI/017); EU: H2020 European Research Council (ERC — 101002463); European Union: European Research Council (BARD No. 101116429, ERC — 948254, ERC 101089007), European Regional Development Fund (HE COFUND GA No.101081355, ERDF), European Union, Future Artificial Intelligence Research (FAIR-NextGenerationEU PE00000013), Italian Center for High Performance Computing, Big Data and Quantum Computing (ICSC, NextGenerationEU), Marie Sklodowska-Curie Actions (ERC Horizon-2020, GA 956086, GAP-101168829); France: Agence Nationale de la Recherche (ANR-21-CE31-0013, ANR-21-CE31-0022, ANR-22-EDIR-0002, ANR-24-CE31-0504-01); Germany: Deutsche Forschungsgemeinschaft (DFG — 469666862, DFG — CR 312/5-2); China: Research Grants Council (GRF); Italy: Istituto Nazionale di Fisica Nucleare (ICSC, NextGenerationEU), Ministero dell'Università e della

JHEP07(2026)028

Ricerca (NextGenEU 153D23001490006 M4C2.1.1, NextGenEU I53D23000820006 M4C2.1.1, NextGenEU I53D23001490006 M4C2.1.1, SOE2024_0000023); Japan: Japan Society for the Promotion of Science (JSPS KAKENHI JP25H0063, JSPS KAKENHI JP22H01227, JSPS KAKENHI JP22H04944, JSPS KAKENHI JP22KK0227, JSPS KAKENHI JP24K23939, JSPS KAKENHI JP24KK0251, JSPS KAKENHI JP25H00650, JSPS KAKENHI JP25H01291, JSPS KAKENHI JP25K01011, JSPS KAKENHI JP25K01023); Norway: Research Council of Norway (RCN-314472); Poland: Ministry of Science and Higher Education (IDUB AGH, POB8, D4 no 9722), Polish National Science Centre (NCN 2021/42/E/ST2/00350, NCN OPUS 2023/51/B/ST2/02507, NCN OPUS nr 2022/47/B/ST2/03059, NCN UMO-2019/34/E/ST2/00393, UMO-2022/47/O/ST2/00148, UMO-2023/49/B/ST2/04085, UMO-2023/51/B/ST2/00920, UMO-2024/53/N/ST2/00869); Portugal: Foundation for Science and Technology (FCT); Spain: Agència de Gestió d'Ajuts Universitaris i de Recerca. (AGAUR — 2023 BP 00141), Generalitat Valenciana (ASFAE/2022/008), Ministry of Science and Innovation (MCIN & NextGenEU PCI2022-135018-2, MICIN & FEDER PID2021-125273NB, RYC2019-028510-I, RYC2020-030254-I, RYC2021-031273-I, RYC2022-038164-I), Ministerio de Ciencia, Innovación y Universidades/Agencia Estatal de Investigación (EU NextGenerationEU (PRTR-C17.I1), PID2022-142604OB-C22); Sweden: Carl Trygger Foundation (Carl Trygger Foundation CTS 22:2312), Swedish Research Council (Swedish Research Council 2023-04654, VR 2021-03651, VR 2022-03845, VR 2022-04683, VR 2023-03403, VR 2024-05451), Knut and Alice Wallenberg Foundation (KAW 2018.0458, KAW 2022.0358, KAW 2023.0366); Switzerland: Swiss National Science Foundation (SNSF — PCEFP2_194658); United Kingdom: Royal Society (NIF-R1-231091); United States of America: U.S. Department of Energy (ECA DE-AC02-76SF00515), Neubauer Family Foundation.

Data Availability Statement. This article has no associated data or the data will not be deposited.

Code Availability Statement. This article has no associated code or the code will not be deposited.

Open Access. This article is distributed under the terms of the Creative Commons Attribution License (CC-BY4.0), which permits any use, distribution and reproduction in any medium, provided the original author(s) and source are credited.

References

[1] L. Evans and P. Bryant, *LHC machine*, 2008 *JINST* **3** S08001 [INSPIRE].

[2] ATLAS collaboration, *Measurements of top-quark pair differential cross-sections in the lepton+jets channel in pp collisions at $\sqrt{s} = 13$ TeV using the ATLAS detector*, *JHEP* **11** (2017) 191 [arXiv:1708.00727] [INSPIRE].

[3] ATLAS collaboration, *Measurements of top-quark pair differential and double-differential cross-sections in the ℓ+jets channel with pp collisions at $\sqrt{s} = 13$ TeV using the ATLAS detector*, *Eur. Phys. J. C* **79** (2019) 1028 [*Erratum ibid.* **80** (2020) 1092] [arXiv:1908.07305] [INSPIRE].

JHEP07(2026)028

[4] ATLAS collaboration, *Measurement of jet substructure in boosted $t\bar{t}$ events with the ATLAS detector using 140 fb^{-1} of 13 TeV pp collisions*, Phys. Rev. D **109** (2024) 112016 [arXiv:2312.03797] [INSPIRE].

[5] ATLAS collaboration, *Measurement of differential cross-sections in $t\bar{t}$ and $t\bar{t}$+jets production in the lepton+jets final state in pp collisions at $\sqrt{s} = 13$ TeV using 140 fb^{-1} of ATLAS data*, JHEP **08** (2024) 182 [arXiv:2406.19701] [INSPIRE].

[6] ATLAS collaboration, *Precise measurement of the $t\bar{t}$ production cross-section and lepton differential distributions in $e\mu$ dilepton events from $\sqrt{s} = 13$ TeV pp collisions with the ATLAS detector*, Eur. Phys. J. C **86** (2026) 470 [arXiv:2509.15066] [INSPIRE].

[7] CMS collaboration, *Measurement of normalized differential $t\bar{t}$ cross sections in the dilepton channel from pp collisions at $\sqrt{s} = 13$ TeV*, JHEP **04** (2018) 060 [arXiv:1708.07638] [INSPIRE].

[8] CMS collaboration, *Measurements of differential cross sections of top quark pair production as a function of kinematic event variables in proton-proton collisions at $\sqrt{s} = 13$ TeV*, JHEP **06** (2018) 002 [arXiv:1803.03991] [INSPIRE].

[9] CMS collaboration, *Measurement of differential cross sections for the production of top quark pairs and of additional jets in lepton+jets events from pp collisions at $\sqrt{s} = 13$ TeV*, Phys. Rev. D **97** (2018) 112003 [arXiv:1803.08856] [INSPIRE].

[10] CMS collaboration, *Measurement of $t\bar{t}$ normalised multi-differential cross sections in pp collisions at $\sqrt{s} = 13$ TeV, and simultaneous determination of the strong coupling strength, top quark pole mass, and parton distribution functions*, Eur. Phys. J. C **80** (2020) 658 [arXiv:1904.05237] [INSPIRE].

[11] M. Czakon and A. Mitov, *Top++: a program for the calculation of the top-pair cross-section at hadron colliders*, Comput. Phys. Commun. **185** (2014) 2930 [arXiv:1112.5675] [INSPIRE].

[12] M. Czakon, D. Heymes and A. Mitov, *High-precision differential predictions for top-quark pairs at the LHC*, Phys. Rev. Lett. **116** (2016) 082003 [arXiv:1511.00549] [INSPIRE].

[13] M. Czakon, D. Heymes and A. Mitov, *Dynamical scales for multi-TeV top-pair production at the LHC*, JHEP **04** (2017) 071 [arXiv:1606.03350] [INSPIRE].

[14] ATLAS collaboration, *Measurement of the cross-section for producing a W boson in association with a single top quark in pp collisions at $\sqrt{s} = 13$ TeV with ATLAS*, JHEP **01** (2018) 063 [arXiv:1612.07231] [INSPIRE].

[15] ATLAS collaboration, *Measurement of differential cross-sections of a single top quark produced in association with a W boson at $\sqrt{s} = 13$ TeV with ATLAS*, Eur. Phys. J. C **78** (2018) 186 [arXiv:1712.01602] [INSPIRE].

[16] ATLAS collaboration, *Measurement of single top-quark production in association with a W boson in pp collisions at $\sqrt{s} = 13$ TeV with the ATLAS detector*, Phys. Rev. D **110** (2024) 072010 [arXiv:2407.15594] [INSPIRE].

[17] CMS collaboration, *Measurement of the production cross section for single top quarks in association with W bosons in proton-proton collisions at $\sqrt{s} = 13$ TeV*, JHEP **10** (2018) 117 [arXiv:1805.07399] [INSPIRE].

[18] CMS collaboration, *Observation of tW production in the single-lepton channel in pp collisions at $\sqrt{s} = 13$ TeV*, JHEP **11** (2021) 111 [arXiv:2109.01706] [INSPIRE].

JHEP07(2026)028

[19] CMS collaboration, *Measurement of inclusive and differential cross sections for single top quark production in association with a W boson in proton-proton collisions at* $\sqrt{s} = 13$ *TeV*, *JHEP* **07** (2023) 046 [arXiv:2208.00924] [INSPIRE].

[20] CMS collaboration, *Measurement of differential cross sections and charge ratios for t-channel single top quark production in proton–proton collisions at* $\sqrt{s} = 13$ *TeV*, *Eur. Phys. J. C* **80** (2020) 370 [arXiv:1907.08330] [INSPIRE].

[21] C.D. White, S. Frixione, E. Laenen and F. Maltoni, *Isolating* Wt *production at the LHC*, *JHEP* **11** (2009) 074 [arXiv:0908.0631] [INSPIRE].

[22] S. Frixione et al., *Single-top hadroproduction in association with a W boson*, *JHEP* **07** (2008) 029 [arXiv:0805.3067] [INSPIRE].

[23] W. Hollik, J.M. Lindert and D. Pagani, *NLO corrections to squark-squark production and decay at the LHC*, *JHEP* **03** (2013) 139 [arXiv:1207.1071] [INSPIRE].

[24] F. Demartin et al., *tWH associated production at the LHC*, *Eur. Phys. J. C* **77** (2017) 34 [arXiv:1607.05862] [INSPIRE].

[25] ATLAS collaboration, *Studies on top-quark Monte Carlo modelling for Top2016*, ATL-PHYS-PUB-2016-020 (2016) [INSPIRE].

[26] ATLAS collaboration, *Inclusive and differential cross-sections for dilepton* $t\bar{t}$ *production measured in* $\sqrt{s} = 13$ *TeV pp collisions with the ATLAS detector*, *JHEP* **07** (2023) 141 [arXiv:2303.15340] [INSPIRE].

[27] ATLAS collaboration, *Evidence for the charge asymmetry in* $pp \to t\bar{t}$ *production at* $\sqrt{s} = 13$ *TeV with the ATLAS detector*, *JHEP* **08** (2023) 077 [arXiv:2208.12095] [INSPIRE].

[28] ATLAS collaboration, *Measurement of double-differential charged-current Drell-Yan cross-sections at high transverse masses in pp collisions at* $\sqrt{s} = 13$ *TeV with the ATLAS detector*, *JHEP* **07** (2025) 026 [arXiv:2502.21088] [INSPIRE].

[29] ATLAS collaboration, *Search for direct top squark pair production in final states with two leptons in* $\sqrt{s} = 13$ *TeV pp collisions with the ATLAS detector*, *Eur. Phys. J. C* **77** (2017) 898 [arXiv:1708.03247] [INSPIRE].

[30] ATLAS collaboration, *ATLAS run 1 searches for direct pair production of third-generation squarks at the Large Hadron Collider*, *Eur. Phys. J. C* **75** (2015) 510 [*Erratum ibid.* **76** (2016) 153] [arXiv:1506.08616] [INSPIRE].

[31] ATLAS collaboration, *Search for bottom squark pair production in proton–proton collisions at* $\sqrt{s} = 13$ *TeV with the ATLAS detector*, *Eur. Phys. J. C* **76** (2016) 547 [arXiv:1606.08772] [INSPIRE].

[32] ATLAS collaboration, *Search for gluinos in events with an isolated lepton, jets and missing transverse momentum at* $\sqrt{s} = 13$ *TeV with the ATLAS detector*, *Eur. Phys. J. C* **76** (2016) 565 [arXiv:1605.04285] [INSPIRE].

[33] ATLAS collaboration, *Search for top-squark pair production in final states with one lepton, jets, and missing transverse momentum using* $36\,fb^{-1}$ *of* $\sqrt{s} = 13$ *TeV pp collision data with the ATLAS detector*, *JHEP* **06** (2018) 108 [arXiv:1711.11520] [INSPIRE].

[34] ATLAS collaboration, *Search for a scalar partner of the top quark in the all-hadronic* $t\bar{t}$ *plus missing transverse momentum final state at* $\sqrt{s} = 13$ *TeV with the ATLAS detector*, *Eur. Phys. J. C* **80** (2020) 737 [arXiv:2004.14060] [INSPIRE].

JHEP07(2026)028

[35] ATLAS collaboration, *Search for new phenomena in pp collisions in final states with tau leptons, b-jets, and missing transverse momentum with the ATLAS detector*, *Phys. Rev. D* **104** (2021) 112005 [arXiv:2108.07665] [INSPIRE].

[36] ATLAS collaboration, *Search for pair-produced scalar and vector leptoquarks decaying into third-generation quarks and first- or second-generation leptons in pp collisions with the ATLAS detector*, *JHEP* **06** (2023) 188 [arXiv:2210.04517] [INSPIRE].

[37] ATLAS collaboration, *Search for pair-produced vector-like top and bottom partners in events with large missing transverse momentum in pp collisions with the ATLAS detector*, *Eur. Phys. J. C* **83** (2023) 719 [arXiv:2212.05263] [INSPIRE].

[38] ATLAS collaboration, *Search for excited τ-leptons and leptoquarks in the final state with τ-leptons and jets in pp collisions at $\sqrt{s} = 13$ TeV with the ATLAS detector*, *JHEP* **06** (2023) 199 [arXiv:2303.09444] [INSPIRE].

[39] ATLAS collaboration, *Search for supersymmetry in final states with missing transverse momentum and three or more b-jets in 139 fb^{-1} of proton–proton collisions at $\sqrt{s} = 13$ TeV with the ATLAS detector*, *Eur. Phys. J. C* **83** (2023) 561 [arXiv:2211.08028] [INSPIRE].

[40] A. Denner, S. Dittmaier, S. Kallweit and S. Pozzorini, *NLO QCD corrections to $WWbb$ production at hadron colliders*, *Phys. Rev. Lett.* **106** (2011) 052001 [arXiv:1012.3975] [INSPIRE].

[41] T. Ježo et al., *An NLO+PS generator for $t\bar{t}$ and Wt production and decay including non-resonant and interference effects*, *Eur. Phys. J. C* **76** (2016) 691 [arXiv:1607.04538] [INSPIRE].

[42] T. Ježo, J.M. Lindert and S. Pozzorini, *Resonance-aware NLOPS matching for off-shell $t\bar{t} + tW$ production with semileptonic decays*, *JHEP* **10** (2023) 008 [arXiv:2307.15653] [INSPIRE].

[43] A. Denner and M. Pellen, *Off-shell production of top-antitop pairs in the lepton+jets channel at NLO QCD*, *JHEP* **02** (2018) 013 [arXiv:1711.10359] [INSPIRE].

[44] L. Mans, D. Stremmer and M. Worek, *Complete NLO corrections to off-shell $t\bar{t}$ production in the $\ell + j$ decay channel*, arXiv:2512.18391 [INSPIRE].

[45] ATLAS collaboration, *Probing the quantum interference between singly and doubly resonant top-quark production in pp collisions at $\sqrt{s} = 13$ TeV with the ATLAS detector*, *Phys. Rev. Lett.* **121** (2018) 152002 [arXiv:1806.04667] [INSPIRE].

[46] ATLAS collaboration, *Measurements of differential cross-sections of $WbWb$ production in the dilepton channel in pp collisions at $\sqrt{s} = 13$ TeV using the ATLAS detector*, *JHEP* **02** (2026) 153 [arXiv:2506.14700] [INSPIRE].

[47] ATLAS collaboration, *Search for top squarks in final states with one isolated lepton, jets, and missing transverse momentum in $\sqrt{s} = 13$ TeV pp collisions with the ATLAS detector*, *Phys. Rev. D* **94** (2016) 052009 [arXiv:1606.03903] [INSPIRE].

[48] ATLAS collaboration, *Search for a scalar partner of the top quark in the jets plus missing transverse momentum final state at $\sqrt{s} = 13$ TeV with the ATLAS detector*, *JHEP* **12** (2017) 085 [arXiv:1709.04183] [INSPIRE].

[49] ATLAS collaboration, *The ATLAS experiment at the CERN Large Hadron Collider*, 2008 *JINST* **3** S08003 [INSPIRE].

[50] G. Avoni et al., *The new LUCID-2 detector for luminosity measurement and monitoring in ATLAS*, 2018 *JINST* **13** P07017 [INSPIRE].

JHEP07(2026)028

[51] ATLAS collaboration, *Performance of the ATLAS trigger system in 2015*, *Eur. Phys. J. C* **77** (2017) 317 [arXiv:1611.09661] [INSPIRE].

[52] ATLAS collaboration, *Software and computing for run 3 of the ATLAS experiment at the LHC*, *Eur. Phys. J. C* **85** (2025) 234 [arXiv:2404.06335] [INSPIRE].

[53] ATLAS collaboration, *Electron and photon performance measurements with the ATLAS detector using the 2015–2017 LHC proton-proton collision data*, 2019 *JINST* **14** P12006 [arXiv:1908.00005] [INSPIRE].

[54] ATLAS collaboration, *Muon reconstruction and identification efficiency in ATLAS using the full Run 2 pp collision data set at* $\sqrt{s} = 13$ *TeV*, *Eur. Phys. J. C* **81** (2021) 578 [arXiv:2012.00578] [INSPIRE].

[55] ATLAS collaboration, *Evidence for the associated production of the Higgs boson and a top quark pair with the ATLAS detector*, *Phys. Rev. D* **97** (2018) 072003 [arXiv:1712.08891] [INSPIRE].

[56] ATLAS collaboration, *Measurement of the track impact parameters resolution with the ATLAS experiment at LHC using 2016–2018 data*, *Nuovo Cim. C* **44** (2021) 55 [INSPIRE].

[57] ATLAS collaboration, *Electron and photon energy calibration with the ATLAS detector using LHC run 2 data*, 2024 *JINST* **19** P02009 [arXiv:2309.05471] [INSPIRE].

[58] ATLAS collaboration, *Studies of the muon momentum calibration and performance of the ATLAS detector with pp collisions at* $\sqrt{s} = 13$ *TeV*, *Eur. Phys. J. C* **83** (2023) 686 [arXiv:2212.07338] [INSPIRE].

[59] M. Cacciari, G.P. Salam and G. Soyez, *The anti-*k_t *jet clustering algorithm*, *JHEP* **04** (2008) 063 [arXiv:0802.1189] [INSPIRE].

[60] M. Cacciari, G.P. Salam and G. Soyez, *FastJet user manual*, *Eur. Phys. J. C* **72** (2012) 1896 [arXiv:1111.6097] [INSPIRE].

[61] ATLAS collaboration, *Jet reconstruction and performance using particle flow with the ATLAS detector*, *Eur. Phys. J. C* **77** (2017) 466 [arXiv:1703.10485] [INSPIRE].

[62] ATLAS collaboration, *Topological cell clustering in the ATLAS calorimeters and its performance in LHC run 1*, *Eur. Phys. J. C* **77** (2017) 490 [arXiv:1603.02934] [INSPIRE].

[63] ATLAS collaboration, *Performance of pile-up mitigation techniques for jets in pp collisions at* $\sqrt{s} = 8$ *TeV using the ATLAS detector*, *Eur. Phys. J. C* **76** (2016) 581 [arXiv:1510.03823] [INSPIRE].

[64] ATLAS collaboration, *Jet energy scale and resolution measured in proton–proton collisions at* $\sqrt{s} = 13$ *TeV with the ATLAS detector*, *Eur. Phys. J. C* **81** (2021) 689 [arXiv:2007.02645] [INSPIRE].

[65] ATLAS collaboration, *ATLAS flavour-tagging algorithms for the LHC run 2 pp collision dataset*, *Eur. Phys. J. C* **83** (2023) 681 [arXiv:2211.16345] [INSPIRE].

[66] ATLAS collaboration, *The performance of missing transverse momentum reconstruction and its significance with the ATLAS detector using 140* fb^{-1} *of* $\sqrt{s} = 13$ *TeV pp collisions*, *Eur. Phys. J. C* **85** (2025) 606 [arXiv:2402.05858] [INSPIRE].

[67] ATLAS collaboration, *The ATLAS simulation infrastructure*, *Eur. Phys. J. C* **70** (2010) 823 [arXiv:1005.4568] [INSPIRE].

[68] GEANT4 collaboration, *GEANT4 — a simulation toolkit*, *Nucl. Instrum. Meth. A* **506** (2003) 250 [INSPIRE].

JHEP07(2026)028

[69] ATLAS collaboration, *Study of the double Higgs production channel $H(\to b\bar{b})H(\to \gamma\gamma)$ with the ATLAS experiment at the HL-LHC*, ATL-PHYS-PUB-2017-001 (2017) [INSPIRE].

[70] ATLAS collaboration, *Multi-boson simulation for 13 TeV ATLAS analyses*, ATL-PHYS-PUB-2017-005 (2017) [INSPIRE].

[71] ATLAS collaboration, *Improvements in $t\bar{t}$ modelling using NLO+PS Monte Carlo generators for run 2*, ATL-PHYS-PUB-2018-009 (2018) [INSPIRE].

[72] D.J. Lange, *The EvtGen particle decay simulation package*, Nucl. Instrum. Meth. A **462** (2001) 152 [INSPIRE].

[73] T. Sjöstrand, S. Mrenna and P.Z. Skands, *A brief introduction to PYTHIA 8.1*, Comput. Phys. Commun. **178** (2008) 852 [arXiv:0710.3820] [INSPIRE].

[74] R.D. Ball et al., *Parton distributions with LHC data*, Nucl. Phys. B **867** (2013) 244 [arXiv:1207.1303] [INSPIRE].

[75] ATLAS collaboration, *The Pythia 8 A3 tune description of ATLAS minimum bias and inelastic measurements incorporating the Donnachie-Landshoff diffractive model*, ATL-PHYS-PUB-2016-017 (2016) [INSPIRE].

[76] ATLAS collaboration, *Measurement of the inelastic proton-proton cross section at $\sqrt{s} = 13$ TeV with the ATLAS detector at the LHC*, Phys. Rev. Lett. **117** (2016) 182002 [arXiv:1606.02625] [INSPIRE].

[77] S. Frixione, P. Nason and G. Ridolfi, *A positive-weight next-to-leading-order Monte Carlo for heavy flavour hadroproduction*, JHEP **09** (2007) 126 [arXiv:0707.3088] [INSPIRE].

[78] P. Nason, *A new method for combining NLO QCD with shower Monte Carlo algorithms*, JHEP **11** (2004) 040 [hep-ph/0409146] [INSPIRE].

[79] S. Frixione, P. Nason and C. Oleari, *Matching NLO QCD computations with parton shower simulations: the POWHEG method*, JHEP **11** (2007) 070 [arXiv:0709.2092] [INSPIRE].

[80] S. Alioli, P. Nason, C. Oleari and E. Re, *A general framework for implementing NLO calculations in shower Monte Carlo programs: the POWHEG BOX*, JHEP **06** (2010) 043 [arXiv:1002.2581] [INSPIRE].

[81] T. Sjöstrand et al., *An introduction to PYTHIA 8.2*, Comput. Phys. Commun. **191** (2015) 159 [arXiv:1410.3012] [INSPIRE].

[82] M. Beneke, P. Falgari, S. Klein and C. Schwinn, *Hadronic top-quark pair production with NNLL threshold resummation*, Nucl. Phys. B **855** (2012) 695 [arXiv:1109.1536] [INSPIRE].

[83] M. Cacciari et al., *Top-pair production at hadron colliders with next-to-next-to-leading logarithmic soft-gluon resummation*, Phys. Lett. B **710** (2012) 612 [arXiv:1111.5869] [INSPIRE].

[84] P. Bärnreuther, M. Czakon and A. Mitov, *Percent level precision physics at the Tevatron: first genuine NNLO QCD corrections to $q\bar{q} \to t\bar{t} + X$*, Phys. Rev. Lett. **109** (2012) 132001 [arXiv:1204.5201] [INSPIRE].

[85] M. Czakon and A. Mitov, *NNLO corrections to top-pair production at hadron colliders: the all-fermionic scattering channels*, JHEP **12** (2012) 054 [arXiv:1207.0236] [INSPIRE].

[86] M. Czakon and A. Mitov, *NNLO corrections to top pair production at hadron colliders: the quark-gluon reaction*, JHEP **01** (2013) 080 [arXiv:1210.6832] [INSPIRE].

[87] M. Czakon, P. Fiedler and A. Mitov, *Total top-quark pair-production cross section at hadron colliders through $O(\alpha_S^4)$*, Phys. Rev. Lett. **110** (2013) 252004 [arXiv:1303.6254] [INSPIRE].

JHEP07(2026)028

[88] N. Kidonakis and N. Yamanaka, *Higher-order corrections for tW production at high-energy hadron colliders*, *JHEP* **05** (2021) 278 [arXiv:2102.11300] [INSPIRE].

[89] N. Kidonakis, *Two-loop soft anomalous dimensions for single top quark associated production with a W^- or H^-*, *Phys. Rev. D* **82** (2010) 054018 [arXiv:1005.4451] [INSPIRE].

[90] N. Kidonakis, *Top quark production*, in the proceedings of the *Helmholtz International Summer School on Physics of Heavy Quarks and Hadrons*, Dubna, Russian Federation, July 15–28 (2013) [DOI:10.3204/DESY-PROC-2013-03/Kidonakis] [arXiv:1311.0283] [INSPIRE].

[91] M. Bähr et al., *Herwig++ physics and manual*, *Eur. Phys. J. C* **58** (2008) 639 [arXiv:0803.0883] [INSPIRE].

[92] J. Bellm et al., *Herwig 7.0/Herwig++ 3.0 release note*, *Eur. Phys. J. C* **76** (2016) 196 [arXiv:1512.01178] [INSPIRE].

[93] J. Bellm et al., *Herwig 7.1 release note*, arXiv:1705.06919 [INSPIRE].

[94] J. Bellm et al., *Herwig 7.2 release note*, *Eur. Phys. J. C* **80** (2020) 452 [arXiv:1912.06509] [INSPIRE].

[95] S. Höche et al., *A study of QCD radiation in VBF Higgs production with Vincia and Pythia*, *SciPost Phys.* **12** (2022) 010 [arXiv:2106.10987] [INSPIRE].

[96] E. Bothmann, M. Schönherr and S. Schumann, *Reweighting QCD matrix-element and parton-shower calculations*, *Eur. Phys. J. C* **76** (2016) 590 [arXiv:1606.08753] [INSPIRE].

[97] J. Butterworth et al., *PDF4LHC recommendations for LHC run II*, *J. Phys. G* **43** (2016) 023001 [arXiv:1510.03865] [INSPIRE].

[98] J. Mazzitelli et al., *Next-to-Next-to-Leading Order event generation for top-quark pair production*, *Phys. Rev. Lett.* **127** (2021) 062001 [arXiv:2012.14267] [INSPIRE].

[99] SHERPA collaboration, *Event generation with Sherpa 2.2*, *SciPost Phys.* **7** (2019) 034 [arXiv:1905.09127] [INSPIRE].

[100] T. Gleisberg and S. Höche, *Comix, a new matrix element generator*, *JHEP* **12** (2008) 039 [arXiv:0808.3674] [INSPIRE].

[101] F. Buccioni et al., *OpenLoops 2*, *Eur. Phys. J. C* **79** (2019) 866 [arXiv:1907.13071] [INSPIRE].

[102] F. Cascioli, P. Maierhöfer and S. Pozzorini, *Scattering amplitudes with OpenLoops*, *Phys. Rev. Lett.* **108** (2012) 111601 [arXiv:1111.5206] [INSPIRE].

[103] A. Denner, S. Dittmaier and L. Hofer, *Collier: a fortran-based Complex One-Loop LIbrary in Extended Regularizations*, *Comput. Phys. Commun.* **212** (2017) 220 [arXiv:1604.06792] [INSPIRE].

[104] S. Schumann and F. Krauss, *A parton shower algorithm based on Catani-Seymour dipole factorisation*, *JHEP* **03** (2008) 038 [arXiv:0709.1027] [INSPIRE].

[105] S. Höche, F. Krauss, M. Schönherr and F. Siegert, *A critical appraisal of NLO+PS matching methods*, *JHEP* **09** (2012) 049 [arXiv:1111.1220] [INSPIRE].

[106] S. Höche, F. Krauss, M. Schönherr and F. Siegert, *QCD matrix elements + parton showers: the NLO case*, *JHEP* **04** (2013) 027 [arXiv:1207.5030] [INSPIRE].

[107] S. Catani, F. Krauss, R. Kuhn and B.R. Webber, *QCD matrix elements + parton showers*, *JHEP* **11** (2001) 063 [hep-ph/0109231] [INSPIRE].

[108] S. Höche, F. Krauss, S. Schumann and F. Siegert, *QCD matrix elements and truncated showers*, *JHEP* **05** (2009) 053 [arXiv:0903.1219] [INSPIRE].

JHEP07(2026)028

[109] S. Kallweit et al., *NLO electroweak automation and precise predictions for W+multijet production at the LHC*, *JHEP* **04** (2015) 012 [arXiv:1412.5157] [INSPIRE].

[110] S. Kallweit et al., *NLO QCD+EW predictions for V + jets including off-shell vector-boson decays and multijet merging*, *JHEP* **04** (2016) 021 [arXiv:1511.08692] [INSPIRE].

[111] J. Alwall et al., *The automated computation of tree-level and next-to-leading order differential cross sections, and their matching to parton shower simulations*, *JHEP* **07** (2014) 079 [arXiv:1405.0301] [INSPIRE].

[112] M. Aliev et al., *HATHOR: HAdronic Top and Heavy quarks crOss section calculatoR*, *Comput. Phys. Commun.* **182** (2011) 1034 [arXiv:1007.1327] [INSPIRE].

[113] P. Kant et al., *HatHor for single top-quark production: updated predictions and uncertainty estimates for single top-quark production in hadronic collisions*, *Comput. Phys. Commun.* **191** (2015) 74 [arXiv:1406.4403] [INSPIRE].

[114] LHC Higgs Cross section Working Group collaboration, *Handbook of LHC Higgs cross sections: 4. Deciphering the nature of the Higgs sector*, *CERN Yellow Rep. Monogr.* **2** (2017) 1 [arXiv:1610.07922] [INSPIRE].

[115] ATLAS collaboration, *Luminosity determination in pp collisions at $\sqrt{s} = 13$ TeV using the ATLAS detector at the LHC*, *Eur. Phys. J. C* **83** (2023) 982 [arXiv:2212.09379] [INSPIRE].

[116] ATLAS collaboration, *ATLAS data quality operations and performance for 2015–2018 data-taking*, 2020 *JINST* **15** P04003 [arXiv:1911.04632] [INSPIRE].

[117] ATLAS collaboration, *Performance of electron and photon triggers in ATLAS during LHC run 2*, *Eur. Phys. J. C* **80** (2020) 47 [arXiv:1909.00761] [INSPIRE].

[118] ATLAS collaboration, *Performance of the ATLAS muon triggers in run 2*, 2020 *JINST* **15** P09015 [arXiv:2004.13447] [INSPIRE].

[119] ATLAS collaboration, *Vertex reconstruction performance of the ATLAS detector at $\sqrt{s} = 13$ TeV*, ATL-PHYS-PUB-2015-026 (2015) [INSPIRE].

[120] S. Schmitt, *Data unfolding methods in high energy physics*, *EPJ Web Conf.* **137** (2017) 11008 [arXiv:1611.01927] [INSPIRE].

[121] V. Blobel, *Unfolding methods in particle physics*, in the proceedings of the *PHYSTAT 2011*, Geneva, Switzerland, January 17–20 (2011) [DOI:10.5170/CERN-2011-006.240] [INSPIRE].

[122] S. Schmitt, *TUnfold: an algorithm for correcting migration effects in high energy physics*, 2012 *JINST* **7** T10003 [arXiv:1205.6201] [INSPIRE].

[123] A.N. Tikhonov, A.V. Goncharsky, V.V. Stepanov and A.G. Yagola, *Numerical methods for the solution of ill-posed problems*, Springer, Dordrecht, The Netherlands (1995) [DOI:10.1007/978-94-015-8480-7].

[124] D.L. Phillips, *A technique for the numerical solution of certain integral equations of the first kind*, *J. Assoc. Comput. Machinery* **9** (1962) 84 [INSPIRE].

[125] ATLAS collaboration, *Tools for estimating fake/non-prompt lepton backgrounds with the ATLAS detector at the LHC*, 2023 *JINST* **18** T11004 [arXiv:2211.16178] [INSPIRE].

[126] ATLAS collaboration, *ATLAS b-jet identification performance and efficiency measurement with $t\bar{t}$ events in pp collisions at $\sqrt{s} = 13$ TeV*, *Eur. Phys. J. C* **79** (2019) 970 [arXiv:1907.05120] [INSPIRE].

JHEP07(2026)028

[127] ATLAS collaboration, *Measurement of the c-jet mistagging efficiency in $t\bar{t}$ events using pp collision data at $\sqrt{s} = 13$ TeV collected with the ATLAS detector*, Eur. Phys. J. C **82** (2022) 95 [arXiv:2109.10627] [INSPIRE].

[128] ATLAS collaboration, *Calibration of the light-flavour jet mistagging efficiency of the b-tagging algorithms with Z+jets events using 139 fb^{-1} of ATLAS proton–proton collision data at $\sqrt{s} = 13$ TeV*, Eur. Phys. J. C **83** (2023) 728 [arXiv:2301.06319] [INSPIRE].

[129] P. Artoisenet, R. Frederix, O. Mattelaer and R. Rietkerk, *Automatic spin-entangled decays of heavy resonances in Monte Carlo simulations*, JHEP **03** (2013) 015 [arXiv:1212.3460] [INSPIRE].

[130] ATLAS collaboration, *ATLAS computing acknowledgements*, ATL-SOFT-PUB-2026-001 (2026).

JHEP07(2026)028

The ATLAS collaboration

G. Aad[103], E. Aakvaag[17], B. Abbott[121], S. Abdelhameed[84b], K. Abeling[55], N.J. Abicht[49], S.H. Abidi[30], M. Aboelela[45], A. Aboulhorma[36e], H. Abramowicz[155], Y. Abulaiti[118], B.S. Acharya[69a,69b,a], A. Ackermann[63a], C. Adam Bourdarios[4], L. Adamczyk[86a], S.V. Addepalli[147], M. J. Addison[102], J. Adelman[117], A. Adiguzel[22c], T. Adye[135], A.A. Affolder[137], Y. Afik[40], M.N. Agaras[13], A. Aggarwal[101], C. Agheorghiesei[28c], F. Ahmadov[39,b], S. Ahuja[96], S. Ahuja[167], X. Ai[141b], G. Aielli[76a,76b], A. Aikot[167], M. Ait Tamlihat[36e], B. Aitbenchikh[36a], T.P.A. Åkesson[99], A.V. Akimov[149], D. Akiyama[172], N.N. Akolkar[25], S. Aktas[170], G.L. Alberghi[24b], J. Albert[169], U. Alberti[20], P. Albicocco[53], G.L. Albouy[60], S. Alderweireldt[52], Z.L. Alegria[122], M. Aleksa[37], I.N. Aleksandrov[39], C. Alexa[28b], T. Alexopoulos[10], F. Alfonsi[24b], M. Algren[56], M. Alhroob[171], B. Ali[133], H. M. J. Ali[92,c], S. Ali[32], S.W. Alibocus[93], M. Aliev[34c], G. Alimonti[71a], W. Alkakhi[55], C. Allaire[66], B.M.M. Allbrooke[150], D. R. Allen[122], J. S. Allen[102], J.F. Allen[52], P.P. Allport[21], A. Aloisio[72a,72b], F. Alonso[91], C. Alpigiani[140], Z.M.K. Alsolami[92], A. Alvarez Fernandez[101], M. Alves Cardoso[56], M.G. Alviggi[72a,72b], M. Aly[102], Y. Amaral Coutinho[82b], A. Ambler[105], C. Amelung[37], M. Amerl[102], C.G. Ames[110], T. Amezza[128], D. Amidei[107], B. Amini[54], K. Amirie[159], A. Amirkhanov[39], S.P. Amor Dos Santos[131a], K.R. Amos[167], D. Amperiadou[156], S. An[83], C. Anastopoulos[143], T. Andeen[11], J.K. Anders[93], A. C. Anderson[59], A. Andreazza[71a,71b], S. Angelidakis[9], A. Angerami[42], A.V. Anisenkov[39], A. Annovi[74a], C. Antel[37], E. Antipov[149], M. Antonelli[53], F. Anulli[75a], M. Aoki[83], T. Aoki[157], M.A. Aparo[150], L. Aperio Bella[48], M. Apicella[31], C. Appelt[155], A. Apyan[27], M. Arampatzi[10], S. J. Arbiol Val[87], C. Arcangeletti[53], A.T.H. Arce[51], J-F. Arguin[109], S. Argyropoulos[156], J.-H. Arling[48], O. Arnaez[4], H. Arnold[149], G. Artoni[75a,75b], H. Asada[112], K. Asai[119], S. Asatryan[177], N.A. Asbah[37], R. A. Ashby Pickering[171], A. M. Aslam[96], K. Assamagan[30], R. Astalos[29a], K. S. V. Astrand[99], S. Atashi[163], R.J. Atkin[34a], H. Atmani[36f], P.A. Atmasiddha[129], K. Augsten[133], A.D. Auriol[41], V.A. Austrup[102], A.S. Avad[95], G. Avolio[37], K. Axiotis[56], A. Azzam[13], D. Babal[29b], H. Bachacou[136], K. Bachas[156,d], A. Bachiu[35], E. Bachmann[50], M. J. Backes[63a], A. Badea[40], T.M. Baer[107], P. Bagnaia[75a,75b], M. Bahmani[19], D. Bahner[54], K. Bai[124], J.T. Baines[135], L. Baines[95], O.K. Baker[176], E. Bakos[16], D. Bakshi Gupta[8], L.E. Balabram Filho[82b], V. Balakrishnan[121], R. Balasubramanian[4], E.M. Baldin[38], P. Balek[86a], E. Ballabene[24b,24a], F. Balli[136], L.M. Baltes[63a], W.K. Balunas[33], J. Balz[101], I. Bamwidhi[84c], E. Banas[87], M. Bandieramonte[130], A. Bandyopadhyay[25], S. Bansal[25], L. Barak[155], M. Barakat[48], E.L. Barberio[106], D. Barberis[18b], M. Barbero[103], M. Z. Barel[116], T. Barillari[111], M-S. Barisits[37], T. Barklow[147], P. Baron[134], D.A. Baron Moreno[102], A. Baroncelli[62], A.J. Barr[127], J.D. Barr[97], F. Barreiro[100], J. Barreiro Guimarães da Costa[14], M.G. Barros Teixeira[131a], S. Barsov[38], F. Bartels[63a], R. Bartoldus[147], A.E. Barton[92], P. Bartos[29a], M. Baselga[49], S. Bashiri[87], A. Bassalat[66,e], M.J. Basso[160a], S. Bataju[45], R. Bate[168], R.L. Bates[59], S. Batlamous[100], M. Battaglia[137], D. Battulga[19], M. Bauce[75a,75b], M. Bauer[79], P. Bauer[25], L. T. Bayer[48], L.T. Bazzano Hurrell[31], J.B. Beacham[111], T. Beau[128], J.Y. Beaucamp[91], P.H. Beauchemin[162], P. Bechtle[25], H.P. Beck[20,f], K. Becker[171], A.J. Beddall[81], V.A. Bednyakov[39], C.P. Bee[149],

JHEP07(2026)028

L.J. Beemster[16], M. Begalli[82d], M. Begel[30], J.K. Behr[48], J.F. Beirer[37], F. Beisiegel[25], M. Belfkir[84c], G. Bella[155], L. Bellagamba[24b], A. Bellerive[35], C.D. Bellgraph[68], P. Bellos[21], K. Beloborodov[38], I. Benaoumeur[21], D. Benchekroun[36a], F. Bendebba[36a], Y. Benhammou[155], K.C. Benkendorfer[61], L. Beresford[48], M. Beretta[53], E. Bergeaas Kuutmann[165], N. Berger[4], B. Bergmann[133], J. Beringer[18a], G. Bernardi[5], C. Bernius[147], F.U. Bernlochner[25], A. Berrocal Guardia[13], T. Berry[96], P. Berta[134], A. Berti[131a], R. Bertrand[103], S. Bethke[111], A. Betti[75a,75b], A.J. Bevan[95], L. Bezio[56], N.K. Bhalla[54], S. Bharthuar[111], S. Bhatta[149], P. Bhattarai[147], Z.M. Bhatti[118], K. D. Bhide[54], V.S. Bhopatkar[122], R.M. Bianchi[130], G. Bianco[24b,24a], O. Biebel[110], M. Biglietti[77a], C. S. Billingsley[45], Y. Bimgdi[36f], M. Bindi[55], A. Bingham[175], A. Bingul[22b], C. Bini[75a,75b], G.A. Bird[33], M. Birman[173], M. Biros[134], S. Biryukov[150], T. Bisanz[49], E. Bisceglie[24b,24a], J.P. Biswal[135], D. Biswas[145], I. Bloch[48], A. Blue[59], U. Blumenschein[95], V.S. Bobrovnikov[39], L. Boccardo[57b,57a], M. Boehler[54], B. Boehm[170], D. Bogavac[13], A.G. Bogdanchikov[38], L. S. Boggia[128], V. Boisvert[96], P. Bokan[37], T. Bold[86a], M. Bomben[5], M. Bona[95], M. Boonekamp[136], A.G. Borbély[59], I.S. Bordulev[38], G. Borissov[92], D. Bortoletto[127], D. Boscherini[24b], M. Bosman[13], K. Bouaouda[36a], N. Bouchhar[167], L. Boudet[4], J. Boudreau[130], E.V. Bouhova-Thacker[92], D. Boumediene[41], R. Bouquet[57b,57a], A. Boveia[120], J. Boyd[37], D. Boye[30], I.R. Boyko[39], L. Bozianu[56], J. Bracinik[21], N. Brahimi[4], G. Brandt[175], O. Brandt[33], B. Brau[104], J.E. Brau[124], R. Brener[173], L. Brenner[116], R. Brenner[165], S. Bressler[173], G. Brianti[78a,78b], D. Britton[59], D. Britzger[111], I. Brock[25], R. Brock[108], G. Brooijmans[42], A.J. Brooks[68], E. M. Brooks[160b], E. Brost[30], L.M. Brown[169,160a], L.E. Bruce[61], T.L. Bruckler[127], P.A. Bruckman de Renstrom[87], B. Brüers[48], A. Bruni[24b], G. Bruni[24b], D. Brunner[47a,47b], M. Bruschi[24b], N. Bruscino[75a,75b], T. Buanes[17], Q. Buat[140], D. Buchin[111], A.G. Buckley[59], O. Bulekov[81], B.A. Bullard[147], S. Burdin[93], C.D. Burgard[49], A.M. Burger[90], B. Burghgrave[8], O. Burlayenko[54], J. Burleson[166], J.C. Burzynski[146], E.L. Busch[42], V. Büscher[101], P.J. Bussey[59], O. But[25], J.M. Butler[26], C.M. Buttar[59], J.M. Butterworth[97], P. Butti[37], W. Buttinger[135], C.J. Buxo Vazquez[108], A.R. Buzykaev[39], S. Cabrera Urbán[167], L. Cadamuro[66], H. Cai[37], Y. Cai[24b,113c,24a], Y. Cai[113a], V.M.M. Cairo[37], O. Cakir[3a], N. Calace[37], P. Calafiura[18a], G. Calderini[128], P. Calfayan[35], L. Calic[99], G. Callea[59], L.P. Caloba[82b], D. Calvet[41], S. Calvet[41], R. Camacho Toro[128], S. Camarda[37], D. Camarero Munoz[27], P. Camarri[76a,76b], C. Camincher[169], M. Campanelli[97], A. Camplani[43], V. Canale[72a,72b], A.C. Canbay[3a], E. Canonero[96], J. Cantero[167], Y. Cao[166], F. Capocasa[27], M. Capua[44b,44a], A. Carbone[71a,71b], R. Cardarelli[76a], J.C.J. Cardenas[8], M. P. Cardiff[27], G. Carducci[44b,44a], T. Carli[37], G. Carlino[72a], J.I. Carlotto[13], B.T. Carlson[130,g], E.M. Carlson[169], J. Carmignani[93], L. Carminati[71a,71b], A. Carnelli[4], M. Carnesale[37], S. Caron[115], E. Carquin[138g], I.B. Carr[106], S. Carrá[73a,73b], G. Carratta[24b,24a], C. Carrion Martinez[167], A.M. Carroll[124], M.P. Casado[13,h], P. Casolaro[72a,72b], M. Caspar[48], W.R. Castiglioni[40], F.L. Castillo[4], L. Castillo Garcia[13], V. Castillo Gimenez[167], N.F. Castro[131a,131e], A. Catinaccio[37], J.R. Catmore[126], T. Cavaliere[4], V. Cavaliere[30], L.J. Caviedes Betancourt[23b], E. Celebi[81], S. Cella[37], V. Cepaitis[56], K. Cerny[123], A.S. Cerqueira[82a], A. Cerri[74a,i], L. Cerrito[76a,76b], F. Cerutti[18a], B. Cervato[71a,71b],

JHEP07(2026)028

A. Cervelli[24b], G. Cesarini[53], S.A. Cetin[81], P.M. Chabrillat[128], R. Chakkappai[66], S. Chakraborty[171], A. Chambers[61], J. Chan[18a], W.Y. Chan[157], J.D. Chapman[33], E. Chapon[136], B. Chargeishvili[153b], D.G. Charlton[21], C. Chauhan[134], Y. Che[113a], S. Chekanov[6], G.A. Chelkov[39,j], B. Chen[155], B. Chen[169], H. Chen[30], J. Chen[142a], J. Chen[146], M. Chen[127], S. Chen[88], S.J. Chen[113a], X. Chen[142a], X. Chen[15,k], Z. Chen[62], C.L. Cheng[174], H.C. Cheng[64a], S. Cheong[147], A. Cheplakov[39], E. Cherepanova[116], R. Cherkaoui El Moursli[36e], E. Cheu[7], K. Cheung[65], L. Chevalier[136], V. Chiarella[53], G. Chiarelli[74a], G. Chiodini[70a], A.S. Chisholm[21], A. Chitan[28b], M. Chitishvili[167], M.V. Chizhov[39,l], K. Choi[11], Y. Chou[140], E.Y.S. Chow[115], K.L. Chu[173], M.C. Chu[64a], X. Chu[14,113c], Z. Chubinidze[53], J. Chudoba[132], J.J. Chwastowski[87], D. Cieri[111], K.M. Ciesla[86a], V. Cindro[94], A. Ciocio[18a], F. Cirotto[72a,72b], Z.H. Citron[173], M. Citterio[71a], D.A. Ciubotaru[28b], A. Clark[56], P.J. Clark[52], N. Clarke Hall[97], C. Clarry[159], S.E. Clawson[48], C. Clement[47a,47b], L. Clissa[24b,24a], Y. Coadou[103], M. Cobal[69a,69c], A. Coccaro[57b], R.F. Coelho Barrue[131a], R. Coelho Lopes De Sa[104], S. Coelli[71a], M.M. Cohen[129], L. S. Colangeli[159], B. Cole[42], P. Collado Soto[100], J. Collot[60], M.R. Coluccia[70a], P. Conde Muiño[131a,131g], M.P. Connell[34c], S.H. Connell[34c], E.I. Conroy[127], M. Contreras Cossio[11], F. Conventi[72a,m], A.M. Cooper-Sarkar[127], L. Corazzina[75a,75b], F. A. Corchia[24b,24a], A. Cordeiro Oudot Choi[140], L.D. Corpe[41], M. Corradi[75a,75b], F. Corriveau[105,n], A. Cortes-Gonzalez[157], M.J. Costa[167], F. Costanza[4], D. Costanzo[143], J. Couthures[4], G. Cowan[96], K. Cranmer[174], L. Cremer[49], D. Cremonini[24b,24a], S. Crépé-Renaudin[60], F. Crescioli[128], T. Cresta[73a,73b], M. Cristinziani[145], M. Cristoforetti[78a,78b], E. Critelli[97], V. Croft[116], G. Crosetti[44b,44a], A. Cueto[100], H. Cui[97], Z. Cui[7], B.M. Cunnett[150], W.R. Cunningham[59], F. Curcio[167], J. R. Curran[52], G. D'amen[30], V. D'Amico[110], M. D'Andrea[57b,57a], G. D'anniballe[74a,74b], S. D'Auria[71a,71b], A. D'Avanzo[72a,72b], L. D'Eramo[41], A. D'Onofrio[72a,72b], M. D'Onofrio[93], M. D'uffizi[102], M.J. Da Cunha Sargedas De Sousa[57b,57a], J.V. Da Fonseca Pinto[82b], C. Da Via[102], W. Dabrowski[86a], T. Dado[37], S. Dahbi[152], T. Dai[107], D. Dal Santo[20], C. Dallapiccola[104], M. Dam[43], J.R. Dandoy[35], D. Dannheim[37], M. Danninger[146], V. Dao[149], G. Darbo[57b], S.J. Das[30], F. Dattola[48], T. Davidek[134], J. Davidson[171], I. Dawson[95], K. De[8], C. De Almeida Rossi[159], R. De Asmundis[72a], N. De Biase[48], S. De Castro[24b,24a], N. De Groot[115], P. de Jong[116], H. De la Torre[117], A. De Maria[113a], A. De Salvo[75a], U. De Sanctis[76a,76b], F. De Santis[70a,70b], A. De Santo[150], J.B. De Vivie De Regie[60], J. Debevc[94], D.V. Dedovich[39], J. Degens[93], A.M. Deiana[45], J. Del Peso[100], L. Delagrange[128], F. Deliot[136], C.M. Delitzsch[49], A. Dell'Acqua[37], L. Dell'Asta[71a,71b], M. Della Pietra[72a,72b], D. Della Volpe[56], M. Delmastro[4], C.C. Delogu[57b,57a], P.A. Delsart[60], S. Demers[176], M. Demichev[39], S.P. Denisov[38], H. Denizli[22a,o], M.G. Depala[93], D. Derendarz[87], F. Derue[128], P. Dervan[93,†], A. M. Desai[1], K. Desch[25], F.A. Di Bello[74a,74b], A. Di Ciaccio[76a,76b], L. Di Ciaccio[4], A. Di Domenico[75a,75b], C. Di Donato[72a,72b], A. Di Girolamo[37], G. Di Gregorio[66], A. Di Luca[78a,78b], B. Di Micco[77a,77b], R. Di Nardo[77a,77b], K.F. Di Petrillo[40], M. Diamantopoulou[35], F.A. Dias[116], M.A. Diaz[138a,138b], A. R. Didenko[39], M. Didenko[167], S.D. Diefenbacher[18a], E.B. Diehl[107], S. Díez Cornell[48], C. Diez Pardos[145], C. Dimitriadi[148], A. Dimitrievska[21], A. Dimri[149], Y. Ding[62], J. Dingfelder[25],

JHEP07(2026)028

T. Dingley[127], I-M. Dinu[28b], S.J. Dittmeier[63b], F. Dittus[37], M. Divisek[134], B. Dixit[93], F. Djama[103], T. Djobava[153b], C. Doglioni[102,99], A. Dohnalova[29a], Z. Dolezal[134], K. Domijan[86a], K.M. Dona[40], M. Donadelli[82d], B. Dong[108], J. Donini[41], J. Dopke[135], A. Doria[72a], N. Dos Santos Fernandes[131a], I.A. Dos Santos Luz[82e], P. Dougan[102], M.T. Dova[91], A.T. Doyle[59], M.P. Drescher[55], E. Dreyer[173], I. Drivas-koulouris[10], M. Drnevich[118], D. Du[62], T.A. du Pree[116], Z. Duan[113a], M. Dubau[4], F. Dubinin[39], M. Dubovsky[29a], E. Duchovni[173], G. Duckeck[110], P. K. Duckett[97], O.A. Ducu[28b], D. Duda[52], A. Dudarev[37], M.M. Dudek[87], E. R. Duden[27], L. Duflot[66], M. Dührssen[37], I. Duminica[28g], A.E. Dumitriu[28b], M. Dunford[63a], K. Dunne[47a,47b], A. Duperrin[103], H. Duran Yildiz[3a], A. Durglishvili[153b], G.I. Dyckes[18a], M. Dyndal[86a], B.S. Dziedzic[37], Z.O. Earnshaw[150], G.H. Eberwein[127], B. Eckerova[29a], S. Eggebrecht[55], E. Egidio Purcino De Souza[82e], G. Eigen[17], K. Einsweiler[18a], T. Ekelof[165], P.A. Ekman[99], S. El Farkh[36b], Y. El Ghazali[62], H. El Jarrari[105], A. El Moussaouy[36a], D. Elitez[37], M. Ellert[165], F. Ellinghaus[175], T.A. Elliot[96], N. Ellis[37], J. Elmsheuser[30], M. Elsawy[84b], M. Elsing[37], D. Emeliyanov[135], Y. Enari[83], S. Epari[109], D. Ernani Martins Neto[87], F. Ernst[37], M. Escalier[66], C. Escobar[167], E. Etzion[155], G. Evans[131a,131b], H. Evans[68], L.S. Evans[48], A. Ezhilov[38], S. Ezzarqtouni[36a], F. Fabbri[24b,24a], L. Fabbri[24b,24a], G. Facini[97], V. Fadeyev[137], R.M. Fakhrutdinov[38], D. Fakoudis[101], S. Falciano[75a], L.F. Falda Ulhoa Coelho[27], F. Fallavollita[111], G. Falsetti[44b,44a], J. Faltova[134], C. Fan[166], K. Y. Fan[64b], Y. Fan[14], Y. Fang[14,113c], M. Fanti[71a,71b], M. Faraj[69a,69b], Z. Farazpay[98], A. Farbin[8], A. Farilla[77a], K. Farman[152], T. Farooque[108], J. N. Farr[176], M. S. Farrington[61], S.M. Farrington[135,52], F. Fassi[36e], D. Fassouliotis[9], L. Fayard[66], P. Federic[134], P. Federicova[132], O.L. Fedin[38,j], M. Feickert[174], L. Feligioni[103], D.E. Fellers[18a], C. Feng[141a], Y. Feng[14], Z. Feng[116], M.J. Fenton[163], L. Ferencz[48], B. Fernandez Barbadillo[92], P. Fernandez Martinez[67], M.J.V. Fernoux[103], J. Ferrando[92], A. Ferrari[165], P. Ferrari[116,115], R. Ferrari[73a], D. Ferrere[56], C. Ferretti[107], M. P. Fewell[1], D. Fiacco[75a,75b], F. Fiedler[101], P. Fiedler[133], S. Filimonov[39], M.S. Filip[28b,p], A. Filipčič[94], E.K. Filmer[160a], F. Filthaut[115], M.C.N. Fiolhais[131a,131c,q], L. Fiorini[167], W.C. Fisher[108], T. Fitschen[102], P. M. Fitzhugh[136], I. Fleck[145], P. Fleischmann[107], T. Flick[175], M. Flores[34d,r], L.R. Flores Castillo[64a], M. Foll[126], F.M. Follega[78a,78b], N. Fomin[33], J.H. Foo[159], A. Formica[136], A.C. Forti[102], E. Fortin[37], A.W. Fortman[18a], L. Foster[18a], L. Fountas[9,s], D. Fournier[66], H. Fox[92], P. Francavilla[74a,74b], S. Francescato[61], S. Franchellucci[56], M. Franchini[24b,24a], S. Franchino[63a], D. Francis[37], L. Franco[48], L. Franconi[48], M. Franklin[61], G. Frattari[27], Y.Y. Frid[155], J. Friend[59], N. Fritzsche[37], A. Froch[56], D. Froidevaux[37], J.A. Frost[135], Y. Fu[108], S. Fuenzalida Garrido[138g], M. Fujimoto[149], K. Y. Fung[64a], E. Furtado De Simas Filho[82e], M. Furukawa[157], M. Fuste Costa[48], J. Fuster[167], A. Gaa[55], A. Gabrielli[24b,24a], A. Gabrielli[159], P. Gadow[37], G. Gagliardi[57b,57a], L.G. Gagnon[18a], S. Gaid[84d], S. Galantzan[155], J. Gallagher[1], E.J. Gallas[127], A.L. Gallen[165], B.J. Gallop[135], K.K. Gan[120], S. Ganguly[157], Y. Gao[52], A. Garabaglu[140], F.M. Garay Walls[138a,138b], C. García[167], A. Garcia Alonso[116], A.G. Garcia Caffaro[176], J.E. García Navarro[167], M. A. Garcia Ruiz[23b], M. Garcia-Sciveres[18a], G.L. Gardner[129], R.W. Gardner[40], N. Garelli[162], R.B. Garg[147], J.M. Gargan[33], C.A. Garner[159], C.M. Garvey[34a],

JHEP07(2026)028

V. K. Gassmann[162], G. Gaudio[73a], V. Gautam[13], P. Gauzzi[75a,75b], J. Gavranovic[94], I.L. Gavrilenko[131a], A. Gavrilyuk[38], C. Gay[168], G. Gaycken[124], E.N. Gazis[10], A. Gekow[120], C. Gemme[57b], M.H. Genest[60], A. D. Gentry[114], S. George[96], T. Geralis[46], A. A. Gerwin[121], P. Gessinger-Befurt[37], M. Ghani[171], K. Ghorbanian[95], A. Ghosal[145], A. Ghosh[163], A. Ghosh[7], B. Giacobbe[24b], S. Giagu[75a,75b], T. Giani[116], A. Giannini[62], S.M. Gibson[96], M. Gignac[137], D.T. Gil[86b], A.K. Gilbert[86a], B.J. Gilbert[42], D. Gillberg[35], G. Gilles[116], D.M. Gingrich[2,t], M.P. Giordani[69a,69c], P.F. Giraud[136], G. Giugliarelli[69a,69c], D. Giugni[71a], F. Giuli[76a,76b], I. Gkialas[9,s], L.K. Gladilin[38], C. Glasman[100], M. Glazewska[20], R. M. Gleason[163], G. Glemža[48], M. Glisic[124], I. Gnesi[44b], Y. Go[30], M. Goblirsch-Kolb[37], B. Gocke[49], D. Godin[109], B. Gokturk[22a], S. Goldfarb[106], T. Golling[56], M.G.D. Gololo[34c], A. Golub[140], D. Golubkov[38], J.P. Gombas[108], A. Gomes[131a,131b], G. Gomes Da Silva[145], A.J. Gomez Delegido[37], R. Gonçalo[131a], L. Gonella[21], A. Gongadze[153c], F. Gonnella[21], J.L. Gonski[147], R.Y. González Andana[52], S. González de la Hoz[167], M. V. Gonzalez Rodrigues[48], R. Gonzalez Suarez[165], S. Gonzalez-Sevilla[56], L. Goossens[37], B. Gorini[37], E. Gorini[70a,70b], A. Gorišek[94], T.C. Gosart[129], A.T. Goshaw[51], M.I. Gostkin[39], S. Goswami[122], C.A. Gottardo[37], S. A. Gotz[110], M. Gouighri[36b], A.G. Goussiou[140], N. Govender[34c], R. P. Grabarczyk[127], I. Grabowska-Bold[86a], K. Graham[35], E. Gramstad[126], S. Grancagnolo[70a,70b], C.M. Grant[1], P.M. Gravila[28f], F.G. Gravili[70a,70b], H.M. Gray[18a], M. Greco[111], M. J. Green[1], C. Grefe[25], A. S. Grefsrud[17], I.M. Gregor[48], K.T. Greif[163], P. Grenier[147], S.G. Grewe[111], A.A. Grillo[137], K. Grimm[32], S. Grinstein[13,u], J.-F. Grivaz[66], E. Gross[173], J. Grosse-Knetter[55], L.H. Grossman[18b], L. Guan[107], G. Guerrieri[37], R. Guevara[126], R. Gugel[101], J.A.M. Guhit[107], A. Guida[19], E. Guilloton[171], S. Guindon[37], F. Guo[14,113c], J. Guo[142a], L. Guo[48], L. Guo[113b,v], Y. Guo[107], Y. Guo[42], A. Gupta[49], R. Gupta[130], S. Gupta[27], S. Gurbuz[25], S.S. Gurdasani[48], G. Gustavino[75a,75b], P. Gutierrez[121], L.F. Gutierrez Zagazeta[129], M. Gutsche[50], C. Gutschow[97], C. Gwenlan[127], C.B. Gwilliam[93], E.S. Haaland[126], A. Haas[118], M. Habedank[59], C. Haber[18a], H.K. Hadavand[8], A. Haddad[41], A. Hadef[50], A.I. Hagan[92], J. J. Hahn[145], E.H. Haines[97], M. Haleem[170], J. Haley[122], G.D. Hallewell[103], J.A. Hallford[48], K. Hamano[169], H. Hamdaoui[165], M. Hamer[25], S. E. D. Hammoud[66], E.J. Hampshire[96], J. Han[141a], L. Han[113a], L. Han[62], S. Han[14], K. Hanagaki[83], M. Hance[137], D.A. Hangal[42], H. Hanif[146], M.D. Hank[129], J.B. Hansen[43], P.H. Hansen[43], T. Harenberg[175], S. Harkusha[177], M.L. Harris[104], Y.T. Harris[25], J. Harrison[13], P.F. Harrison[171], M. L. E. Hart[97], N.M. Hartman[111], N.M. Hartmann[110], R. Z. Hasan[96,135], Y. Hasegawa[144], F. Haslbeck[127], S. Hassan[17], R. Hauser[108], M. Haviernik[134], C.M. Hawkes[21], R.J. Hawkings[37], Y. Hayashi[157], D. Hayden[108], C. Hayes[107], R.L. Hayes[116], C.P. Hays[127], J.M. Hays[95], H.S. Hayward[93], M. He[14,113c], Y. He[48], Y. He[97], N.B. Heatley[95], V. Hedberg[99], J. Heilman[35], S. Heim[48], T. Heim[18a], J.J. Heinrich[124], L. Heinrich[111], J. Hejbal[132], M. Helbig[50], A. Held[174], S. Hellesund[17], C.M. Helling[168], S. Hellman[47a,47b], A.M. Henriques Correia[37], H. Herde[99], Y. Hernández Jiménez[149], L.M. Herrmann[25], T. Herrmann[50], G. Herten[54], R. Hertenberger[110], L. Hervas[37], M.E. Hesping[101], N.P. Hessey[160a], J. Hessler[111], M. Hidaoui[36b], N. Hidic[134], E. Hill[159], T. S. Hillersoy[17], S.J. Hillier[21], J.R. Hinds[108], F. Hinterkeuser[25], M. Hirose[125],

JHEP07(2026)028

S. Hirose[161], D. Hirschbuehl[175], T.G. Hitchings[102], B. Hiti[94], J. Hobbs[149], R. Hobincu[28e], N. Hod[173], A.M. Hodges[166], M.C. Hodgkinson[143], B.H. Hodkinson[127], A. Hoecker[37], D. D. Hofer[107], J. Hofer[167], J. Hofner[101], M. Holzbock[37], L.B.A.H. Hommels[33], V. Homsak[127], J. J. Hong[68], T.M. Hong[130], B.H. Hooberman[166], W.H. Hopkins[6], M. C. Hoppesch[166], Y. Horii[112], M. E. Horstmann[111], S. Hou[152], M. R. Housenga[166], J. Howarth[59], J. Hoya[6], M. Hrabovsky[123], T. Hryn'ova[4], P.J. Hsu[65], S.-C. Hsu[140], T. Hsu[66], M. Hu[18a], Q. Hu[62], S. Huang[33], X. Huang[14,113c], Y. Huang[134], Y. Huang[113b], Y. Huang[14], Z. Huang[66], Z. Hubacek[133], F. Huegging[25], T.B. Huffman[127], M. Hufnagel Maranha De Faria[82a], C. A. Hugli[48], M. Huhtinen[37], S.K. Huiberts[126], R. Hulsken[105], C. E. Hultquist[18a], D.L. Humphreys[104], N. Huseynov[12], J. Huston[108], B. Huth[37], J. Huth[61], L. Huth[48], R. Hyneman[7], G. Iacobucci[56], G. Iakovidis[30], L. Iconomidou-Fayard[66], J. P. Iddon[37], P. Iengo[72a,72b], Y. Iiyama[157], T. Iizawa[157], Y. Ikegami[83], D. Iliadis[156], N. Ilic[159], H. Imam[36a], G. Inacio Goncalves[82d], S. A. Infante Cabanas[138c], T. Ingebretsen Carlson[47a,47b], J. M. Inglis[95], G. Introzzi[73a,73b], M. Iodice[77a], V. Ippolito[75a,75b], R. K. Irwin[93], M. Ishino[157], W. Islam[174], C. Issever[19], S. Istin[22a,w], K. Itabashi[125], H. Ito[172], R. Iuppa[78a,78b], A. Ivina[173], S. Izumiyama[112], V. Izzo[72a], P. Jacka[133], P. Jackson[1], P. Jain[48], K. Jakobs[54], T. Jakoubek[173], J. Jamieson[59], W. Jang[157], S. Jankovych[134], M. Javurkova[104], P. Jawahar[102], L. Jeanty[124], J. Jejelava[153a,x], P. Jenni[54,y], C.E. Jessiman[35], C. Jia[141a], H. Jia[168], J. Jia[149], X. Jia[111,113c], Z. Jia[113a], C. Jiang[52], Q. Jiang[64b], S. Jiggins[48], M. Jimenez Ortega[167], J. Jimenez Pena[13], S. Jin[113a], A. Jinaru[28b], O. Jinnouchi[139], P. Johansson[143], K.A. Johns[7], J.W. Johnson[137], F. A. Jolly[48], D.M. Jones[150], E. Jones[48], K.S. Jones[8], P. Jones[33], R.W.L. Jones[92], T.J. Jones[93], H.L. Joos[55], R. Joshi[120], J. Jovicevic[16], X. Ju[18a], J.J. Junggeburth[37], T. Junkermann[63a], A. Juste Rozas[13,u], M.K. Juzek[87], S. Kabana[138f], A. Kaczmarska[87], S. A. Kadir[147], M. Kado[111], H. Kagan[120], M. Kagan[147], A. Kahn[129], C. Kahra[101], T. Kaji[157], E. Kajomovitz[154], N. Kakati[173], N. Kakoty[13], I. Kalaitzidou[54], S. Kandel[8], N. Kanellos[10], N.J. Kang[137], D. Kar[34j,†], E. Karentzos[25], K. Karki[8], O. Karkout[116], S.N. Karpov[39], Z.M. Karpova[39], V. Kartvelishvili[92,153b], A.N. Karyukhin[38], E. Kasimi[156], J. Katzy[48], S. Kaur[35], K. Kawade[144], M.P. Kawale[121], C. Kawamoto[88], T. Kawamoto[62], E.F. Kay[37], S. Kazakos[108], V.F. Kazanin[38], J.M. Keaveney[34a], R. Keeler[169], G.V. Kehris[61], J.S. Keller[35], J. M. Kelly[169], J.J. Kempster[150], O. Kepka[132], J. Kerr[160b], B.P. Kerridge[135], B.P. Kerševan[94], L. Keszeghova[29a], R. A. Khan[130], A. Khanov[122], A.G. Kharlamov[38], T. Kharlamova[38], E.E. Khoda[140], M. Kholodenko[131a], T.J. Khoo[19], G. Khoriauli[170], Y. Khoulaki[36a], Y.A.R. Khwaira[128], B. Kibirige[34j], D. Kim[6], D.W. Kim[18b], Y.K. Kim[40], N. Kimura[97], M.K. Kingston[55], A. Kirchhoff[55], C. Kirfel[25], F. Kirfel[25], J. Kirk[135], A.E. Kiryunin[111], S. Kita[161], O. Kivernyk[25], M. Klassen[162], C. Klein[35], L. Klein[170], M.H. Klein[45], S.B. Klein[56], U. Klein[93], A. Klimentov[30], T. Klioutchnikova[37], P. Kluit[116], S. Kluth[111], E. Kneringer[79], T.M. Knight[159], A. Knue[49], M. Kobel[50], D. Kobylianskii[173], S.F. Koch[127], M. Kocian[147], P. Kodyš[134], D.M. Koeck[124], T. Koffas[35], O. Kolay[50], I. Koletsou[4], T. Komarek[87], K. Köneke[55], A.X.Y. Kong[1], T. Kono[119], N. Konstantinidis[97], P. Kontaxakis[56], B. Konya[99], R. Kopeliansky[42], S. Koperny[86a], R. Koppenhofer[54], K. Korcyl[87], K. Kordas[156,z],

JHEP07(2026)028

A. Korn[97], S. Korn[55], I. Korolkov[13], N. Korotkova[38], B. Kortman[116], O. Kortner[111], S. Kortner[111], W.H. Kostecka[117], M. Kostov[29a], V.V. Kostyukhin[145], A. Kotsokechagia[37], A. Kotwal[51], A. Koulouris[37], A. Kourkoumeli-Charalampidi[73a,73b], C. Kourkoumelis[9], E. Kourlitis[111], O. Kovanda[124], R. Kowalewski[169], W. Kozanecki[124], A.S. Kozhin[38], V.A. Kramarenko[38], G. Kramberger[94], P. Kramer[25], M.W. Krasny[128], A. Krasznahorkay[104], A. C. Kraus[117], J.W. Kraus[175], J.A. Kremer[48], N. B. Krengel[145], T. Kresse[50], L. Kretschmann[175], J. Kretzschmar[93], P. Krieger[159], K. Krizka[21], K. Kroeninger[49], H. Kroha[111], J. Kroll[132], J. Kroll[129], K.S. Krowpman[108], U. Kruchonak[39], H. Krüger[25], N. Krumnack[80], M.C. Kruse[51], O. Kuchinskaia[39], S. Kuday[3a], S. Kuehn[37], R. Kuesters[54], T. Kuhl[48], V. Kukhtin[39], Y. Kulchitsky[39], S. Kuleshov[138d,138b], J. Kull[1], E. V. Kumar[110], M. Kumar[34j], N. Kumari[48], P. Kumari[160b], A. Kupco[132], A. Kupich[38], O. Kuprash[54], H. Kurashige[85], L.L. Kurchaninov[160a], O. Kurdysh[4], A. Kurova[38], M. Kuze[139], A.K. Kvam[104], J. Kvita[123], N.G. Kyriacou[140], M. Laassiri[30], C. Lacasta[167], F. Lacava[75a,75b], H. Lacker[19], D. Lacour[128], N.N. Lad[97], E. Ladygin[39], A. Lafarge[41], B. Laforge[128], T. Lagouri[176], F.Z. Lahbabi[36a], S. Lai[55,37], W. S. Lai[97], I.K. Lakomiec[55], J.E. Lambert[169], S. Lammers[68], W. Lampl[7], C. Lampoudis[156,z], G. Lamprinoudis[170], A.N. Lancaster[117], E. Lançon[30], U. Landgraf[54], M.P.J. Landon[95], V.S. Lang[54], A.J. Lankford[163], F. Lanni[37], C. S. Lantz[166], K. Lantzsch[25], A. Lanza[73a], M. Lanzac Berrocal[167], J.F. Laporte[136], T. Lari[71a], D. Larsen[17], L. Larson[11], F. Lasagni Manghi[24b], M. Lassnig[37], S.D. Lawlor[143], R. Lazaridou[163], M. Lazzaroni[71a,71b], E. T. T. Le[163], H. D. M. Le[108], E.M. Le Boulicaut[176], L.T. Le Pottier[18a], B. Leban[24b,24a], F. Ledroit-Guillon[60], T.F. Lee[160b], L.L. Leeuw[34c], M. Lefebvre[169], C. Leggett[18a], G. Lehmann Miotto[37], M. Leigh[56], W.A. Leight[104], W. Leinonen[115], A. Leisos[156,aa], M.A.L. Leite[82c], C.E. Leitgeb[19], R. Leitner[134], K.J.C. Leney[45], T. Lenz[25], S. Leone[74a], C. Leonidopoulos[52], A. Leopold[148], J. LePage-Bourbonnais[35], R. Les[108], C.G. Lester[33], M. Levchenko[38], J. Levêque[4], L.J. Levinson[173], G. Levrini[24b,24a], M.P. Lewicki[87], C. Lewis[140], D.J. Lewis[4], L. Lewitt[143], A. Li[30], B. Li[141a], C-Q. Li[111], C. Li[107], H. Li[141a], H. Li[102], H. Li[15], H. Li[62], H. Li[141a], J. Li[142a], K. Li[14], L. Li[142a], R. Li[176], S. Li[14,113c], S. Li[142b,142a], T. Li[5], X. Li[105], Y. Li[14], Z. Li[157], Z. Li[14,113c], Z. Li[62], S. Liang[14,113c], Z. Liang[14], M. Liberatore[136], B. Liberti[76a], G. B. Libotte[82d], K. Lie[64c], J. Lieber Marin[82e], H. Lien[68], H. Lin[107], S. F. Lin[149], L. Linden[110], R.E. Lindley[7], J.H. Lindon[37], J. Ling[61], E. Lipeles[129], A. Lipniacka[17], A. Lister[168], J.D. Little[68], B. Liu[14], B.X. Liu[113b], D. Liu[154], D. Liu[137], E. H. L. Liu[21], J.K.K. Liu[118], K. Liu[142b], K. Liu[142b,142a], M. Liu[62], M.Y. Liu[62], P. Liu[14], Q. Liu[147], S. Liu[149], X. Liu[141a], Y. Liu[113b,113c], Y. Liu[166], Y.L. Liu[141a], Y.W. Liu[62], Z. Liu[66,ab], S.L. Lloyd[95], E.M. Lobodzinska[48], P. Loch[7], E. Lodhi[159], K. Lohwasser[143], E. Loiacono[48], J. D. Lomas[21], J.D. Long[42], I. Longarini[163], R. Longo[166], A. Lopez Solis[13], N.A. Lopez-canelas[7], N. Lorenzo Martinez[4], A.M. Lory[110], M. Losada[84b], G. Löschcke Centeno[4], X. Lou[47a,47b], X. Lou[14,113c], A. Lounis[66], P.A. Love[92], M. Lu[66], S. Lu[129], Y.J. Lu[152], H.J. Lubatti[140], C. Luci[75a,75b], F.L. Lucio Alves[113a], F. Luehring[68], B. S. Lunday[129], O. Lundberg[148], J. Lunde[37], N.A. Luongo[6], M.S. Lutz[37], A.B. Lux[26], D. Lynn[30], R. Lysak[132], V. Lysenko[133], E. Lytken[99],

JHEP07(2026)028

V. Lyubushkin[39], T. Lyubushkina[39], M.M. Lyukova[149], H. Ma[30], K. Ma[62], L.L. Ma[141a], W. Ma[62], Y. Ma[122], J.C. MacDonald[101], B. Maček[94], P.C. Machado De Abreu Farias[82e], D. Macina[37], R. Madar[41], T. Madula[97], J. Maeda[85], T. Maeno[30], P.T. Mafa[34c,ac], H. Maguire[143], M. Maheshwari[33], V. Maiboroda[66], A. Maio[131a,131b,131d], K. Maj[86a], O. Majersky[48], S. Majewski[124], R. Makhmanazarov[38], N. Makovec[66], V. Maksimovic[16], B. Malaescu[128], J. Malamant[126], Pa. Malecki[87], V.P. Maleev[38], F. Malek[60,ad], M. Mali[94], D. Malito[96], A. Maloizel[5], S. Maltezos[10], A. Malvezzi Lopes[82d], S. Malyukov[39], J. Mamuzic[94], G. Mancini[53], M. N. Mancini[27], G. Manco[73a,73b], J.P. Mandalia[95], S.S. Mandarry[150], I. Mandić[94], L. Manhaes de Andrade Filho[82a], I.M. Maniatis[173], J. Manjarres Ramos[90], D.C. Mankad[173], A. Mann[110], T. Manoussos[37], M.N. Mantinan[40], S. Manzoni[37], L. Mao[142a], X. Mapekula[34c], A. Marantis[156], R.R. Marcelo Gregorio[95], G. Marchiori[5], C. Marcon[71a], E. Maricic[16], M. Marinescu[48], S. Marium[48], M. Marjanovic[121], A. Markhoos[54], M. Markovitch[66], M. K. Maroun[104], M. C. Marr[146], G. T. Marsden[102], E.J. Marshall[92], Z. Marshall[18a], S. Marti-Garcia[167], J. Martin[97], T.A. Martin[135], V.J. Martin[52], B. Martin dit Latour[17], S. Martin-Haugh[135], L. Martinelli[75a,75b], M. Martinez[13,u], P. Martinez Agullo[167], V.I. Martinez Outschoorn[104], P. Martinez Suarez[37], G. Martinovicova[134], V.S. Martoiu[28b], A.C. Martyniuk[97], A. Marzin[37], D. Mascione[78a,78b], L. Masetti[101], J. Masik[102], A.L. Maslennikov[39], S.L. Mason[42], P. Massarotti[72a,72b], P. Mastrandrea[74a,74b], A. Mastroberardino[44b,44a], T. Masubuchi[125], T.T. Mathew[124], J. Matousek[134], D.M. Mattern[49], K. Mauer[48], J. Maurer[28b], T. Maurin[59], A.J. Maury[66], C. Mavungu Tsava[103], D.A. Maximov[38], A. E. May[102], E. Mayer[41], R. Mazini[34j], I. Maznas[117], S.M. Mazza[137], E. Mazzeo[37], J.P. Mc Gowan[169], S.P. Mc Kee[107], C.A. Mc Lean[6], C.C. McCracken[168], E.F. McDonald[106], A.E. McDougall[116], L. F. Mcelhinney[92], J.A. Mcfayden[150], R.P. McGovern[129], R.P. Mckenzie[34j], T.C. Mclachlan[48], D.J. Mclaughlin[97], S.J. McMahon[135], C.M. Mcpartland[93], R.A. McPherson[169,n], S. Mehlhase[110], A. Mehta[93], D. Melini[167], B.R. Mellado Garcia[34j], A.H. Melo[55], F. Meloni[48], A.M. Mendes Jacques Da Costa[102], L. Meng[92], S. Menke[111], M. Mentink[37], E. Meoni[44b,44a], G. Mercado[117], S. Merianos[156], C. Merlassino[69a,69c], C. Meroni[71a,71b], J. Metcalfe[6], A.S. Mete[6], E. Meuser[101], C. Meyer[68], J-P. Meyer[136], Y. Miao[113a], R.P. Middleton[135], M. Mihovilovic[66], L. Mijović[52], G. Mikenberg[173], M. Mikestikova[132], M. Mikuž[94], H. Mildner[101], A. Milic[37], D.W. Miller[40], E. H. Miller[147], A. Milov[173], D.A. Milstead[47a,47b], T. Min[113a], A.A. Minaenko[38], I.A. Minashvili[153b], A.I. Mincer[118], B. Mindur[86a], M. Mineev[39], Y. Mino[88], L.M. Mir[13], M. Miralles Lopez[59], M. Mironova[18a], M. Missio[41], A. Mitra[171], V.A. Mitsou[167], Y. Mitsumori[112], O. Miu[159], P.S. Miyagawa[95], T. Mkrtchyan[37], M. Mlinarevic[97], T. Mlinarevic[97], M. Mlynarikova[134], L. Mlynarska[86a], C. Mo[142a], S. Mobius[20], M. H. Mohamed Farook[114], S. Mohapatra[42], M.F. Mohd Soberi[52], S. Mohiuddin[122], G. Mokgatitswane[34j], L. Moleri[173], U. Molinatti[127], L.G. Mollier[20], B. Mondal[132], S. Mondal[133], K. Mönig[48], E. Monnier[103], L. Monsonis Romero[167], J. Montejo Berlingen[13], A. Montella[47a,47b], M. Montella[120], F. Montereali[77a,77b], F. Monticelli[91], S. Monzani[69a,69c], A. Morancho Tarda[43], N. Morange[66], A.L. Moreira De Carvalho[48], M. Moreno Llácer[167], C. Moreno Martinez[56], J.M. Moreno Perez[23b], P. Morettini[57b], S. Morgenstern[37], M. Morii[61], M. Morinaga[157],

JHEP07(2026)028

M. Moritsu[89], F. Morodei[75a,75b], P. Moschovakos[37], B. Moser[54], M. Mosidze[153b], T. Moskalets[45], P. Moskvitina[115], J. Moss[32], P. Moszkowicz[86a], T. Motta Quirino[82d], A. Moussa[36d], Y. Moyal[173], H. Moyano Gomez[13], E.J.W. Moyse[104], T.G. Mroz[87], S. Muanza[103], M. Mucha[25], J. Mueller[130], G.A. Mullier[165], A.J. Mullin[33], J.J. Mullin[51], A.C. Mullins[45], A.E. Mulski[61], D.P. Mungo[159], D. Munoz Perez[167], F.J. Munoz Sanchez[102], W.J. Murray[171,135], M. Muškinja[94], C. Mwewa[48], A.G. Myagkov[38,j], A.J. Myers[8], G. Myers[107], M. Myska[133], B.P. Nachman[147], K. Nagai[127], K. Nagano[83], R. Nagasaka[157], J.L. Nagle[30,ae], E. Nagy[103], A.M. Nairz[37], Y. Nakahama[83], K. Nakamura[83], K. Nakkalil[5], A. Nandi[63b], H. Nanjo[125], E.A. Narayanan[45], Y. Narukawa[157], I. Naryshkin[38], L. Nasella[71a,71b], S. Nasri[84c], C. Nass[25], G. Navarro[23a], A. Nayaz[19], P.Y. Nechaeva[38], S. Nechaeva[24b,24a], F. Nechansky[132], L. Nedic[127], T.J. Neep[21], A. Negri[73a,73b], M. Negrini[24b], C. Nellist[116], C. Nelson[105], K. Nelson[107], S. Nemecek[132], M. Nessi[37,af], M.S. Neubauer[166], J. Newell[93], P.R. Newman[21], Y.W.Y. Ng[166], B. Ngair[84b], H.D.N. Nguyen[109], J.D. Nichols[121], R.B. Nickerson[127], R. Nicolaidou[136], J. Nielsen[137], M. Niemeyer[55], J. Niermann[37], N. Nikiforou[37], V. Nikolaenko[38,j], I. Nikolic-Audit[128], P. Nilsson[30], I. Ninca[48], G. Ninio[155], A. Nisati[75a], R. Nisius[111], N. Nitika[173], E.K. Nkadimeng[34b], T. Nobe[157], D. Noll[147], T. Nommensen[151], M.B. Norfolk[143], B.J. Norman[35], L.C. Nosler[18a], M. Noury[36a], J. Novak[94], T. Novak[94], P. Novotny[173], R. Novotny[133], L. Nozka[123], K. Ntekas[163], D. Ntounis[147], N.M.J. Nunes De Moura Junior[82b], A.P. O'Neill[20], J. Ocariz[128], I. Ochoa[131a], A. Odella Rodriguez[13], S. Oerdek[48], J.T. Offermann[40], A. Ogrodnik[87], A. Oh[102], C.C. Ohm[148], H. Oide[83], M.L. Ojeda[37], Y. Okumura[157], L.F. Oleiro Seabra[131a], I. Oleksiyuk[56], G. Oliveira Correa[13], D. Oliveira Damazio[30], J.L. Oliver[1], R. Omar[68], Ö.O. Öncel[54], Y. Onoda[139], A. Onofre[131a,131e,ag], P.U.E. Onyisi[11], M.J. Oreglia[40], D. Orestano[77a,77b], R. Orlandini[77a,77b], R.S. Orr[159], L.M. Osojnak[42], Y. Osumi[112], G. Otero y Garzón[31], H. Otono[89], M. Ouchrif[36d], F. Ould-Saada[126], T. Ovsiannikova[140], M. Owen[59], R.E. Owen[135], V.E. Ozcan[22a], F. Ozturk[87], N. Ozturk[8], S. Ozturk[81], H.A. Pacey[127], K. Pachal[160a], A. Pacheco Pages[13], C. Padilla Aranda[13], G. Padovano[75a,75b], S. Pagan Griso[18a], J. Pampel[25], J. Pan[176], D.K. Panchal[11], C.E. Pandini[60], J.G. Panduro Vazquez[135], H.D. Pandya[1], H. Pang[136], P. Pani[48], G. Panizzo[69a,69c], L. Panwar[128], L. Paolozzi[56], S. Parajuli[166], A. Paramonov[6], C. Paraskevopoulos[53], D. Paredes Hernandez[64b], S.R. Paredes Saenz[52], A. Pareti[73a,73b], K.R. Park[42], T.H. Park[111], F. Parodi[57b,57a], J.A. Parsons[42], U. Parzefall[54], B. Pascual Dias[41], L. Pascual Dominguez[100], E. Pasqualucci[75a], S. Passaggio[57b], F. Pastore[96], P. Patel[87], U.M. Patel[51], J.R. Pater[102], T. Pauly[37], F. Pauwels[134], C.I. Pazos[162], M. Pedersen[126], R. Pedro[131a], S.V. Peleganchuk[38], O. Penc[132], S. Peng[15], G. D. Penn[176], K.E. Penski[110], M. Penzin[38], B.S. Peralva[82d], A.P. Pereira Peixoto[140], L. Pereira Sanchez[147], D.V. Perepelitsa[30,ae], G. Perera[104], E. Perez Codina[37], M. Perganti[10], H. Pernegger[37], S. Perrella[75a,75b], K. Peters[48], R.F.Y. Peters[102], B.A. Petersen[37], T.C. Petersen[43], E. Petit[103], V. Petousis[133], A. R. Petri[71a,71b], C. Petridou[156,z], T. Petru[134], M. Pettee[18a], A. Petukhov[81], K. Petukhova[37], R. Pezoa[138g], L. Pezzotti[24b,24a], G. Pezzullo[176], L. Pfaffenbichler[37], A. J. Pfleger[79], T. Pham[106], T.M. Pham[174], P.W. Phillips[135], G. Piacquadio[149], E. Pianori[18a],

JHEP07(2026)028

F. Piazza[124], R. Piegaia[31], D. Pietreanu[28b], A.D. Pilkington[102], M. Pinamonti[69a,69c], J.L. Pinfold[2], G. Pinheiro Matos[42], B.C. Pinheiro Pereira[131a], J. Pinol Bel[13], A. E. Pinto Pinoargote[128], L. Pintucci[69a,69c], K. M. Piper[150], A. Pirttikoski[56], D.A. Pizzi[35], L. Pizzimento[64b], A. Plebani[33], M.-A. Pleier[30], V. Pleskot[134], E. Plotnikova[39], G. Poddar[95], R. Poettgen[99], L. Poggioli[128], S. Polacek[134], G. Polesello[73a], A. Poley[146], A. Polini[24b], C.S. Pollard[171], Z.B. Pollock[120], E. Pompa Pacchi[121], N. I. Pond[97], D. Ponomarenko[68], L. Pontecorvo[37], S. Popa[28a], G.A. Popeneciu[28d], A. Poreba[37], D.M. Portillo Quintero[160a], S. Pospisil[133], M. A. Postill[143], P. Postolache[28c], K. Potamianos[171], P.A. Potepa[86a], I.N. Potrap[39], C.J. Potter[33], H. Potti[151], J. Poveda[167], M.E. Pozo Astigarraga[37], R. Pozzi[37], A. Prades Ibanez[76a,76b], S.R. Pradhan[143], J. Pretel[169], D. Price[102], M. Primavera[70a], L. Primomo[69a,69c], M.A. Principe Martin[100], R. Privara[123], T. Procter[86b], M.L. Proffitt[140], N. Proklova[129], K. Prokofiev[64c], G. Proto[111], J. Proudfoot[6], M. Przybycien[86a], W.W. Przygoda[86b], A. Psallidas[46], J.E. Puddefoot[143], D. Pudzha[53], H. I. Purnell[1], D. Pyatiizbyantseva[115], J. Qian[107], R. Qian[108], D. Qichen[127], Y. Qin[13], T. Qiu[52], A. Quadt[55], M. Queitsch-Maitland[102], G. Quetant[56], R.P. Quinn[168], G. Rabanal Bolanos[61], D. Rafanoharana[111], F. Raffaeli[76a,76b], F. Ragusa[71a,71b], J.L. Rainbolt[40], S. Rajagopalan[30], E. Ramakoti[39], L. Rambelli[57b,57a], I.A. Ramirez-Berend[35], K. Ran[107,113c], D. S. Rankin[129], N.P. Rapheeha[34j], H. Rasheed[28b], A. Rastogi[18a], S. Rave[101], S. Ravera[57b,57a], B. Ravina[37], I. Ravinovich[173], M. Raymond[37], A.L. Read[126], N.P. Readioff[143], D.M. Rebuzzi[73a,73b], A. S. Reed[59], K. Reeves[27], D. Reikher[37], A. Rej[49], C. Rembser[37], H. Ren[62], M. Renda[28b], F. Renner[48], A.G. Rennie[59], M. Repik[56], A.L. Rescia[57b,57a], S. Resconi[71a], M. Ressegotti[57b], S. Rettie[116], W.F. Rettie[35], M. M. Revering[33], E. Reynolds[18a], O.L. Rezanova[39], P. Reznicek[134], H. Riani[36d], N. Ribaric[51], B. Ricci[69a,69c], E. Ricci[78a,78b], R. Richter[111], S. Richter[47a,47b], E. Richter-Was[86b], M. Ridel[128], S. Ridouani[36d], P. Rieck[118], P. Riedler[37], E.M. Riefel[47a,47b], J. O. Rieger[116], M. Rijssenbeek[149], M. Rimoldi[34c], L. Rinaldi[24b,24a], P. Rincke[165,55], G. Ripellino[165], I. Riu[13], J.C. Rivera Vergara[169], F. Rizatdinova[122], E. Rizvi[95], B.R. Roberts[40], S.S. Roberts[137], D. Robinson[33], A. Robson[59], A. Rocchi[76a,76b], C. Roda[74a,74b], F.A. Rodriguez[117], S. Rodriguez Bosca[37], Y. Rodriguez Garcia[23a], A.M. Rodríguez Vera[117], S. Roe[37], J.T. Roemer[37], O. Røhne[126], R.A. Rojas[37], C.P.A. Roland[128], A. Romaniouk[79], E. Romano[73a,73b], M. Romano[24b], A.C. Romero Hernandez[166], N. Rompotis[93], L. Roos[128], S. Rosati[75a], B.J. Rosser[40], E. Rossi[127], E. Rossi[72a,72b], L.P. Rossi[61], L. Rossini[54], R. Rosten[120], M. Rotaru[28b], R. Roth[37], D. Rousseau[66], D. Rousso[48], S. Roy-Garand[159], A. Rozanov[103], Z. M. A. Rozario[59], Y. Rozen[154], A. Rubio Jimenez[167], V.H. Ruelas Rivera[19], T.A. Ruggeri[1], A. Ruggiero[127], A. Ruiz-Martinez[167], A. Rummler[37], G.B. Rupnik Boero[37], Z. Rurikova[54], N.A. Rusakovich[39], S. Ruscelli[49], H.L. Russell[169], G. Russo[75a,75b], J.P. Rutherfoord[7], S. Rutherford Colmenares[33], M. Rybar[134], P. Rybczynski[86a], A. Ryzhov[45], H.F-W. Sadrozinski[137], F. Safai Tehrani[75a], S. Saha[1], M. Sahinsoy[81], B. Sahoo[173], A. Saibel[167], B. T. Saifuddin[121], M. Saimpert[136], G.T. Saito[82c], M. Saito[157], T. Saito[157], A. Sala[71a,71b], A. Salnikov[147], J. Salt[167], A. Salvador Salas[155], F. Salvatore[150], A. Salzburger[37], D. Sammel[54], E. Sampson[92], D. Sampsonidis[156,z], D. Sampsonidou[124], M.A.A. Samy[59], J. Sánchez[167],

JHEP07(2026)028

V. Sanchez Sebastian[167], H. Sandaker[126], C.O. Sander[48], J.A. Sandesara[174], M. Sandhoff[175], C. Sandoval[23b], L. Sanfilippo[63a], D.P.C. Sankey[135], T. Sano[88], A. Sansoni[53], M. Santana Queiroz[18b], L. Santi[37], C. Santoni[41], H. Santos[131a,131b], A. Santra[173], E. Sanzani[24b,24a], K.A. Saoucha[84d], J.G. Saraiva[131a,131d], J. Sardain[7], O. Sasaki[83], K. Sato[161], C. Sauer[37], E. Sauvan[4], P. Savard[159,t], R. Sawada[157], C. Sawyer[135], L. Sawyer[98], A. M. Sayed[27], C. Sbarra[24b], A. Sbrizzi[24b,24a], T. Scanlon[97], J. Schaarschmidt[140], U. Schäfer[101], A.C. Schaffer[66,45], D. Schaile[110], R.D. Schamberger[149], C. Scharf[19], M.M. Schefer[20], V.A. Schegelsky[38], D. Scheirich[134], M. Schernau[138f], C. Scheulen[56], C. Schiavi[57b,57a], M. Schioppa[44b,44a], B. Schlag[147], S. Schlenker[37], J. Schmeing[175], E. Schmidt[111], M. A. Schmidt[175], K. Schmieden[25], C. Schmitt[101], N. Schmitt[101], S. Schmitt[48], N.A. Schneider[110], L. Schoeffel[136], A. Schoening[63b], P.G. Scholer[35], E. Schopf[145], M. Schott[25], S. Schramm[56], T. Schroer[56], H-C. Schultz-Coulon[63a], M. Schumacher[54], B.A. Schumm[137], Ph. Schune[136], H.R. Schwartz[7], A. Schwartzman[147], T.A. Schwarz[107], Ph. Schwemling[136], R. Schwienhorst[108], F.G. Sciacca[20], A. Sciandra[30], G. Sciolla[27], F. Scuri[74a], C.D. Sebastiani[37], K. Sedlaczek[117], S.C. Seidel[114], A. Seiden[137], B.D. Seidlitz[42], C. Seitz[48], J.M. Seixas[82b], G. Sekhniaidze[72a], L. Selem[60], N. Semprini-Cesari[24b,24a], A. Semushin[177], D. Sengupta[56], V. Senthilkumar[167], L. Serin[66], M. Sessa[72a,72b], H. Severini[121], F. Sforza[57b,57a], A. Sfyrla[56], Q. Sha[14], H. Shaddix[117], A.H. Shah[33], R. Shaheen[148], J.D. Shahinian[129], M. Shamim[37], L.Y. Shan[14], M. Shapiro[18a], A. Sharma[37], A.S. Sharma[168], P. Sharma[30], P.B. Shatalov[38], K. Shaw[150], S.M. Shaw[102], Q. Shen[14], D.J. Sheppard[146], P. Sherwood[97], L. Shi[97], X. Shi[14], S. Shimizu[83], I.P.J. Shipsey[127,†], S. Shirabe[89], M. Shiyakova[39,ah], M.J. Shochet[40], D.R. Shope[126], B. Shrestha[121], S. Shrestha[120,ai], I. Shreyber[39], M.J. Shroff[169], P. Sicho[132], A.M. Sickles[166], E. Sideras Haddad[34j,164], A. C. Sidley[116], A. Sidoti[24b], F. Siegert[50], Dj. Sijacki[16], F. Sili[62], J.M. Silva[52], I. Silva Ferreira[82b], M.V. Silva Oliveira[30], S.B. Silverstein[47a], S. Simion[66], R. Simoniello[37], E.L. Simpson[102], H. Simpson[150], L.R. Simpson[6], S. Simsek[81], S. Sindhu[55], P. Sinervo[159], S. Singh[30], S. N. Singh[27], S. Sinha[48], S. Sinha[102], M. Sioli[24b,24a], K. Sioulas[9], I. Siral[37], E. Sitnikova[48], J. Sjölin[47a,47b], A. Skaf[55], E. Skorda[21], P. Skubic[121], M. Slawinska[87], I. Slazyk[17], I. Sliusar[126], V. Smakhtin[173], B.H. Smart[135], S.Yu. Smirnov[138b], Y. Smirnov[34c], L.N. Smirnova[38,j], O. Smirnova[99], A.C. Smith[42], D.R. Smith[163], J.L. Smith[102], M. B. Smith[35], R. Smith[147], H. Smitmanns[101], M. Smizanska[92], K. Smolek[133], P. Smolyanskiy[133], A.A. Snesarev[39], H.L. Snoek[116], R. M. Snyder[51], S. Snyder[30], R. Sobie[169,n], A. Soffer[155], C.A. Solans Sanchez[37], E.Yu. Soldatov[39], U. Soldevila[167], A.A. Solodkov[34j], S. Solomon[27], A. Soloshenko[39], K. Solovieva[54], O.V. Solovyanov[41], P. Sommer[50], A. Sonay[13], A. Sopczak[133], A.L. Sopio[52], F. Sopkova[29b], J. D. Sorenson[114], I.R. Sotarriva Alvarez[139], V. Sothilingam[63a], O. J. Soto Sandoval[138c,138b], S. Sottocornola[68], R. Soualah[84a], Z. Soumaimi[36e], D. South[48], N. Soybelman[173], S. Spagnolo[70a,70b], D. Sperlich[54], B. Spisso[72a,72b], D.P. Spiteri[59], L. Splendori[103], M. Spousta[134], E.J. Staats[35], R. Stamen[63a], E. Stanecka[87], W. Stanek-Maslouska[48], M.V. Stange[50], B. Stanislaus[18a], M.M. Stanitzki[48], E.A. Starchenko[38], G.H. Stark[137], J. Stark[90], P. Staroba[132], P. Starovoitov[84d], R. Staszewski[87], C. Stauch[110],

JHEP07(2026)028

G. Stavropoulos[46], A. Stefl[37], A. Stein[101], P. Steinberg[30], B. Stelzer[146,160a], H.J. Stelzer[130], O. Stelzer[160a], H. Stenzel[58], T.J. Stevenson[150], G.A. Stewart[37], J.R. Stewart[122], G. Stoicea[28b], M. Stolarski[131a], S. Stonjek[111], A. Straessner[50], J. Strandberg[148], S. Strandberg[47a,47b], M. Stratmann[175], M. Strauss[121], T. Strebler[103], P. Strizenec[29b], R. Ströhmer[170], D.M. Strom[124], R. Stroynowski[45], A. Strubig[47a,47b], S.A. Stucci[30], B. Stugu[17], J. Stupak[121], N.A. Styles[48], D. Su[147], S. Su[62], X. Su[62], D. Suchy[29a], A. D. Sudhakar Ponnu[55], L. Sudit[173], K. Sugizaki[129], V.V. Sulin[38], D.M.S. Sultan[127], L. Sultanaliyeva[25], S. Sultansoy[3b], S. Sun[174], W. Sun[14], N. Sur[99], N. Suri Jr[176], M.R. Sutton[150], M. Svatos[132], P. N. Swallow[33], M. Swiatlowski[160a], A. Swoboda[37], I. Sykora[29a], M. Sykora[134], T. Sykora[134], D. Ta[101], K. Tackmann[48,aj], A. Taffard[163], R. Tafirout[160a], Y. Takubo[83], M. Talby[103], A.A. Talyshev[38], K.C. Tam[64b], N.M. Tamir[155], A. Tanaka[157], J. Tanaka[157], R. Tanaka[66], M. Tanasini[149], Z. Tao[168], S. Tapia Araya[138g], S. Tapprogge[101], A. Tarek Abouelfadl Mohamed[37], S. Tarem[154], K. Tariq[14], G. Tarna[37], G.F. Tartarelli[71a], M. J. Tartarin[90], P. Tas[134], M. Tasevsky[132], E. Tassi[44b,44a], A.C. Tate[166], Y. Tayalati[36e,ak], G.N. Taylor[106], W. Taylor[160b], R.J. Taylor Vara[167], A.S. Tegetmeier[90], P. Teixeira-Dias[96], J.J. Teoh[159], K. Terashi[157], J. Terron[100], S. Terzo[13], M. Testa[53], R.J. Teuscher[159,n], A. Thaler[79], O. Theiner[56], T. Theveneaux-Pelzer[103], D.W. Thomas[96], J.P. Thomas[21], E.A. Thompson[18a], P.D. Thompson[21], E. Thomson[129], R. E. Thornberry[45], C. Tian[62], Y. Tian[56], V. Tikhomirov[81], Yu.A. Tikhonov[39], S. Timoshenko[38], D. Timoshyn[134], E.X.L. Ting[1], P. Tipton[176], A. Tishelman-Charny[30], K. Todome[139], S. Todorova-Nova[134], L. Toffolin[69a,69c], M. Togawa[83], J. Tojo[89], S. Tokár[29a], O. Toldaiev[68], G. Tolkachev[103], M. Tomoto[83], L. Tompkins[147,al], E. Torrence[124], H. Torres[90], D. I. Torres Arza[138g], E. Torró Pastor[167], M. Toscani[31], C. Tosciri[40], M. Tost[11], D.R. Tovey[143], T. Trefzger[170], P.M. Tricarico[13], A. Tricoli[30], I.M. Trigger[160a], S. Trincaz-Duvoid[128], D.A. Trischuk[169], A. Tropina[39], D. Truncali[76a,76b], L. Truong[34c], M. Trzebinski[87], A. Trzupek[87], F. Tsai[149], M. Tsai[107], A. Tsiamis[156], P.V. Tsiareshka[39], S. Tsigaridas[160a], A. Tsirigotis[156,aa], V. Tsiskaridze[153a], E.G. Tskhadadze[153a], Y. Tsujikawa[88], I.I. Tsukerman[38], V. Tsulaia[18a], S. Tsuno[83], K. Tsuri[119], D. Tsybychev[149], Y. Tu[64b], A. Tudorache[28b], V. Tudorache[28b], S. B. Tuncay[127], S. Turchikhin[57b,57a], I. Turk Cakir[3a], R. Turra[71a], T. Turtuvshin[39,am], P.M. Tuts[42], S. Tzamarias[156,z], Y. Uematsu[83], F. Ukegawa[161], P.A. Ulloa Poblete[138c,138b], E.N. Umaka[30], G. Unal[37], A. Undrus[30], G. Unel[163], J. Urban[29b], P. Urrejola[138e], G. Usai[8], R. Ushioda[158], M. Usman[109], F. Ustuner[52], Z. Uysal[81], V. Vacek[133], B. Vachon[105], T. Vafeiadis[37], A. Vaitkus[97], C. Valderanis[110], E. Valdes Santurio[47a,47b], M. Valente[37], S. Valentinetti[24b,24a], A. Valero[167], E. Valiente Moreno[167], A. Vallier[90], J.A. Valls Ferrer[167], D. R. Van Arneman[116], A. Van Der Graaf[49], H. Z. Van Der Schyf[34j], P. Van Gemmeren[6], M. Van Rijnbach[37], S. Van Stroud[97], I. Van Vulpen[116], P. Vana[134], M. Vanadia[76a,76b], U. M. Vande Voorde[148], W. Vandelli[37], E.R. Vandewall[147], D. Vannicola[155], L. Vannoli[53], R. Vari[75a], M. Varma[176], E.W. Varnes[7], C. Varni[79], D. Varouchas[66], L. Varriale[167], K.E. Varvell[151], M.E. Vasile[28b], L. Vaslin[83], M. D. Vassilev[147], A. Vasyukov[39], L. M. Vaughan[122], R. Vavricka[134], T. Vazquez Schroeder[13], J. Veatch[32], V. Vecchio[102], M.J. Veen[104], I. Veliscek[30], I. Velkovska[94], L.M. Veloce[159], F. Veloso[131a,131c], A.G. Veltman[52], S.H. Venetianer[162],

JHEP07(2026)028

S. Veneziano[75a], A. Ventura[70a,70b], A. Verbytskyi[111], M. Verducci[74a,74b], C. Vergis[95], M. Verissimo De Araujo[82b], W. Verkerke[116], J.C. Vermeulen[116], C. Vernieri[147], M. Vessella[163], M.C. Vetterli[146,t], A. Vgenopoulos[101], N. Viaux Maira[138g,an], T. Vickey[143], O.E. Vickey Boeriu[143], G.H.A. Viehhauser[127], L. Vigani[63b], M. Vigl[111], M. Villa[24b,24a], M. Villaplana Perez[167], E.M. Villhauer[40], E. Vilucchi[53], M. Vincent[167], M.G. Vincter[35], A. Visibile[116], A. Visive[116], C. Vittori[37], I. Vivarelli[24b,24a], M.I. Vivas Albornoz[48], E. Voevodina[111], F. Vogel[110], J.C. Voigt[50], P. Vokac[133], Yu. Volkotrub[86b], L. Vomberg[25], E. Von Toerne[25], B. Vormwald[37], K. Vorobev[51], M. Vos[167], K. Voss[145], M. Vozak[37], L. Vozdecky[121], N. Vranjes[16], M. Vranjes Milosavljevic[16], M. Vreeswijk[116], N.K. Vu[142b,142a], R. Vuillermet[37], O. Vujinovic[101], I. Vukotic[40], I. K. Vyas[35], J.F. Wack[33], S. Wada[161], C. Wagner[147], J.M. Wagner[18a], W. Wagner[175], S. Wahdan[175], H. Wahlberg[91], C. H. Waits[121], J. Walder[135], R. Walker[110], K. Walkingshaw Pass[59], W. Walkowiak[145], A. Wall[129], E.J. Wallin[99], T. Wamorkar[18a], K. Wandall-Christensen[167], A. Wang[62], A.Z. Wang[137], C. Wang[48], C. Wang[11], H. Wang[18a], J. Wang[64c], P. Wang[102], P. Wang[97], R. Wang[61], R. Wang[6], S. Wang[14], S.M. Wang[152], T. Wang[115], T. Wang[62], W. Wang[14], W.T. Wang[127], X. Wang[166], X. Wang[142a], X. Wang[48], Y. Wang[149], Y. Wang[114], Z. Wang[107], Z. Wang[142b], Z. Wang[107], C. Wanotayaroj[83], A. Warburton[105], A.L. Warnerbring[145], S. Waterhouse[96], A.T. Watson[21], H. Watson[52], M.F. Watson[21], E. Watton[37], G. Watts[140], B.M. Waugh[97], J. M. Webb[54], C. Weber[30], M.S. Weber[20], S.M. Weber[63a], C. Wei[62], Y. Wei[54], A.R. Weidberg[127], E.J. Weik[118], J. Weingarten[49], C. Weiser[54], C.J. Wells[48], T. Wenaus[30], T. Wengler[37], N.S. Wenke[111], N. Wermes[25], M. Wessels[63a], A.M. Wharton[92], A. White[8], A.S. White[61], M.J. White[1], D. Whiteson[163], L. Wickremasinghe[125], W. Wiedenmann[174], M. Wielers[135], R. Wierda[148], C. Wiglesworth[43], H.G. Wilkens[37], J. J. H. Wilkinson[33], D.M. Williams[42], H.H. Williams[129], S. Williams[33], S. Willocq[104], B.J. Wilson[102], D.J. Wilson[102], P.J. Windischhofer[40], F.I. Winkel[31], F. Winklmeier[124], B.T. Winter[54], M. Wittgen[147], M. Wobisch[98], T. Wojtkowski[60], Z. Wolffs[116], J. Wollrath[37], M.W. Wolter[87], H. Wolters[131a,131c], M.C. Wong[137], E.L. Woodward[42], S.D. Worm[48], B.K. Wosiek[87], K.W. Woźniak[87], S. Wozniewski[55], K. Wraight[59], C. Wu[159], C. Wu[21], J. Wu[157], M. Wu[113b], M. Wu[115], S. Wu[14,ao], S.L. Wu[174], X. Wu[62], Y. Wu[62], Y.Q. Wu[159], Z. Wu[4], Z. Wu[113a], J. Wuerzinger[111], T.R. Wyatt[102], B.M. Wynne[52], S. Xella[43], L. Xia[113a], M. Xie[62], A. Xiong[124], D. Xu[14], H. Xu[62], L. Xu[62], R. Xu[129], T. Xu[107], W. Xu[113a], Y. Xu[140], Z. Xu[52], R. Xue[130], B. Yabsley[151], S. Yacoob[34a], Y. Yamaguchi[83], E. Yamashita[157], H. Yamauchi[161], T. Yamazaki[18a], Y. Yamazaki[85], S. Yan[59], Z. Yan[104], H.J. Yang[142a,142b], H.T. Yang[62], S. Yang[62], T. Yang[64c], X. Yang[37], X. Yang[14], Y. Yang[157], Y. Yang[62], W-M. Yao[18a], C. L. Yardley[150], J. Ye[14], S. Ye[30], X. Ye[62], Y. Yeh[97], I. Yeletskikh[39], B. Yeo[18b], M.R. Yexley[97], T. P. Yildirim[127], K. Yorita[172], C. Young[147], C.J.S. Young[37], I.N.L. Young[59], N.D. Young[124], Y. Yu[62], J. Yuan[14,113c,ao], M. Yuan[107], R. Yuan[142b], L. Yue[97], M. Zaazoua[62], B. Zabinski[87], I. Zahir[36a], A. Zaio[57b,57a], Z.K. Zak[87], T. Zakareishvili[167], S. Zambito[56], J.A. Zamora Saa[138d], J. Zang[157], R. Zanzottera[71a,71b], O. Zaplatilek[133], C. Zeitnitz[175], H. Zeng[14], D.T. Zenger Jr[27], O. Zenin[38], T. Ženiš[29a], S. Zenz[95], D. Zerwas[66], B. Zhang[171], D.F. Zhang[143], G. Zhang[14,ao], J. Zhang[141a], J. Zhang[6], L. Zhang[62], L. Zhang[113a],

JHEP07(2026)028

P. Zhang[14,113c], R. Zhang[113a], S. Zhang[90], T. Zhang[157], Y. Zhang[140], Y. Zhang[97], Y. Zhang[62], Y. Zhang[113a], Z. Zhang[18a], Z. Zhang[141a], Z. Zhang[66], H. Zhao[140], T. Zhao[141a], Y. Zhao[35], Z. Zhao[62], Z. Zhao[62], A. Zhemchugov[39], J. Zheng[113a], K. Zheng[166], X. Zheng[62], Z. Zheng[147], D. Zhong[166], B. Zhou[107], B. Zhou[142b,142a], H. Zhou[7], N. Zhou[142a], Y. Zhou[15], Y. Zhou[113a], Y. Zhou[7], J. Zhu[107], X. Zhu[142b], Y. Zhu[142a], Y. Zhu[62], X. Zhuang[14], K. Zhukov[68], N.I. Zimine[39], J. Zinsser[63b], M. Ziolkowski[145], L. Živković[16], A. Zoccoli[24b,24a], K. Zoch[61], A. Zografos[37], T.G. Zorbas[143], O. Zormpa[46], L. Zwalinski[37]

[1] *Department of Physics, University of Adelaide, Adelaide, Australia*
[2] *Department of Physics, University of Alberta, Edmonton AB, Canada*
[3a] *Department of Physics, Ankara University, Ankara, Türkiye*
[3b] *Division of Physics, TOBB University of Economics and Technology, Ankara, Türkiye*
[4] *LAPP, Université Savoie Mont Blanc, CNRS/IN2P3, Annecy, France*
[5] *APC, Université Paris Cité, CNRS/IN2P3, Paris, France*
[6] *High Energy Physics Division, Argonne National Laboratory, Argonne IL, United States of America*
[7] *Department of Physics, University of Arizona, Tucson AZ, United States of America*
[8] *Department of Physics, University of Texas at Arlington, Arlington TX, United States of America*
[9] *Physics Department, National and Kapodistrian University of Athens, Athens, Greece*
[10] *Physics Department, National Technical University of Athens, Zografou, Greece*
[11] *Department of Physics, University of Texas at Austin, Austin TX, United States of America*
[12] *Institute of Physics, Azerbaijan Academy of Sciences, Baku, Azerbaijan*
[13] *Institut de Física d'Altes Energies (IFAE), Barcelona Institute of Science and Technology, Barcelona, Spain*
[14] *Institute of High Energy Physics, Chinese Academy of Sciences, Beijing, China*
[15] *Physics Department, Tsinghua University, Beijing, China*
[16] *Institute of Physics, University of Belgrade, Belgrade, Serbia*
[17] *Department for Physics and Technology, University of Bergen, Bergen, Norway*
[18a] *Physics Division, Lawrence Berkeley National Laboratory, Berkeley CA, United States of America*
[18b] *University of California, Berkeley CA, United States of America*
[19] *Institut für Physik, Humboldt Universität zu Berlin, Berlin, Germany*
[20] *Albert Einstein Center for Fundamental Physics and Laboratory for High Energy Physics, University of Bern, Bern, Switzerland*
[21] *School of Physics and Astronomy, University of Birmingham, Birmingham, United Kingdom*
[22a] *Department of Physics, Bogazici University, Istanbul, Türkiye*
[22b] *Department of Physics Engineering, Gaziantep University, Gaziantep, Türkiye*
[22c] *Department of Physics, Istanbul University, Istanbul, Türkiye*
[23a] *Facultad de Ciencias y Centro de Investigaciónes, Universidad Antonio Nariño, Bogotá, Colombia*
[23b] *Departamento de Física, Universidad Nacional de Colombia, Bogotá, Colombia*
[24a] *Dipartimento di Fisica e Astronomia A. Righi, Università di Bologna, Bologna, Italy*
[24b] *INFN Sezione di Bologna, Italy*
[25] *Physikalisches Institut, Universität Bonn, Bonn, Germany*
[26] *Department of Physics, Boston University, Boston MA, United States of America*
[27] *Department of Physics, Brandeis University, Waltham MA, United States of America*
[28a] *Transilvania University of Brasov, Brasov, Romania*
[28b] *Horia Hulubei National Institute of Physics and Nuclear Engineering, Bucharest, Romania*
[28c] *Department of Physics, Alexandru Ioan Cuza University of Iasi, Iasi, Romania*
[28d] *National Institute for Research and Development of Isotopic and Molecular Technologies, Physics Department, Cluj-Napoca, Romania*
[28e] *National University of Science and Technology Politechnica, Bucharest, Romania*
[28f] *West University in Timisoara, Timisoara, Romania*
[28g] *Faculty of Physics, University of Bucharest, Bucharest, Romania*

JHEP07(2026)028

[29a] Faculty of Mathematics, Physics and Informatics, Comenius University, Bratislava, Slovak Republic
[29b] Department of Subnuclear Physics, Institute of Experimental Physics of the Slovak Academy of Sciences, Kosice, Slovak Republic
[30] Physics Department, Brookhaven National Laboratory, Upton NY, United States of America
[31] Universidad de Buenos Aires, Facultad de Ciencias Exactas y Naturales, Departamento de Física, y CONICET, Instituto de Física de Buenos Aires (IFIBA), Buenos Aires, Argentina
[32] California State University, CA, United States of America
[33] Cavendish Laboratory, University of Cambridge, Cambridge, United Kingdom
[34a] Department of Physics, University of Cape Town, Cape Town, South Africa
[34b] iThemba Labs, Western Cape, South Africa
[34c] Department of Mechanical Engineering Science, University of Johannesburg, Johannesburg, South Africa
[34d] National Institute of Physics, University of the Philippines Diliman (Philippines), Philippines
[34e] Department of Physics, Stellenbosch University, Matieland, South Africa
[34f] University of KwaZulu-Natal, School of Agriculture and Science, Mathematics, Westville, South Africa
[34g] University of South Africa, Department of Physics, Pretoria, South Africa
[34h] University of Pretoria, Department of Mechanical and Aeronautical Engineering, Pretoria, South Africa
[34i] University of Zululand, KwaDlangezwa, South Africa
[34j] School of Physics, University of the Witwatersrand, Johannesburg, South Africa
[35] Department of Physics, Carleton University, Ottawa ON, Canada
[36a] Faculté des Sciences Ain Chock, Université Hassan II de Casablanca, Morocco
[36b] Faculté des Sciences, Université Ibn-Tofail, Kénitra, Morocco
[36c] Faculté des Sciences Semlalia, Université Cadi Ayyad, LPHEA-Marrakech, Morocco
[36d] LPMR, Faculté des Sciences, Université Mohamed Premier, Oujda, Morocco
[36e] Faculté des sciences, Université Mohammed V, Rabat, Morocco
[36f] Institute of Applied Physics, Mohammed VI Polytechnic University, Ben Guerir, Morocco
[37] CERN, Geneva, Switzerland
[38] Affiliated with an institute formerly covered by a cooperation agreement with CERN
[39] Affiliated with an international laboratory covered by a cooperation agreement with CERN
[40] Enrico Fermi Institute, University of Chicago, Chicago IL, United States of America
[41] LPC, Université Clermont Auvergne, CNRS/IN2P3, Clermont-Ferrand, France
[42] Nevis Laboratory, Columbia University, Irvington NY, United States of America
[43] Niels Bohr Institute, University of Copenhagen, Copenhagen, Denmark
[44a] Dipartimento di Fisica, Università della Calabria, Rende, Italy
[44b] INFN Gruppo Collegato di Cosenza, Laboratori Nazionali di Frascati, Italy
[45] Physics Department, Southern Methodist University, Dallas TX, United States of America
[46] National Centre for Scientific Research "Demokritos", Agia Paraskevi, Greece
[47a] Department of Physics, Stockholm University, Sweden
[47b] Oskar Klein Centre, Stockholm, Sweden
[48] Deutsches Elektronen-Synchrotron DESY, Hamburg and Zeuthen, Germany
[49] Fakultät Physik, Technische Universität Dortmund, Dortmund, Germany
[50] Institut für Kern- und Teilchenphysik, Technische Universität Dresden, Dresden, Germany
[51] Department of Physics, Duke University, Durham NC, United States of America
[52] SUPA - School of Physics and Astronomy, University of Edinburgh, Edinburgh, United Kingdom
[53] INFN e Laboratori Nazionali di Frascati, Frascati, Italy
[54] Physikalisches Institut, Albert-Ludwigs-Universität Freiburg, Freiburg, Germany
[55] II. Physikalisches Institut, Georg-August-Universität Göttingen, Göttingen, Germany
[56] Département de Physique Nucléaire et Corpusculaire, Université de Genève, Genève, Switzerland
[57a] Dipartimento di Fisica, Università di Genova, Genova, Italy
[57b] INFN Sezione di Genova, Italy
[58] II. Physikalisches Institut, Justus-Liebig-Universität Giessen, Giessen, Germany
[59] SUPA - School of Physics and Astronomy, University of Glasgow, Glasgow, United Kingdom
[60] LPSC, Université Grenoble Alpes, CNRS/IN2P3, Grenoble INP, Grenoble, France

JHEP07(2026)028

[61] *Laboratory for Particle Physics and Cosmology, Harvard University, Cambridge MA, United States of America*
[62] *Department of Modern Physics and State Key Laboratory of Particle Detection and Electronics, University of Science and Technology of China, Hefei, China*
[63a] *Kirchhoff-Institut für Physik, Ruprecht-Karls-Universität Heidelberg, Heidelberg, Germany*
[63b] *Physikalisches Institut, Ruprecht-Karls-Universität Heidelberg, Heidelberg, Germany*
[64a] *Department of Physics, Chinese University of Hong Kong, Shatin, N.T., Hong Kong, China*
[64b] *Department of Physics, University of Hong Kong, Hong Kong, China*
[64c] *Department of Physics and Institute for Advanced Study, Hong Kong University of Science and Technology, Clear Water Bay, Kowloon, Hong Kong, China*
[65] *Department of Physics, National Tsing Hua University, Hsinchu, Taiwan*
[66] *IJCLab, Université Paris-Saclay, CNRS/IN2P3, 91405, Orsay, France*
[67] *Centro Nacional de Microelectrónica (IMB-CNM-CSIC), Barcelona, Spain*
[68] *Department of Physics, Indiana University, Bloomington IN, United States of America*
[69a] *INFN Gruppo Collegato di Udine, Sezione di Trieste, Udine, Italy*
[69b] *ICTP, Trieste, Italy*
[69c] *Dipartimento Politecnico di Ingegneria e Architettura, Università di Udine, Udine, Italy*
[70a] *INFN Sezione di Lecce, Italy*
[70b] *Dipartimento di Matematica e Fisica, Università del Salento, Lecce, Italy*
[71a] *INFN Sezione di Milano, Italy*
[71b] *Dipartimento di Fisica, Università di Milano, Milano, Italy*
[72a] *INFN Sezione di Napoli, Italy*
[72b] *Dipartimento di Fisica, Università di Napoli, Napoli, Italy*
[73a] *INFN Sezione di Pavia, Italy*
[73b] *Dipartimento di Fisica, Università di Pavia, Pavia, Italy*
[74a] *INFN Sezione di Pisa, Italy*
[74b] *Dipartimento di Fisica E. Fermi, Università di Pisa, Pisa, Italy*
[75a] *INFN Sezione di Roma, Italy*
[75b] *Dipartimento di Fisica, Sapienza Università di Roma, Roma, Italy*
[76a] *INFN Sezione di Roma Tor Vergata, Italy*
[76b] *Dipartimento di Fisica, Università di Roma Tor Vergata, Roma, Italy*
[77a] *INFN Sezione di Roma Tre, Italy*
[77b] *Dipartimento di Matematica e Fisica, Università Roma Tre, Roma, Italy*
[78a] *INFN-TIFPA, Italy*
[78b] *Università degli Studi di Trento, Trento, Italy*
[79] *Universität Innsbruck, Department of Astro and Particle Physics, Innsbruck, Austria*
[80] *Department of Physics and Astronomy, Iowa State University, Ames IA, United States of America*
[81] *Istinye University, Sariyer, Istanbul, Türkiye*
[82a] *Departamento de Engenharia Elétrica, Universidade Federal de Juiz de Fora (UFJF), Juiz de Fora, Brazil*
[82b] *Universidade Federal do Rio De Janeiro COPPE/EE/IF, Rio de Janeiro, Brazil*
[82c] *Instituto de Física, Universidade de São Paulo, São Paulo, Brazil*
[82d] *Rio de Janeiro State University, Rio de Janeiro, Brazil*
[82e] *Federal University of Bahia, Bahia, Brazil*
[83] *KEK, High Energy Accelerator Research Organization, Tsukuba, Japan*
[84a] *Khalifa University of Science and Technology, Abu Dhabi, United Arab Emirates*
[84b] *New York University Abu Dhabi, Abu Dhabi, United Arab Emirates*
[84c] *United Arab Emirates University, Al Ain, United Arab Emirates*
[84d] *University of Sharjah, Sharjah, United Arab Emirates*
[85] *Graduate School of Science, Kobe University, Kobe, Japan*
[86a] *AGH University of Krakow, Faculty of Physics and Applied Computer Science, Krakow, Poland*
[86b] *Marian Smoluchowski Institute of Physics, Jagiellonian University, Krakow, Poland*
[87] *Institute of Nuclear Physics Polish Academy of Sciences, Krakow, Poland*
[88] *Faculty of Science, Kyoto University, Kyoto, Japan*

JHEP07(2026)028

[89] *Research Center for Advanced Particle Physics and Department of Physics, Kyushu University, Fukuoka, Japan*
[90] *L2IT, Université de Toulouse, CNRS/IN2P3, UPS, Toulouse, France*
[91] *Instituto de Física La Plata, Universidad Nacional de La Plata and CONICET, La Plata, Argentina*
[92] *Physics Department, Lancaster University, Lancaster, United Kingdom*
[93] *Oliver Lodge Laboratory, University of Liverpool, Liverpool, United Kingdom*
[94] *Department of Experimental Particle Physics, Jožef Stefan Institute and Department of Physics, University of Ljubljana, Ljubljana, Slovenia*
[95] *Department of Physics and Astronomy, Queen Mary University of London, London, United Kingdom*
[96] *Department of Physics, Royal Holloway University of London, Egham, United Kingdom*
[97] *Department of Physics and Astronomy, University College London, London, United Kingdom*
[98] *Louisiana Tech University, Ruston LA, United States of America*
[99] *Fysiska institutionen, Lunds universitet, Lund, Sweden*
[100] *Departamento de Física Teorica C-15 and CIAFF, Universidad Autónoma de Madrid, Madrid, Spain*
[101] *Institut für Physik, Universität Mainz, Mainz, Germany*
[102] *School of Physics and Astronomy, University of Manchester, Manchester, United Kingdom*
[103] *CPPM, Aix-Marseille Université, CNRS/IN2P3, Marseille, France*
[104] *Department of Physics, University of Massachusetts, Amherst MA, United States of America*
[105] *Department of Physics, McGill University, Montreal QC, Canada*
[106] *School of Physics, University of Melbourne, Victoria, Australia*
[107] *Department of Physics, University of Michigan, Ann Arbor MI, United States of America*
[108] *Department of Physics and Astronomy, Michigan State University, East Lansing MI, United States of America*
[109] *Group of Particle Physics, University of Montreal, Montreal QC, Canada*
[110] *Fakultät für Physik, Ludwig-Maximilians-Universität München, München, Germany*
[111] *Max-Planck-Institut für Physik (Werner-Heisenberg-Institut), München, Germany*
[112] *Graduate School of Science and Kobayashi-Maskawa Institute, Nagoya University, Nagoya, Japan*
[113a] *Department of Physics, Nanjing University, Nanjing, China*
[113b] *School of Science, Shenzhen Campus of Sun Yat-sen University, China*
[113c] *University of Chinese Academy of Science (UCAS), Beijing, China*
[114] *Department of Physics and Astronomy, University of New Mexico, Albuquerque NM, United States of America*
[115] *Institute for Mathematics, Astrophysics and Particle Physics, Radboud University/Nikhef, Nijmegen, Netherlands*
[116] *Nikhef National Institute for Subatomic Physics and University of Amsterdam, Amsterdam, Netherlands*
[117] *Department of Physics, Northern Illinois University, DeKalb IL, United States of America*
[118] *Department of Physics, New York University, New York NY, United States of America*
[119] *Ochanomizu University, Otsuka, Bunkyo-ku, Tokyo, Japan*
[120] *Ohio State University, Columbus OH, United States of America*
[121] *Homer L. Dodge Department of Physics and Astronomy, University of Oklahoma, Norman OK, United States of America*
[122] *Department of Physics, Oklahoma State University, Stillwater OK, United States of America*
[123] *Palacký University, Joint Laboratory of Optics, Olomouc, Czech Republic*
[124] *Institute for Fundamental Science, University of Oregon, Eugene, OR, United States of America*
[125] *Graduate School of Science, University of Osaka, Osaka, Japan*
[126] *Department of Physics, University of Oslo, Oslo, Norway*
[127] *Department of Physics, Oxford University, Oxford, United Kingdom*
[128] *LPNHE, Sorbonne Université, Université Paris Cité, CNRS/IN2P3, Paris, France*
[129] *Department of Physics, University of Pennsylvania, Philadelphia PA, United States of America*
[130] *Department of Physics and Astronomy, University of Pittsburgh, Pittsburgh PA, United States of America*
[131a] *Laboratório de Instrumentação e Física Experimental de Partículas - LIP, Lisboa, Portugal*
[131b] *Departamento de Física, Faculdade de Ciências, Universidade de Lisboa, Lisboa, Portugal*
[131c] *Departamento de Física, Universidade de Coimbra, Coimbra, Portugal*

JHEP07(2026)028

[131d] Centro de Física Nuclear da Universidade de Lisboa, Lisboa, Portugal
[131e] Departamento de Física, Escola de Ciências, Universidade do Minho, Braga, Portugal
[131f] Departamento de Física Teórica y del Cosmos, Universidad de Granada, Granada (Spain), Spain
[131g] Departamento de Física, Instituto Superior Técnico, Universidade de Lisboa, Lisboa, Portugal
[132] Institute of Physics of the Czech Academy of Sciences, Prague, Czech Republic
[133] Czech Technical University in Prague, Prague, Czech Republic
[134] Charles University, Faculty of Mathematics and Physics, Prague, Czech Republic
[135] Particle Physics Department, Rutherford Appleton Laboratory, Didcot, United Kingdom
[136] IRFU, CEA, Université Paris-Saclay, Gif-sur-Yvette, France
[137] Santa Cruz Institute for Particle Physics, University of California Santa Cruz, Santa Cruz CA, United States of America
[138a] Departamento de Física, Pontificia Universidad Católica de Chile, Santiago, Chile
[138b] Millennium Institute for Subatomic physics at high energy frontier (SAPHIR), Santiago, Chile
[138c] Instituto de Investigación Multidisciplinario en Ciencia y Tecnología, y Departamento de Física, Universidad de La Serena, Chile
[138d] Universidad Andres Bello, Department of Physics, Santiago, Chile
[138e] Universidad San Sebastian, Recoleta, Chile
[138f] Instituto de Alta Investigación, Universidad de Tarapacá, Arica, Chile
[138g] Departamento de Física, Universidad Técnica Federico Santa María, Valparaíso, Chile
[139] Department of Physics, Institute of Science, Tokyo, Japan
[140] Department of Physics, University of Washington, Seattle WA, United States of America
[141a] Institute of Frontier and Interdisciplinary Science and Key Laboratory of Particle Physics and Particle Irradiation (MOE), Shandong University, Qingdao, China
[141b] School of Physics, Zhengzhou University, China
[142a] State Key Laboratory of Dark Matter Physics, School of Physics and Astronomy, Shanghai Jiao Tong University, Key Laboratory for Particle Astrophysics and Cosmology (MOE), SKLPPC, Shanghai, China
[142b] State Key Laboratory of Dark Matter Physics, Tsung-Dao Lee Institute, Shanghai Jiao Tong University, Shanghai, China
[143] Department of Physics and Astronomy, University of Sheffield, Sheffield, United Kingdom
[144] Department of Physics, Shinshu University, Nagano, Japan
[145] Department Physik, Universität Siegen, Siegen, Germany
[146] Department of Physics, Simon Fraser University, Burnaby BC, Canada
[147] SLAC National Accelerator Laboratory, Stanford CA, United States of America
[148] Department of Physics, Royal Institute of Technology, Stockholm, Sweden
[149] Departments of Physics and Astronomy, Stony Brook University, Stony Brook NY, United States of America
[150] Department of Physics and Astronomy, University of Sussex, Brighton, United Kingdom
[151] School of Physics, University of Sydney, Sydney, Australia
[152] Institute of Physics, Academia Sinica, Taipei, Taiwan
[153a] E. Andronikashvili Institute of Physics, Iv. Javakhishvili Tbilisi State University, Tbilisi, Georgia
[153b] High Energy Physics Institute, Tbilisi State University, Tbilisi, Georgia
[153c] University of Georgia, Tbilisi, Georgia
[154] Department of Physics, Technion, Israel Institute of Technology, Haifa, Israel
[155] Raymond and Beverly Sackler School of Physics and Astronomy, Tel Aviv University, Tel Aviv, Israel
[156] Department of Physics, Aristotle University of Thessaloniki, Thessaloniki, Greece
[157] International Center for Elementary Particle Physics and Department of Physics, University of Tokyo, Tokyo, Japan
[158] Graduate School of Science and Technology, Tokyo Metropolitan University, Tokyo, Japan
[159] Department of Physics, University of Toronto, Toronto ON, Canada
[160a] TRIUMF, Vancouver BC, Canada
[160b] Department of Physics and Astronomy, York University, Toronto ON, Canada
[161] Division of Physics and Tomonaga Center for the History of the Universe, Faculty of Pure and Applied Sciences, University of Tsukuba, Tsukuba, Japan

JHEP07(2026)028

[162] Department of Physics and Astronomy, Tufts University, Medford MA, United States of America
[163] Department of Physics and Astronomy, University of California Irvine, Irvine CA, United States of America
[164] University of West Attica, Athens, Greece
[165] Department of Physics and Astronomy, University of Uppsala, Uppsala, Sweden
[166] Department of Physics, University of Illinois, Urbana IL, United States of America
[167] Instituto de Física Corpuscular (IFIC), Centro Mixto Universidad de Valencia - CSIC, Valencia, Spain
[168] Department of Physics, University of British Columbia, Vancouver BC, Canada
[169] Department of Physics and Astronomy, University of Victoria, Victoria BC, Canada
[170] Fakultät für Physik und Astronomie, Julius-Maximilians-Universität Würzburg, Würzburg, Germany
[171] Department of Physics, University of Warwick, Coventry, United Kingdom
[172] Waseda University, Tokyo, Japan
[173] Department of Particle Physics and Astrophysics, Weizmann Institute of Science, Rehovot, Israel
[174] Department of Physics, University of Wisconsin, Madison WI, United States of America
[175] Fakultät für Mathematik und Naturwissenschaften, Fachgruppe Physik, Bergische Universität Wuppertal, Wuppertal, Germany
[176] Department of Physics, Yale University, New Haven CT, United States of America
[177] Yerevan Physics Institute, Yerevan, Armenia

[a] Also at Department of Physics, King's College London, London, United Kingdom
[b] Also at Institute of Physics, Azerbaijan Academy of Sciences, Baku, Azerbaijan
[c] Also at Imam Mohammad Ibn Saud Islamic University, Saudi Arabia
[d] Also at Department of Physics, University of Thessaly, Greece
[e] Also at An-Najah National University, Nablus, Palestine
[f] Also at Department of Physics, University of Fribourg, Fribourg, Switzerland
[g] Also at Department of Physics, Westmont College, Santa Barbara, United States of America
[h] Also at Departament de Fisica de la Universitat Autonoma de Barcelona, Barcelona, Spain
[i] Also at University of Siena, Italy
[j] Also at Affiliated with an institute formerly covered by a cooperation agreement with CERN
[k] Also at The Collaborative Innovation Center of Quantum Matter (CICQM), Beijing, China
[l] Also at Faculty of Physics, Sofia University, 'St. Kliment Ohridski', Sofia, Bulgaria
[m] Also at Università di Napoli Parthenope, Napoli, Italy
[n] Also at Institute of Particle Physics (IPP), Canada
[o] Also at Department of Physics, Bolu Abant Izzet Baysal University, Bolu, Türkiye
[p] Also at Faculty of Physics, University of Bucharest, Romania
[q] Also at Borough of Manhattan Community College, City University of New York, New York NY, United States of America
[r] Also at National Institute of Physics, University of the Philippines Diliman (Philippines), Philippines
[s] Also at Department of Financial and Management Engineering, University of the Aegean, Chios, Greece
[t] Also at TRIUMF, Vancouver BC, Canada
[u] Also at Institucio Catalana de Recerca i Estudis Avancats, ICREA, Barcelona, Spain
[v] Also at Henan University, China
[w] Also at Yeditepe University, Physics Department, Istanbul, Türkiye
[x] Also at Institute of Theoretical Physics, Ilia State University, Tbilisi, Georgia
[y] Also at CERN, Geneva, Switzerland
[z] Also at Center for Interdisciplinary Research and Innovation (CIRI-AUTH), Thessaloniki, Greece
[aa] Also at Hellenic Open University, Patras, Greece
[ab] Also at Department of Modern Physics and State Key Laboratory of Particle Detection and Electronics, University of Science and Technology of China, Hefei, China
[ac] Also at Department of Mathematical Sciences, University of South Africa, Johannesburg, South Africa
[ad] Also at Department of Physics, Stellenbosch University, South Africa
[ae] Also at University of Colorado Boulder, Department of Physics, Colorado, United States of America
[af] Also at Département de Physique Nucléaire et Corpusculaire, Université de Genève, Genève, Switzerland

JHEP07(2026)028

[ag] *Also at Centre of Physics of the Universities of Minho and Porto (CF-UM-UP), Portugal*
[ah] *Also at Institute for Nuclear Research and Nuclear Energy (INRNE) of the Bulgarian Academy of Sciences, Sofia, Bulgaria*
[ai] *Also at Washington College, Chestertown, MD, United States of America*
[aj] *Also at Institut für Experimentalphysik, Universität Hamburg, Hamburg, Germany*
[ak] *Also at Institute of Applied Physics, Mohammed VI Polytechnic University, Ben Guerir, Morocco*
[al] *Also at Department of Physics, Stanford University, Stanford CA, United States of America*
[am] *Also at Institute of Physics and Technology, Mongolian Academy of Sciences, Ulaanbaatar, Mongolia*
[an] *Also at Millennium Institute for Subatomic physics at high energy frontier (SAPHIR), Santiago, Chile*
[ao] *Also at University of Chinese Academy of Sciences (UCAS), Beijing, China*
[†] *Deceased*

JHEP07(2026)028